

# **THERMAL MODELING OF LITHIUM ION BATTERIES**

## **LİTYUM İYON PİLLERİN ISIL MODELLEMESİ**

**EMRE GÜMÜŞSU**

**ASSIST. PROF. DR. ÖZGÜR EKİCİ**

**Supervisor**

Submitted to Graduate School of Science and Engineering of Hacettepe University  
as a Partial Fulfillment to the Requirements  
for the Award of the Degree of Master of Sciences  
in Mechanical Engineering

2017



This work named “**Thermal Modeling of Lithium Ion Batteries**” by **EMRE GÜMÜŞSU** has been approved as a thesis for the degree of **MASTER OF SCIENCE IN MECHANICAL ENGINEERING** by the below mentioned Examining Committee Members.

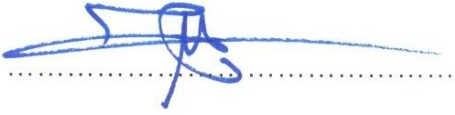
Prof. Dr. Murat KÖKSAL  
Head



Assist. Prof. Dr. Özgür EKİCİ  
Supervisor



Assoc. Prof. Dr. Bora MAVİŞ  
Member



Prof. Dr. Derek BAKER  
Member



Assoc. Prof. Dr. S. Çağlar BAŞLAMIŞLI  
Member



This thesis has been approved as a thesis for the degree of **MASTER OF SCIENCE IN MECHANICAL ENGINEERING** by a board of Directors of the Institute for Graduate School of Science and Engineering.

Prof. Dr. Menemşe GÜMÜŞDERELİOĞLU  
Director of the Institute of Graduate School of Science and Engineering

## YAYINLAMA VE FİKRİ MÜLKİYET HAKLARI BEYANI

Enstitü tarafından onaylanan lisansüstü tezimin/raporumun tamamını veya herhangi bir kısmını, basılı (kağıt) ve elektronik formatta arşivleme ve aşağıda verilen koşullarla kullanıma açma iznini Hacettepe üniversitesine verdiğimi bildiririm. Bu izinle Üniversiteye verilen kullanım hakları dışındaki tüm fikri mülkiyet haklarım bende kalacak, tezimin tamamının ya da bir bölümünün gelecekteki çalışmalarda (makale, kitap, lisans ve patent vb.) kullanım hakları bana ait olacaktır.

Tezin kendi orijinal çalışmam olduğunu, başkalarının haklarını ihlal etmediğimi ve tezimin tek yetkili sahibi olduğumu beyan ve taahhüt ederim. Tezimde yer alan telif hakkı bulunan ve sahiplerinden yazılı izin alınarak kullanması zorunlu metinlerin yazılı izin alarak kullandığımı ve istenildiğinde suretlerini Üniversiteye teslim etmeyi taahhüt ederim.

- Tezimin/Raporumun tamamı dünya çapında erişime açılabilir ve bir kısmı veya tamamının fotokopisi alınabilir.**

(Bu seçenekle teziniz arama motorlarında indekslenebilecek, daha sonra tezinizin erişim statüsünün değiştirilmesini talep etseniz ve kütüphane bu talebinizi yerine getirirse bile, tezinin arama motorlarının önbelleklerinde kalmaya devam edebilecektir.)

- Tezimin/Raporumun ..... tarihine kadar erişime açılmasını ve fotokopi alınmasını (İç Kapak, Özet, İçindekiler ve Kaynakça hariç) istemiyorum.**

(Bu sürenin sonunda uzatma için başvuruda bulunmadığım takdirde, tezimin/raporumun tamamı her yerden erişime açılabilir, kaynak gösterilmek şartıyla bir kısmı ve ya tamamının fotokopisi alınabilir)

- Tezimin/Raporumun ..... tarihine kadar erişime açılmasını istemiyorum, ancak kaynak gösterilmek şartıyla bir kısmı veya tamamının fotokopisinin alınmasını onaylıyorum.**

- Serbest Seçenek/Yazarın Seçimi**

17 / 05 / 2017

  
(İmza)

Emre GÜMÜŞSU

Dedicated to my family

## ETHICS

In this thesis study, prepared in accordance with the spelling rules of Institute of Graduate Studies in Science of Hacettepe University,

I declare that

- all the information and documents have been obtained in the base of the academic rules.
- all audio-visual and written information and results have been presented according to the rules of scientific ethics.
- in case of using others Works, related studies have been cited in accordance with the scientific standards.
- all cited studies have been fully referenced.
- i did not do any distortion in the data set.
- and any part of this thesis has not been presented as another thesis study at this or any other university.

17/05/2017



EMRE GÜMÜŖSU

## ÖZET

### LİTYUM İYON PİLLERİN ISIL MODELLEMESİ

**Emre GÜMÜŞSU**

**Yüksek Lisans, Makina Mühendisliği Bölümü**

**Tez Danışmanı: Yard. Doç. Dr. Özgür EKİCİ**

**Mayıs 2017, 135 Sayfa**

Bu çalışmada, doğal taşınım altındaki bir lityum iyon bataryanın ısı davranışının benzetimi için, probleme özel deneysel yöntemlerle birlikte, 3 boyutlu bir hesaplamalı akışkanlar dinamiği modeli (ANSYS Fluent 14.5 hesaplamalı akışkanlar dinamiği programı kullanılarak) geliştirilmiştir. Bu model, pilin içindeki ısı iletimini ve pilin etrafındaki bütün akış alanını çözebilmektedir. Ayrıca, ana model yapısına – literatürde sıkça kullanılan- bir pil ısı üretim modelinin de yerleştirilmesiyle pilin içerisindeki ısı üretimi doğrudan model içinde hesaplanabilmektedir. Geliştirilen model, ısı açıdan tam kestirim gücüne sahip olduğu için pilin boşaltılması sırasında pil sıcaklığını sadece elektriksel performans verilerini kullanarak hesaplayabilmektedir. Bu model kullanılarak pilin geniş ölçekli ısıfiziksel özelliklerindeki değişimin ve ısı üretimi alt modelinde kullanılan entropik terimin, pilin ısı benzetimine etkisi detaylı bir şekilde incelenmiştir. Sonuçlar göstermiştir ki, özgül ısı, benzetim hesaplarını etkileyen çok önemli bir unsurken, ısı iletkenlik, sonuçlar üzerinde sadece kısıtlı bir etkiye sahiptir. Diğer taraftan entropik terim kullanılmadan koşulan benzetimlerde de deney verilerine oldukça yakın sonuçlar elde edilmiştir. Geliştirilen modelde koşulan benzetimlerde hesaplanan pil yüzey sıcaklıklarının, deneysel verilerle arasındaki fark -pilin kullanım geçmişine bağlı kalmaksızın- 3

$^{\circ}\text{C}$ 'den daha azdır. Geliştirilen model daha ileri seviyelerde deęişik paketleme düzenleri içerisinde bulunan pillerin doğal veya zorlamalı taşınım altında ısı davranışlarının incelenmesi ve benzetimi için de kullanılabilir potansiyele sahiptir.

**Anahtar Sözcükler:** Li-iyon piller, ısı modelleme, ısıfiziksel özellikler, entropik terim, doğal ısıyayım, ısı iletimi, elektriksel performans



## **ABSTRACT**

### **THERMAL MODELING OF LITHIUM ION BATTERIES**

**Emre GÜMÜŞSU**

**Master of Sciences, Department of Mechanical Engineering**

**Thesis Supervisor: Assist. Prof. Dr. Özgür Ekici**

**May 2017, 135 Pages**

In this study, a 3-D computational fluid dynamics model (based on ANSYS Fluent 14.5 CFD program) was developed along with a problem specific experimental procedure for investigating the thermal behavior of lithium ion batteries under natural convection. The model solves the complete flow field around the battery as well as conduction inside the battery using heat generation model widely used in the literature. The model is thermally fully predictive so it requires only electrical performance parameters of the battery to calculate its temperature during discharging. Using the model, detailed investigation of the effects of the variation of the macro-scale thermophysical properties and the entropic term of the heat generation model was carried out. Results show that specific heat is a critical property that has a significant impact on the simulation results, whereas thermal conductivity has relatively minor importance. Moreover, the experimental data can be successfully predicted without taking the entropic term into account in the calculation of the heat generation. The difference between the experimental and predicted battery surface temperature was less than 3 °C for all discharge rates and regardless of the usage history of the battery. The developed model has the potential to be used for the

investigation of the thermal behavior of Li-Ion batteries in different packaging configurations under natural and forced convection.

**Keywords:** Li-ion batteries, thermal modeling, thermophysical properties, entropic term, natural convection, conduction, electrical performance

## ACKNOWLEDGEMENTS

There are lots of people having share in completion of the thesis. First of all, I would like to express my deepest gratitude and respect to my supervisor, Dr. Özgür Ekici, and to Dr. Murat Köksal due to their vital guidance in the course of my thesis. I have always been grateful, as a consequence of having a chance to be a part of their research. Participating in their laboratory, I have entered an academic atmosphere in which I had always an exact freedom to think, to discuss and to realize. I have always become more motivated in my academic path by their priceless presence.

I found always open doors whenever I need, therefore I couldn't miss any of the faculty members of the Mechanical Engineering Department of Hacettepe University. I am also very grateful to my committee members, Dr. Bora Maviş, Dr. Derek Baker and Dr. S. Çağlar Başlamışlı, due to their interest in my thesis.

I should also remind the support of my friends. As before, they have always represented an unreserved friendship.

I would like to thank my family because of their contributions. Especially my parents didn't hesitate even a second to support me in my academical survey. They have always backed my decisions without any reluctance. I couldn't even start without them. My elder sister and my brother in law also deserve a credit for their support. They have followed my studies with an increasing and bewildering interest.

Finally, I would give thanks to the Scientific Research Projects Coordination Unit of Hacettepe University for their financial support in the research project. (project code: FBA-2015-5419)

# TABLE OF CONTENTS

	<b>Page</b>
ÖZET .....	i
ABSTRACT .....	iii
ACKNOWLEDGEMENTS.....	v
LIST OF FIGURES .....	viii
LIST OF TABLES .....	x
LIST OF ABBREVIATIONS .....	xi
NOMENCLATURE .....	xii
CHAPTER 1 .....	1
INTRODUCTION AND LITERATURE REVIEW .....	1
1.1. Introduction .....	1
1.2. Structure of Li-Ion Batteries.....	1
1.3. Thermal Behavior of Li-Ion Batteries .....	3
1.4. Literature Review .....	5
1.5. Aim and Scope of the Thesis .....	8
CHAPTER 2 .....	9
THEORY AND MODELING.....	9
CHAPTER 3 .....	12
EXPERIMENTAL SET UP AND METHODOLOGY .....	12
3.1 Charging and Discharging of Li-Ion Batteries.....	14
3.2 Determination of OCV, V and Entropic Term .....	16
3.2.1 Operating Voltage Measurements .....	16
3.2.2 OCV Measurements .....	20
3.2.3 Entropic Term Measurements.....	23
3.3 Repeatability of Surface Temperature Measurements .....	27
CHAPTER 4 .....	29
IMPLEMENTATION OF NUMERICAL MODEL WITH COMPUTATIONAL FLUID DYNAMICS APPROACH .....	29
4.1 Selection of Computational Tool .....	29

4.2	Solution Parameters .....	33
4.3	Domain, Mesh, Boundary and Initial Conditions .....	33
4.4	Evaluation of the Thermophysical Properties .....	36
CHAPTER 5 .....		38
RESULTS AND DISCUSSIONS.....		38
5.1	Effect of Thermophysical Properties .....	38
5.1.1	Specific Heat.....	38
5.1.2	Thermal Conductivity .....	41
5.2	Effect of Discharge Rate .....	44
5.3	Effect of the Entropic Term .....	47
5.4	Effect of the Usage History .....	50
5.5	Temperature Distribution and Velocity Profile at the End of the Discharge .....	53
CHAPTER 6 .....		55
CONCLUSIONS AND RECOMMENDATIONS FOR FUTURE WORK .....		55
6.1	Conclusions .....	55
6.2	Recommendations for Future Work .....	57
REFERENCES .....		58
APPENDIX A .....		63
Panasonic General Overview about Li-Ion Batteries .....		63
APPENDIX B.....		66
Panasonic Specification Sheet for NCR18650B Type Battery .....		66
APPENDIX C.....		67
UDF Codes.....		67
	Heat generation at 0.5C with 1 <sup>st</sup> approximation for entropic term.....	67
	Heat generation at 1.0C with 1 <sup>st</sup> approximation for entropic term .....	79
	Heat generation at 1.5C with 1 <sup>st</sup> approximation for entropic term .....	89
	Heat generation at 1.0C with 2 <sup>nd</sup> approximation for entropic term .....	98
	Heat generation at 1.0C with 3 <sup>rd</sup> approximation for entropic term .....	107
	Heat generation at 1.0C with 4 <sup>th</sup> approximation for entropic term .....	116
	Heat generation at 1.0C for the new battery.....	124
CURRICULUM VITAE .....		134

## LIST OF FIGURES

	<b>Page</b>
Figure 1.1. Structure of a Li-Ion battery. a) cylindrical cell, b) pouch cell .....	2
Figure 1.2. Working principle of a Li-Ion battery .....	3
Figure 1.3. Classification of literature about modeling of thermal behavior of Li-Ion batteries. a) Methods to handle heat generation, b) Solution approaches for heat transfer problem .....	7
Figure 2.1. Schematic definition of the thermal problem .....	9
Figure 3.1. Experimental equipment. a) Maccor battery test system b) demonstration of a battery during a test c) Nuve natural convection oven .....	13
Figure 3.2. Charging process of Li-Ion battery .....	16
Figure 3.3. Variation of the voltage with time during discharge for different discharge rates .....	18
Figure 3.4. Test procedure of the operating voltage measurement .....	19
Figure 3.5. A screenshot from the battery tester program written for the operating voltage test procedure .....	19
Figure 3.6. Variation of OCV with DoD .....	21
Figure 3.7. Test procedure of the open circuit voltage measurement .....	22
Figure 3.8. A screenshot from the battery tester program written for OCV test procedure .....	22
Figure 3.9. Test procedure of the entropic term measurement .....	24
Figure 3.10. A screenshot from the battery tester program written for entropic term test procedure. a) Reset of the battery b) Test in the oven .....	25
Figure 3.11. Variation of the entropic term with DoD .....	26
Figure 3.12. Variation of surface temperature in different tests during discharge at 1.0C .....	27
Figure 3.13. Test procedure of the temperature measurement .....	28
Figure 4.1. Velocity vectors calculated with compressible flow solvers of both program. a) OpenFOAM b) ANSYS Fluent .....	32
Figure 4.2. Mesh dependency analysis .....	34

Figure 4.3. Mesh Structure. a) 2D view of the region, in the vicinity of the battery, at the middle plane b) 3D view of the region close to the battery .....	35
Figure 5.1. Variation of surface temperature with time for different specific heats at various discharge rates .....	39
Figure 5.2. Variation of surface temperature with time for different thermal conductivities .....	41
Figure 5.3. Variation of the calculated convection coefficient with time in comparison with correlations in the literature .....	43
Figure 5.4. Variation of the Biot number with time for different thermal conductivities .....	44
Figure 5.5. Variation of heat generation in the battery with time for different discharge rates .....	45
Figure 5.6. Variation of the surface temperature with time for different discharge rates .....	46
Figure 5.7. Various approximations for the entropic term .....	48
Figure 5.8. Variation of the surface temperature with time for different entropic term approximations .....	49
Figure 5.9. Variation of surface temperature with time using batteries of different usage history .....	51
Figure 5.10. Model and experimental results for a new and old battery .....	52
Figure 5.11. Temperature distribution ( $^{\circ}\text{C}$ ) and velocity profile (m/s) at the end of discharge. a) Temperature distribution b) Velocity Profile .....	53

## LIST OF TABLES

	<b>Page</b>
Table 3.1. Corresponding currents at each discharge rate for Panasonic NCR18650B type battery .....	17
Table 4.1. Comparison of OpenFOAM and ANSYS Fluent for the investigated flow case in the thesis.....	32
Table 4.2. Boundary and initial conditions .....	35
Table 4.3. Thermophysical properties .....	37
Table 5.1. Root mean square errors ( $^{\circ}\text{C}$ ) for different specific heats at different discharge rates .....	40
Table 5.2. Usage details of five different batteries .....	50
Table 5.3. Maximum temperature variation in the battery at the end of the discharge .....	54



## LIST OF ABBREVIATIONS

DoD	Depth of Discharge
SoC	State of Charge
OCV	Open Circuit Voltage (V)
CFD	Computational Fluid Dynamics
3D	Three Dimensional
SIMPLE	Semi Implicit Method for Pressure Linked Equations
UDF	User Defined Function

## NOMENCLATURE

$c_p$	Specific heat capacity ( $\text{Jkg}^{-1}\text{K}^{-1}$ )
$g$	Gravitational acceleration ( $\text{m}^2\text{s}^{-1}$ )
$I$	Current (A)
$k$	Thermal conductivity ( $\text{Wm}^{-1}\text{K}^{-1}$ )
$p$	Pressure (Pa)
$q$	Heat generation (W)
$\dot{q}$	Volumetric heat generation ( $\text{Wm}^{-3}$ )
$T$	Temperature (K)
$t$	Time (s)
$V$	Air velocity ( $\text{ms}^{-1}$ )
$\frac{dOCV}{dT}$	Entropic term ( $\text{VK}^{-1}$ )
$\rho$	Density ( $\text{kgm}^{-3}$ )
$\beta$	Thermal expansion coefficient ( $\text{K}^{-1}$ )
$\mu$	Dynamic viscosity ( $\text{Nsm}^{-2}$ )

### Subscripts

$\infty$	ambient
$a$	air
$b$	battery

# CHAPTER 1

## INTRODUCTION AND LITERATURE REVIEW

### 1.1 Introduction

Lithium ion (Li-Ion) batteries are one of the most potent sources of energy, which are used to produce and back up electrical energy. Their high energy and power densities make them ideal to power high performance machines and devices [1]. Li-Ion batteries are already used in modern electrical vehicles, cellphones, laptop computers and many other devices [2]. However, substantial safety issues were faced during the operations of systems using Li-Ion batteries [3]. These issues were generally related to thermal behavior of these batteries [3, 4].

In the near future it can be expected that these batteries will have minimum five times as much higher energy and power density as a result of rigorous research aiming to make them sufficient enough to satisfy the power requirements of the future machines and equipment [5]. On the other hand, while even today's Li-Ion batteries cannot be used as completely safe equipment, the higher performance batteries of the future will possibly create more safety problems due to their higher energy and power densities. Therefore, understanding and modeling of thermal behavior of Li-Ion batteries is essential.

### 1.2 Structure of Li-Ion Batteries

A typical Li-Ion battery structure is composed of anode, cathode, solid electrolyte interphase, electrolyte and current collectors [6]. Anode material of Li-Ion batteries is generally composed of carbon based composites, while most of the cathodes consist of metal oxides [2]. Today, most common cathode materials are  $\text{LiCoO}_2$ ,  $\text{LiFePO}_4$  and Nickel based Cobalt oxide solutions. As electrolyte, Li salt in a non-aqueous solvent is widely preferred in Li-Ion batteries [6, 7]. Materials of current collectors, copper and aluminum [6], are nearly the same for all types of Li-Ion batteries. Copper is used at

the anode side, whereas aluminum is utilized at the cathode. Having the same basic structure, geometrical layout of a Li-Ion battery can vary with respect to its external shape, as shown in Fig. 1.1.

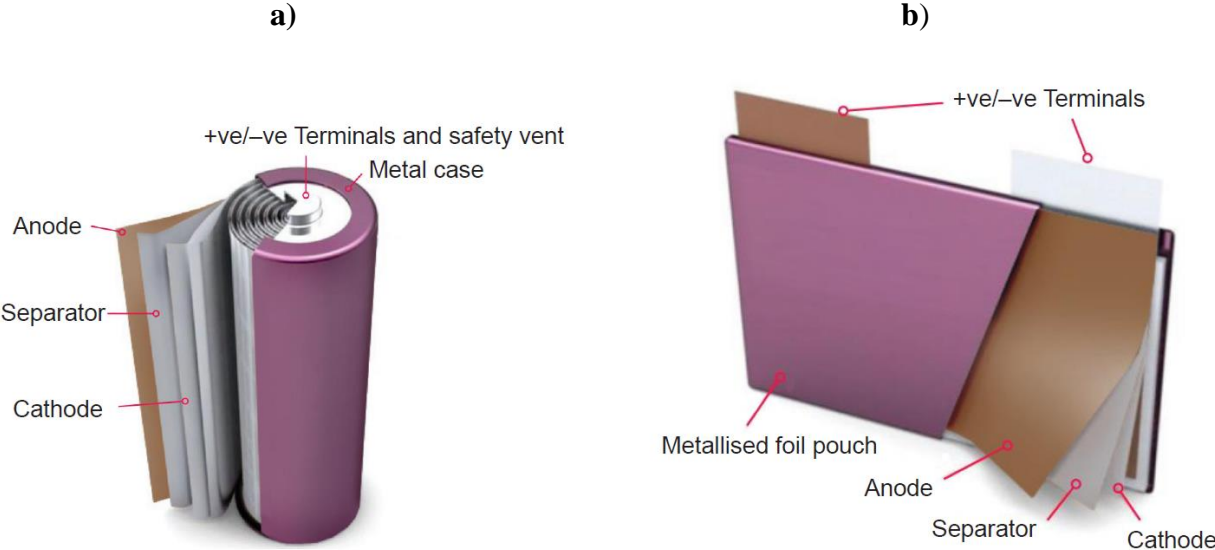


Figure 1.1: Structure of a Li-Ion battery: a) cylindrical cell, b) pouch cell [8].

In Li-Ion batteries, lithium ions are stored in the host structures (anode and cathode) and this process is called as Li insertion/intercalation [9]. The main mechanism producing electrical power is the transportation of lithium ions between anode and cathode while electrons move on a closed external circuit [10], Fig. 1.2. During discharge, lithium ions are inserted into the positive electrode and extracted from the negative electrode [11, 12]; while the same process takes place in the reverse order during charge. Reactions of one of the most widely used types of Li-Ion batteries -  $\text{LiCoO}_2$  (cathode) and graphite (anode) based battery- are represented below as an example from the technical document issued by Panasonic [13], (see Appendix A):

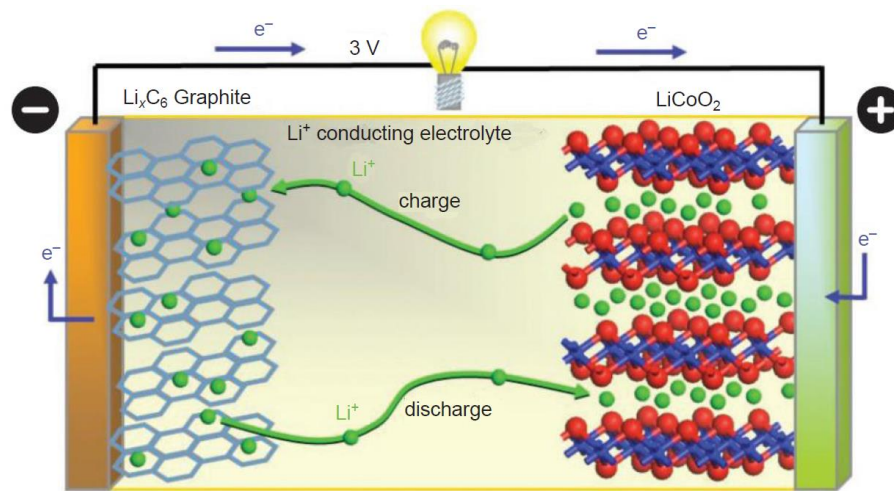
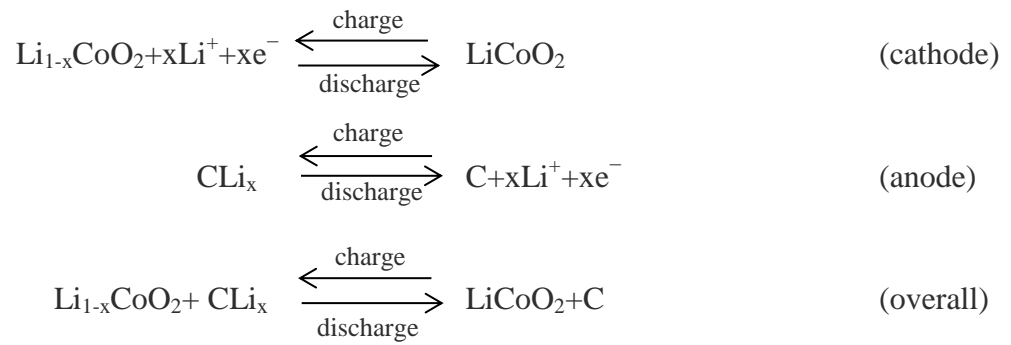


Figure 1.2: Working principle of a Li-Ion battery [8].

### 1.3 Thermal Behavior of Li-Ion Batteries

Thermal behavior of Li-Ion batteries is an important element in operations of these batteries and it is strictly related to both battery performance and safety, as stated above. It is a complex phenomenon depending on many factors.

The foremost reason behind thermal behavior of a Li-Ion battery is heat generation in the battery. During operation of the battery some of its energy is lost through heat generation. The heat generation decreases energy efficiency of the battery in terms of energy conversion from chemical to electrical energy [14]. Main factors causing heat generation in the battery are ohmic resistances, charge transfer over potentials, mass transfer limitations, phase changes, mixing and entropic heating [15]. Among these

factors, effect of mixing can be neglected assuming that the battery is not large enough to have spatially non-uniform reaction rates causing concentration gradients in the battery [3]. In addition, phase changes are usually ignored by assuming that material phases do not change in the battery during its operation [15].

Once heat is generated, it is dissipated through conduction in the battery and heat transfer to the surrounding medium via convection or conduction [14]. Therefore, environmental conditions are also important for understanding the thermal behavior of a Li-Ion battery. As long as heat generation is compensated through heat dissipation so that the critical temperature limit is not exceeded, the battery will be reliable in terms of its thermal behavior. However, if the heat generation increases disproportionately with respect to heat dissipation, that might cause the battery to reach critical temperatures at which the battery will lose its thermal stability leading thermal runaway [16, 17]. In addition to heat generation, environmental conditions could also cause thermal runaway of the battery, when the environment temperature is high enough to increase the battery temperature to the critical level. After such a temperature increase, a series of events preceding thermal runaway take place in the battery [17].

Although, in theory, main reactions in secondary Li-Ion batteries are reversible [9], they are not and batteries lose capacity and power due to some irreversibilities in real life. Since these batteries were initially preferred in low power demanding applications having relatively short lifetime, ageing was not a serious concern for these batteries [18, 19]. However, increasing efforts to use these batteries in new areas -such as high performance and durable machines- bring ageing to the stage as a critical and determinant parameter to enable the utilization of these batteries in the new applications [18, 20]. Therefore, investigating thermal behavior of contemporary Li-Ion batteries, effect of ageing should also be considered regarding its possible and important effects on the battery's thermal behavior.

Ageing of Li-Ion batteries depends on their usage history and calendar life [18, 20]. Ageing can change the structure of a battery through several mechanisms. Solid electrolyte interface (SEI) growing or dissolution, electrolyte decomposition, structural changes in electrodes, Li-plating on the anode and loss of active materials in the electrodes through secondary reactions are some of these ageing mechanisms [19]. One of the possible consequences of these ageing mechanisms is an increase in the internal resistances of the battery which can cause drastic changes in thermal behavior of Li-Ion batteries as well as in their electrical performance [18].

#### **1.4 Literature Review**

Chen and Evans, Newman and Tiedemann, Evans and White and Al Hallaj and his research group carried out extensive research on thermal behavior of Li-Ion batteries [21–31]. These studies comprise a large area of research from cell level to cell stack (battery) and even battery pack levels. Effect of material properties [22, 23], geometrical assumptions [26] and dynamic power profiles [25] were investigated in some of these studies. In addition, thermal management and cooling methods have been among the topics under investigation especially in recent years [27–30, 32–42] including forced convection in a specified layout or in a battery package [32, 34, 35, 37], variable patterns of forced convection [33, 42] and usage of phase change materials for cooling instead of air [27–30, 36, 40].

Broadly, thermal modeling of a Li-Ion battery includes the heat generation problem inside the battery due to electrochemical reactions and heat transfer problem as conduction inside the battery and free or forced convection between the battery surface and the surrounding medium. Therefore, the thermal models of Li-Ion batteries can be classified based on the methods to handle the heat generation and solution approaches used for the heat transfer problem. In the literature, there are various approaches for handling the heat generation inside the battery and the heat transfer problem during the course of thermal modeling.

As seen in Fig. 1.3(a), the heat generation in the battery can be specified either based on direct experimental measurements or based on calculations, which in turn

may use empirical data. Models using direct measurement techniques [27–30, 36, 37, 40, 41] usually employ accelerated rate calorimeter or a similar experimental set up to measure heat generation of the battery. Models calculating heat generation can be generally discussed in two major groups. In the first group [6, 43–46] heat generation is calculated via electrochemical reactions. These reactions can be utilized for calculation of heat generation [6, 43, 44, 46] or for calculation of electrical properties of the battery [45], as preferred. In the second group [45], specified electrical properties are used in a model calculating heat generation separately. Electrochemical models are generally based on concentrated solution theory proposed by Newman [47]. These models have intrinsically high accuracy obtained at the expense of simplicity; hence, they are not suitable to investigate characteristics of more complex systems such as a battery (cell stack) or a battery pack from practical point of view. They require quite a high number of parameters (>50) as they consider all the details of a battery operation such as anode and cathode reactions, transport of Li ions etc. Therefore, these models are generally used to analyze electrical performance and thermal behavior of a single cell.

Models based on experimentally measured electrical properties of the battery [11, 12, 21–26, 31–35, 38, 39, 42, 48–50] calculate the heat generation using the equation of Bernardi et al. [15] or ohmic law. These models are relatively simple compared to electrochemical models and they are suitable for more complex systems like battery packs. The equation of Bernardi et al. [15] is one of the most popular relations used in these kinds of studies [51] and it demonstrates a good agreement with experimental results [14]. It consists of two parts; irreversible heat generation and reversible heat generation. In the literature there are different approaches about the usage of this equation. Evans and White [26] completely neglected reversible heat generation by assuming zero entropic term, while Chen and Evans [22–25] used constant entropic term which indeed demonstrates significant change with respect to depth of discharge (DoD) [52]. In addition, open circuit voltage (OCV) is assumed constant in some studies [22, 23, 25, 26, 31] during the calculation of irreversible heat generation, although it is known that OCV has a substantial variation during discharge similar to



the entropic term [21]. On the other hand, Al Hallaj et al. and Rad et al. considered variable OCV and entropic term with respect to DoD in their studies [21, 49].

The classification of thermal models of Li-Ion batteries based on the solution approach is given in Fig. 1.3(b) and can be discussed in two groups. One of these groups includes models focusing only on conduction inside the battery by introducing convection just as a boundary condition with a specified convection coefficient [6, 11, 12, 21–26, 28–31, 35, 38–41, 43–45, 48–50], while the other group of models solves both conduction throughout the battery and convection around the battery [27, 32–34, 36, 37, 42, 46]. The convection solution inherently involves in the solution of the flow field around the battery under free or forced convection conditions.

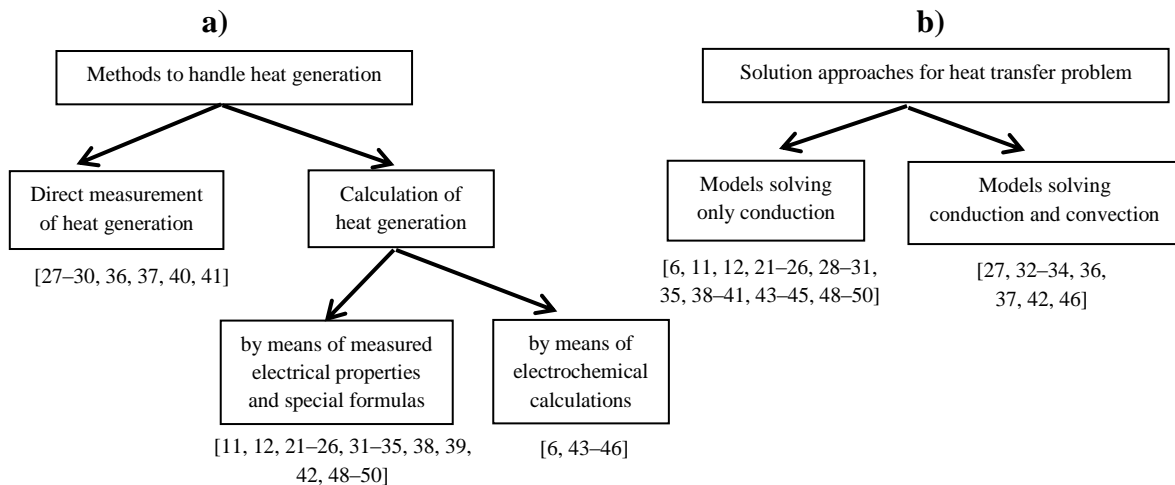


Figure 1.3: Classification of literature about modeling of thermal behavior of Li-Ion batteries. a) Methods to handle heat generation, b) Solution approaches for heat transfer problem

## **1.5 Aim and Scope of the Thesis**

Understanding and predicting the thermal behavior of Li-Ion batteries is one of the most crucial aspects of this technology for realizing its widespread usage. Although a considerable research volume on thermal behavior of Li-Ion batteries has been accumulated in the literature, there is still a need for reliable and fully predictive models for analysis and design of systems using Li-Ion batteries. Furthermore, as far as the CFD based models are concerned, the systematic investigation of the effects of the operating conditions and design parameters on the model results are still lacking in the literature. A reliable modeling approach can only be developed by a direct investigation of the effects of these parameters related to battery operation.

Therefore, the aims of the current study are:

- **To develop a reliable CFD based model for the thermal behavior of Li-Ion batteries,**
- **To validate the accuracy of the model through rigorous experimental testing,**
- **To analyze the effects of design parameters and operating conditions on the model results,**

The scope of the study was limited to a cylindrical battery standing horizontally. Moreover, modeling and investigation of related parameters were performed for discharge operations and under the conditions of natural convection.

## CHAPTER 2

### THEORY AND MODELING

The thermal behavior of Li-ion batteries during discharge is modeled using a 3D CFD approach. The model, composed of a cylindrically shaped battery with internal heat generation and the surrounding air, solves the fundamental mass, momentum and energy equations as required. Internal heat generation occurs as a result of electrochemical reactions taking place during charge or discharge of batteries. Schematic definition of the thermal problem is shown in Fig. 2.1.

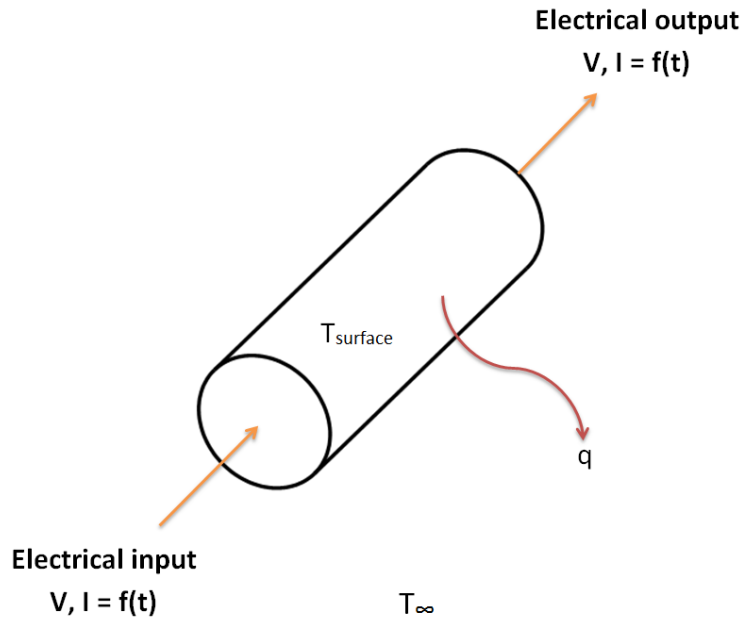


Figure 2.1: Schematic definition of the thermal problem.

$$\nabla \cdot V_a = 0 \quad (1)$$

$$\rho_a \frac{DV_a}{Dt} = \rho_a g - \nabla p_a + \mu_a (\nabla^2 V_a) \quad (2)$$

$$\rho_a c_{p,a} \frac{\partial T_a}{\partial t} + \rho_a c_{p,a} \nabla \cdot (T_a V_a) = \nabla \cdot (k_a \nabla T_a) \quad (3)$$

Due to low velocities, flow is assumed incompressible and as a result of that continuity equation can be written in the form of Eq. (1). Conservation of momentum

for an incompressible flow is represented with Eq. (2) whereas conservation of energy is shown in Eq. (3). Buoyancy forces due to temperature difference in the air should be incorporated in the momentum equation and this is accomplished by employing Boussinesq approximation as shown in Eq. (4).

$$\rho_a \cong \rho_\infty [1 - \beta(T_a - T_\infty)] \quad (4)$$

$$\rho_b c_{p,b} \frac{\partial T_b}{\partial t} = k_b \nabla \cdot (\nabla T_b) + \dot{q} \quad (5)$$

Eq. (5) shows the energy transport equation for the battery. Source term for heat generation in this equation is modeled using the well-known equation of Bernardi et al. [15]:

$$q = I[(OCV - V) - T_b \frac{dOCV}{dT}] \quad (6)$$

In Eq. (6), the first group of terms in parenthesis represents irreversible heat generation (Joule heating) while the second term stands for reversible heat generation in the battery. In this study, all of the terms (OCV, V, I and  $\frac{dOCV}{dT}$ ) in Eq. (6) with the exception of temperature are experimentally determined as a function of DoD specifically for the battery used in this work, which can be also expressed as a function of time as required. Although the battery temperature is measured and recorded during discharge tests, predicted temperature values by the model are preferred to be used in the simulations for the calculation of reversible heat generation term in order to provide a self-consistent model.

Based on initial tests that were performed, the OCV variation with respect to temperature was found to affect the irreversible heat generation at most %2, so this dependency on temperature is neglected for the calculation of the irreversible heat. In the equation of Bernardi et al. [15], any change in OCV is multiplied only by current for the calculation of the irreversible heat. Consequently, -contrary to the reversible heat- temperature dependent OCV variation does not have an important impact for

the irreversible heat. Neglecting this variation, the irreversible heat is determined only as a function of DoD.

In this study, galvanostatic discharge is applied so that DoD varies linearly as a function of time. Therefore, for each discharge rate, Eq. (6) can be written in terms of time and this time dependent equation can be used to calculate the heat generation within the battery in the model.

## **CHAPTER 3**

### **EXPERIMENTAL SET-UP AND METHODOLOGY**

The experimental part of the study involves the measurement of the performance of Li-ion batteries (Panasonic NCR18650B type) with a battery testing system (MACCOR model 4300) as well as the measurement of battery surface temperature during discharge. A natural convection oven (Nüve FN300) was used to carry out the measurements at higher temperatures than the ambient. A platform was employed to hold the battery from its tips and the contact between battery and battery holder was small enough that the battery was treated as being fully exposed to air without any contact. Experimental equipment including Maccor battery test system, Nüve natural convection oven, Panasonic battery and its connections during a test can be seen in Fig. 3.1.

a)



b)



c)



Figure 3.1: Experimental equipment. a) Maccor battery test system b) Demonstration of a battery during a test c) Nüve natural convection oven

The battery was placed horizontally on the holder. In order to measure the surface temperature of the battery a capillary J type thermocouple was used. The acquisition and processing of temperature data were carried out with a data acquisition system (NI USB 6341). Surface temperature values were collected from the top surface of the battery.

### **3.1 Charging and Discharging of Li-Ion Batteries**

Battery operations should be carefully planned regarding operational features of Li-Ion batteries for charging and discharging in order to utilize these batteries safely and efficiently. Otherwise, serious problems can take place in the battery such as quick capacity fade, lithium plating, over-charge, over-discharge, short circuits, thermal runaway and structural degradation of the battery [18, 19, 53–55].

Two important factors should be explained before introducing the details of Li-Ion battery charging and discharging, namely, battery cycle and battery cycle life. A basic battery cycle can be defined as one sequential procedure of complete charging and discharging of the battery, whereas battery cycle life is generally assumed in the literature as the time of cycling until the battery's capacity reduces below 70% of its initial value [56]. As long as battery's features are well known, maximum cycle life of the battery can be easily achieved. On the contrary, uncontrolled cycles will decrease the cycle life substantially.

The first operational feature of a Li-Ion battery is charging pattern of the battery. A suitable charging pattern for the battery should be employed to have a long battery cycle life [56]. There are numerous patterns which can be employed to charge a Li-Ion battery [53]. Among these patterns constant current-constant voltage is probably the most preferred and traditional method [53, 56]. This method is adopted for charging of batteries in this study.



Electrical and thermal limits of the battery, such as highest and lowest values of voltage and ambient temperature, are also important. Electrical performance demanded from the battery and environmental conditions in which the battery will perform should be adjusted regarding these limits.

Throughout this study, operations were carefully planned with respect to the correct charging pattern and limits of the battery for both charging and discharging by referring to the specification sheet issued by the producer [57] (see Appendix B). According to this sheet, the battery's charging pattern should be kept at constant current until 4.2 V after which the topping charge step (constant voltage) starts until current decreases to 0.065 A, as shown in Fig. 3.2. It is worth noting that the time consuming part of the charging process -topping charge or constant voltage step- corresponds to relatively small part of the charging in terms of battery's state of charge. In the specifications sheet limits for discharge are stated as 2.5 V cut off voltage and ambient temperatures of -20 °C and 60°C, while limits for charging are explained as maximum charging rate of 0.5C where C-rate represents the applied current in terms of battery's nominal capacity (see Table 3.1 for details), highest potential of 4.2 V and ambient temperatures of 0°C to 45°C. In all test procedures performed in this study these limits and charging pattern were strictly followed.

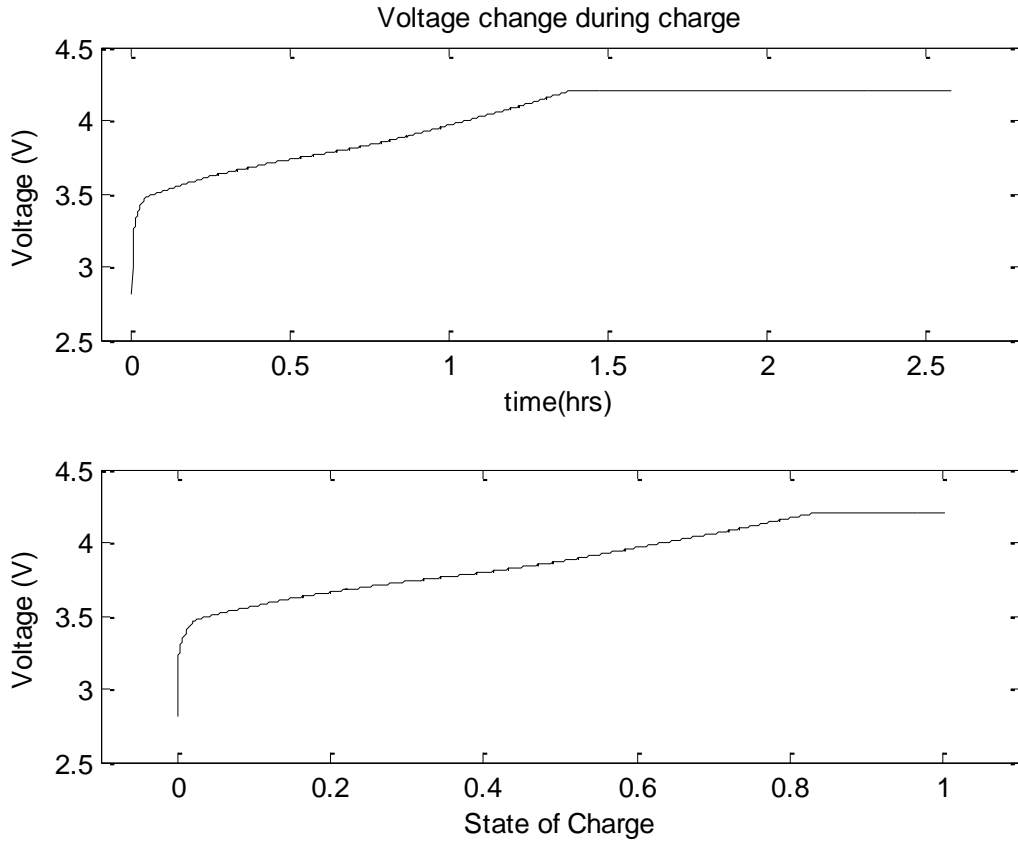


Figure 3.2: Charging process of Li-Ion battery

### 3.2 Determination of OCV, V and Entropic Term

#### 3.2.1 Operating Voltage Measurements

Voltage measurements were performed during galvanostatic discharge (constant current) via Maccor battery testing system showing operating voltage of the battery. Before the galvanostatic discharge, the battery was fully charged and rested for 14 hours to become electrochemically stable. This duration was determined experimentally by recording the variation of the OCV after charge and discharge processes and observing the electrochemical behavior of the battery during this time interval. The next step after charging the battery is the determination of discharge rate. Since the operating voltage changes with respect to discharge rate, tests were conducted separately for each discharge rate modeled in this study, as seen in Fig.

3.3. Considering Panasonic NCR18650B type battery's nominal capacity, current values at galvanostatic discharge process are specified for each discharge rate as shown in Table 3.1. Defining a discharge rate, the battery was discharged to its cut off voltage at galvanostatic discharge by recording operating voltages and temperatures at the same time. The test procedure is explained in Fig. 3.4 step by step. Implementation of these procedures in the Maccor battery test system software is demonstrated in Fig. 3.5.

Table 3.1: Corresponding currents at each discharge rate for Panasonic NCR18650B type battery

<b>Discharge Rate</b>	<b>Current (Ampere)</b>
0.5C	1.625
1.0C	3.25
1.5C	4.875

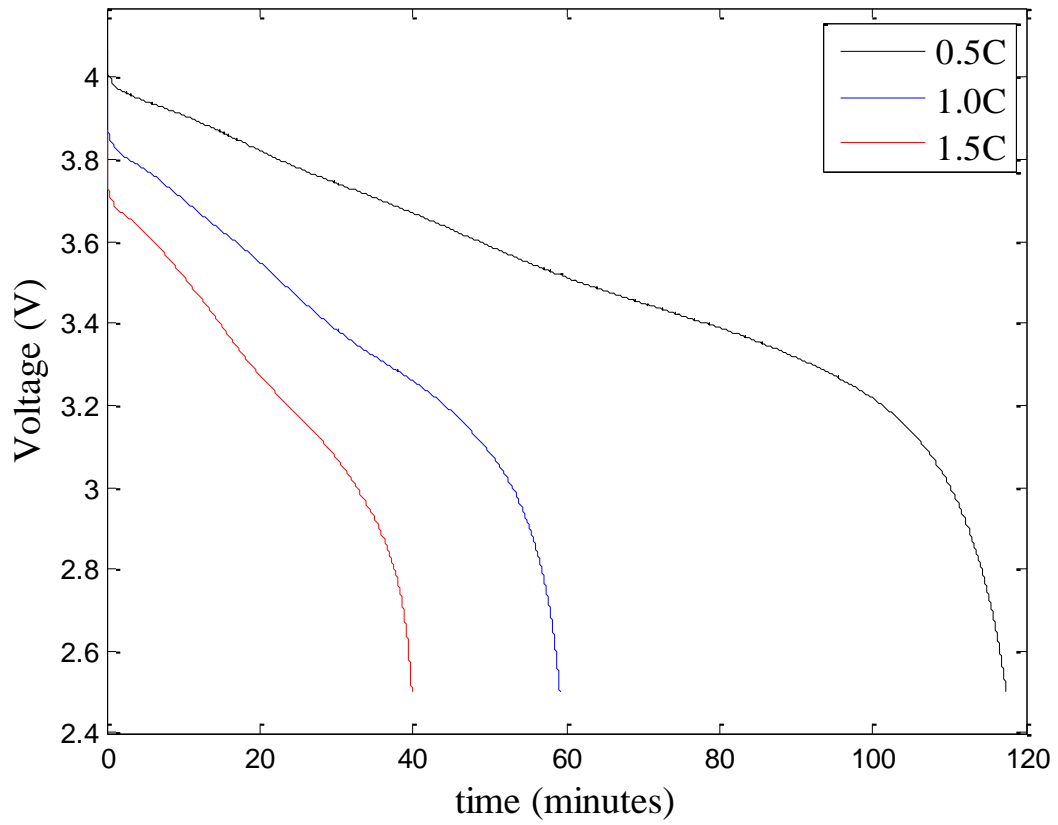


Figure 3.3: Variation of the voltage with time during discharge for different discharge rates.

- charge the battery to 1.0 SOC
- wait for 14 hours for the battery to become electrochemically stable

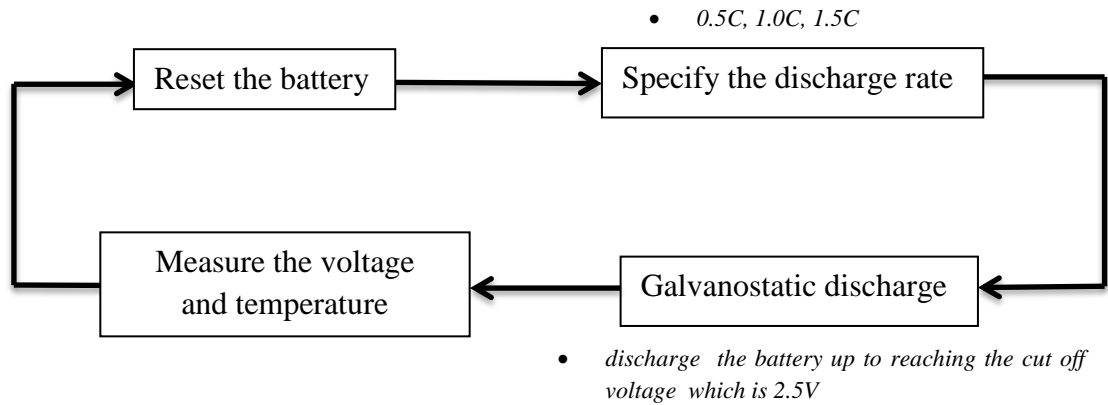


Figure 3.4: Test procedure of the operating voltage measurement.

Step	Type	Mode	Value	Limit	Value	End Type	Op	Value	Goto	Report Type	Value	Options
1	Rest					Step Time	=	00:00:05	002	Step Time	00:00:01	ANNN
2	Charge	Current	0.5C			Step Time	=	00:00:05	003	Step Time	00:00:01	ANNN
3	Charge	Current	0.5C	Voltage	4.2	Current	<=	0.065	004	Step Time	00:05:00	ANNN
4	Rest					Step Time	=	14:00:00	005	Step Time	00:01:00	ANNN
5	Discharge	Current	1.0C			Voltage	<=	2.5	006	Step Time	00:00:01	ANNN
6	End											

Figure 3.5: A screenshot from the battery tester program written for the operating voltage test procedure.

It is worth noting that test procedure obtained in the Maccor includes some extra sequential commands that were not stated in the test procedure shown in Fig. 3.4. The first step provides the last check to observe if everything is working properly at the very beginning of the test. Charge procedure is divided into two parts because of the logic of the test system software according to which the system needs to be given the first input without any limitation in order to reach a continuous charge process with the determined boundary conditions. The rest of the sequential commands in the

Maccor battery test system software are the same as the test procedure stated above.

### **3.2.2 OCV Measurements**

The variation of the OCV with respect to DoD was determined with a set of experiments in which battery's OCV was measured in 0.1 DoD intervals. In preparation of each test the battery was reset in order to relieve it from any possible effects of the self-discharge. In reset procedure the battery was discharged at 1.0C to consume remaining charges from previous test and then it was completely charged again. After each step, the battery was allowed to cool to ambient temperature. Following reset it was discharged to the specified DoD at 1.0C and rested for 14 hours to become electrochemically stable. The recorded value after the rest was taken as the OCV value corresponding to the specified DoD. All tests were performed in ambient conditions. The results of the tests show an almost linear relationship between OCV and DoD as depicted in Fig. 3.6. Detailed test procedure and sequential commands obtained in the Maccor battery test system can be seen in Fig. 3.7 and Fig. 3.8.

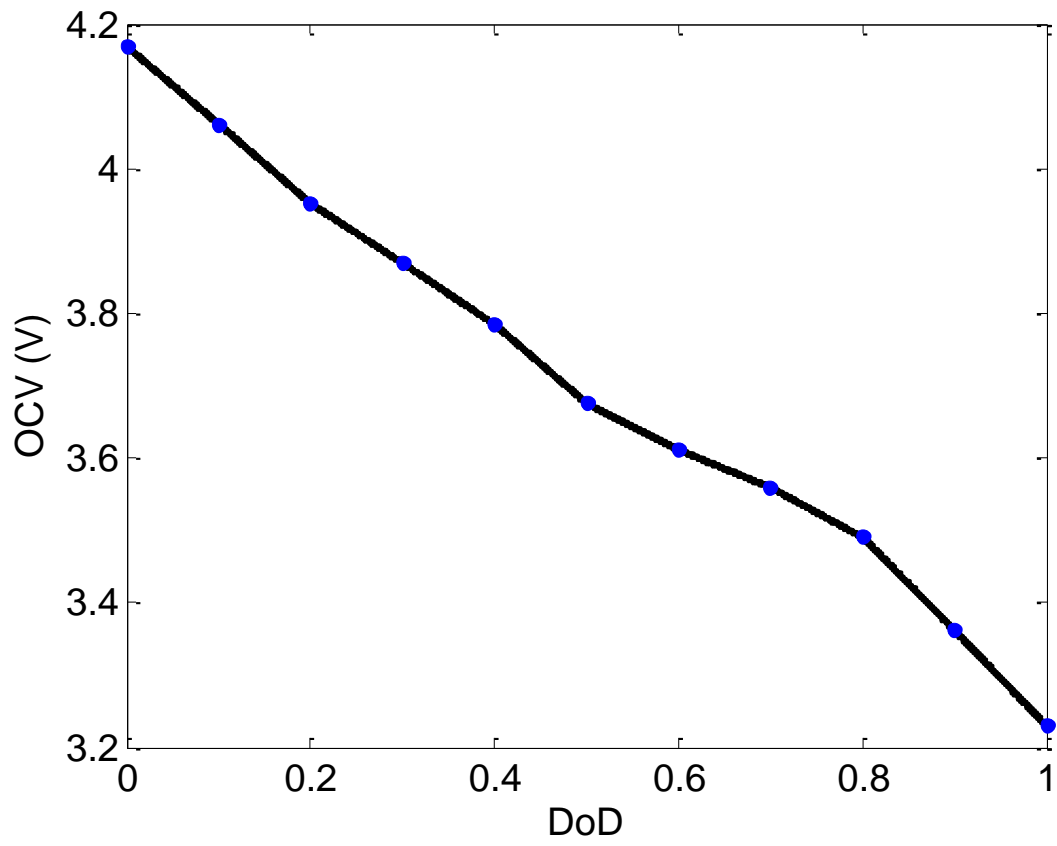


Figure 3.6: Variation of OCV with DoD.

- discharge the battery up to reaching the cut off voltage being equal to 2.5V
- wait for surface temperature to reach the ambient temperature
- charge the battery to 1.0 SOC
- wait for surface temperature to reach the ambient temperature
- discharge the battery to the determined DoD at 1C
- wait for 14 hours for battery to become electrochemically stable

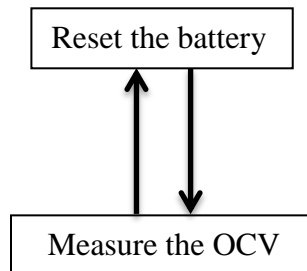


Figure 3.7: Test procedure of the open circuit voltage measurement.

Step	Type	Mode	Value	Limit	Value	End Type	Op	Value	Goto	Report Type	Value	Options
1	Rest					Step Time	=	00:00:05	002	Step Time	00:00:01	ANNN
2	Discharge	Current	1.0C			Voltage	<=	2.5	003	Step Time	00:00:01	ANNN
3	Rest					Thermocouple	<=	3 / 26.0	004	Step Time	00:01:00	ANNN
4	Charge	Current	0.5C			Step Time	=	00:00:05	005	Step Time	00:00:01	ANNN
5	Charge	Current	0.5C	Voltage	4.2	Current	<=	0.065	006	Step Time	00:05:00	ANNN
6	Rest					Thermocouple	<=	3 / 26.0	007	Step Time	00:01:00	ANNN
7	Discharge	Current	1.0C			Amp Hour	>=	0.325	008	Step Time	00:01:00	ANNN
8	Rest					Step Time	=	14:00:00	009	Step Time	00:01:00	ANNN
9	End											

Figure 3.8: A screenshot from the battery tester program written for OCV test procedure.

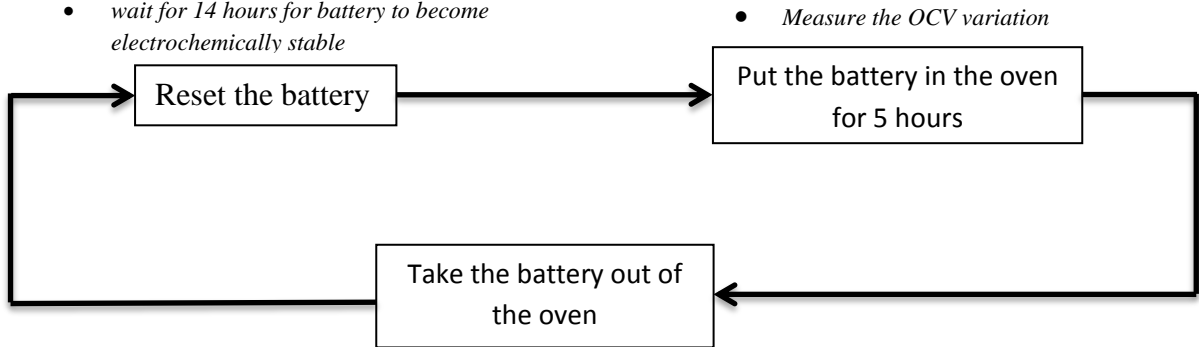


### 3.2.3 Entropic Term ( $\frac{dOCV}{dT}$ ) Measurements

In order to calculate the reversible heat generation in the battery, the entropic term should be determined experimentally as a function of DoD. Test procedure for entropic term measurement is the same as the OCV measurement test in terms of preparatory test procedures. The same reset procedure was applied and the battery was adjusted to the specified DoD using the same way. Then, it was rested for the stabilization as done in the OCV measurement test. After these preparatory procedures the battery was placed in an oven kept at 55 °C. The oven temperature was set considering the operating range of the battery in this study. The battery was kept inside the oven for five hours to provide an isothermal temperature distribution throughout the battery while being connected to the battery tester in open circuit state. In this duration, the variation of OCV was recorded and compared with the values measured at the ambient temperature. Using these data, the entropic term was calculated by employing a finite difference approximation for the first order derivative as shown below. Test procedure is illustrated in Fig. 3.9, while sequential commands developed for this test in the battery tester software are shown in Fig. 3.10. The test program contains two different parts; first one is the preparatory step or reset of the battery which is the same as the OCV measurement test, while the second one is the entropic term measurement in the oven.

$$\text{Entropic term} = \frac{dOCV}{dT} \cong \frac{OCV(T_2) - OCV(T_\infty)}{(T_2 - T_\infty)} \quad (7)$$

- discharge the battery up to reaching the cut off voltage being equal to 2.5V
- wait for surface temperature to reach the ambient temperature
- charge the battery to 1.0 SOC
- wait for surface temperature to reach the ambient temperature
- discharge the battery to the determined DoD at 1C
- wait for 14 hours for battery to become electrochemically stable



- Measure the OCV variation

- Wait for the battery until its surface temperature become equal to the ambient temperature

Figure 3.9: Test procedure of the entropic term measurement.

**a)**

Step	Type	Mode	Value	Limit	Value	End Type	Op	Value	Goto	Report Type	Value	Options
1	Rest					Step Time	=	00:00:05	002	Step Time	00:00:01	ANNN
2	Discharge	Current	1.0C			Voltage	<=	2.5	003	Step Time	00:00:01	ANNN
3	Rest					Thermocouple	<=	3 / 26.0	004	Step Time	00:01:00	ANNN
4	Charge	Current	0.5C			Step Time	=	00:00:05	005	Step Time	00:00:01	ANNN
5	Charge	Current	0.5C	Voltage	4.2	Current	<=	0.065	006	Step Time	00:05:00	ANNN
6	Rest					Thermocouple	<=	3 / 26.0	007	Step Time	00:01:00	ANNN
7	Discharge	Current	1.0C			Amp Hour	>=	0.325	008	Step Time	00:01:00	ANNN
8	Rest					Step Time	=	14:00:00	009	Step Time	00:01:00	ANNN
9	End											

**b)**

Step	Type	Mode	Value	Limit	Value	End Type	Op	Value	Goto	Report Type	Value	Options
1	Rest					Step Time	=	05:00:00	002	Step Time	00:01:00	ANNN
2	End											

Figure 3.10: A screenshot from the battery tester program written for entropic term test procedure.

a) Reset of the battery, b) Test in the oven.

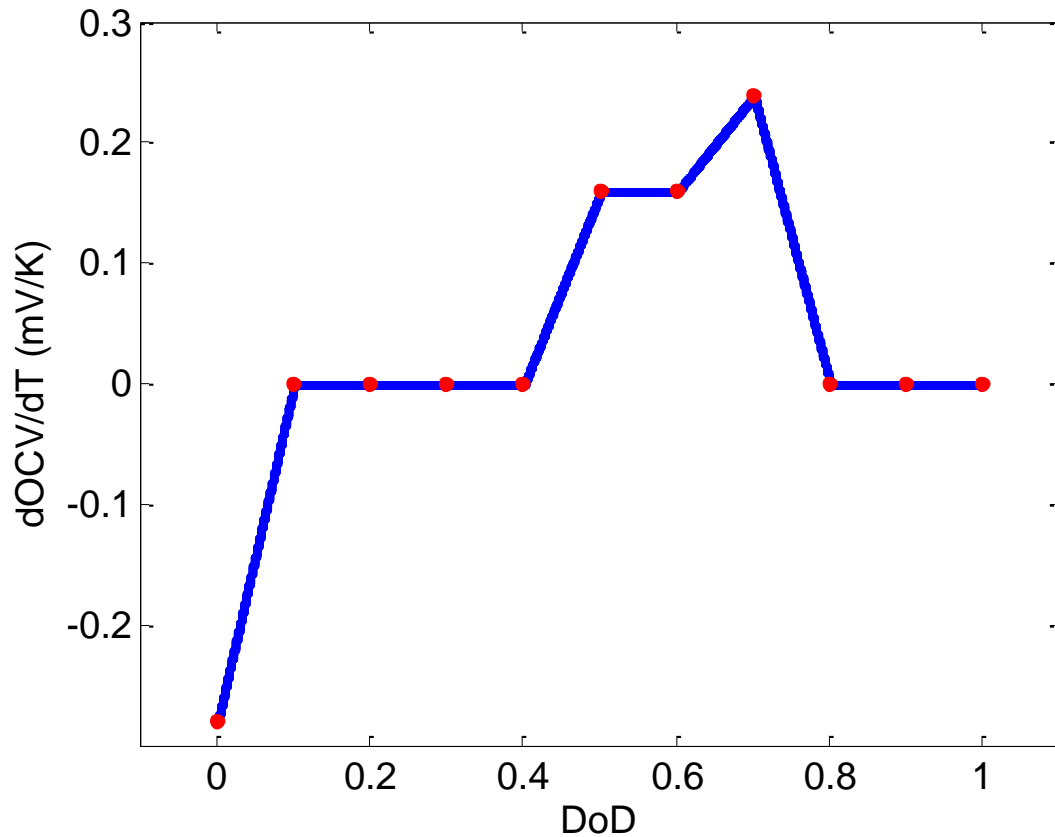


Figure 3.11: Variation of the entropic term with DoD.

The variation of the entropic term with respect to DoD is nonlinear in the entire range of the discharge as shown in Fig. 3.11. A similar entropic term behavior was also observed by Bandhauer et al. [51]. Considering the nonlinear behavior of the entropic term, a piecewise linear approximation was initially specified to approximate the reversible heat generation in this study. This approximation is discussed in section 5.3 in detail.

### 3.3 Repeatability of Surface Temperature Measurements

Repeatability tests were conducted at 1.0C discharge rate under ambient temperature of 31°C. All of these tests were performed with a fully charged battery rested for stabilization. In total, five tests were completed in consecutive days. Results of these tests are shown in Fig. 3.12. The test procedure can be seen in Fig. 3.13 in detail. Commands in the Maccor battery test system for this test are the same as the operating voltage measurement test.

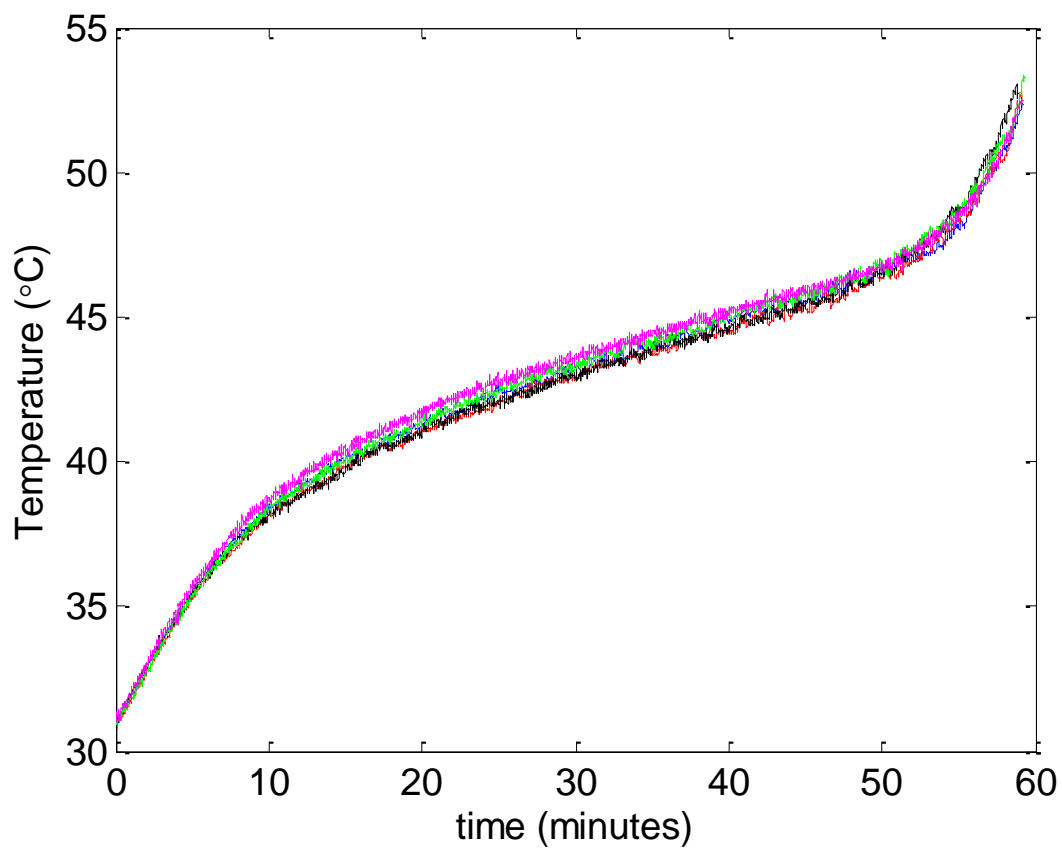


Figure 3.12: Variation of surface temperature in different tests during discharge at 1.0C.

It is seen that results of repeatability tests exhibit a set of curves which are quite similar to each other, qualitatively and quantitatively. The mean of the standard deviation of all results was found to be 0.2 °C with a maximum of 0.5 °C. Therefore the test procedure and results are confirmed to be repeatable.

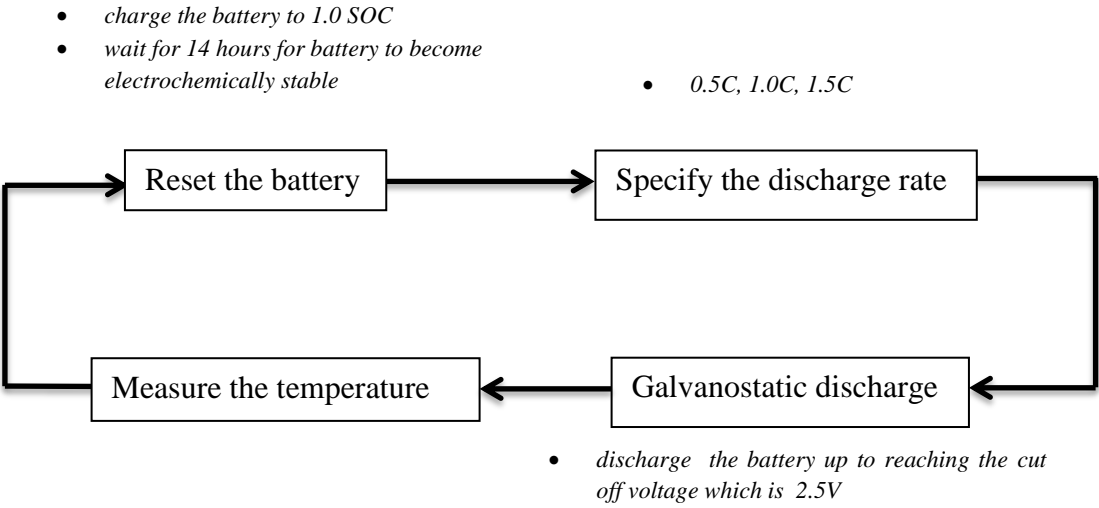


Figure 3.13: Test procedure of the temperature measurement.

## CHAPTER 4

### CFD MODELING OF THERMAL BEHAVIOUR OF LI-ION BATTERIES

#### 4.1 Selection of Computational Tool

Two different computational tools, OpenFOAM 2.3.0 and ANSYS Fluent 14.5, were considered in this study. Selection between them was made with respect to their specifications, appropriateness to the study and potential for further improvements in the model.

OpenFOAM is an open source CFD software mainly operated in Linux based systems, whereas ANSYS Fluent is a commercial software which can be employed in several operating systems but usually in Microsoft Windows. In order to compare both programs several simulations were performed before designing the main model. Results of these performed simulations were used to reveal detailed characteristics of these programs and evaluate their potentials for this study.

In order to be able to assess features of both programs in detail, the selection process was conducted with a step by step approach. Simulations were designed in a sequence in which their complexity increases. Initially, basic flow simulations were performed and they were followed by flows including transport of energy. Then, solid region was included in the solution -representing the battery- along with constant heat generation. Time dependent heat generation was utilized later to obtain a more realistic case closer to the real battery operation. Regarding that the nature of the battery operation is transient, mainly transient simulations were performed in both programs.

The first criterion for the selection is the structure of the program. Software having an open source structure is advantageous in scientific research projects, because they

allow researchers to improve directly the software, if required. In this respect, as opposed to ANSYS Fluent, OpenFOAM provides a flexible structure to improve and modify.

In terms of geometry and mesh design ANSYS Fluent provides a visual interface, while OpenFOAM has nothing visual in preparation of mesh and geometry, so that coordinates of geometry and details of mesh structure must be obtained as computer codes in C++ language. This system needs to proceed from coordinates of vertices to blocks of geometry with right handed orientation of vertices. Indeed, designing a geometry in the three dimensional planar coordinate system by only writing their coordinates in the system is a very tedious process to overcome. Therefore, geometries and meshes obtained in the ANSYS Fluent were later preferred to be used also in OpenFoam for the multiple region case (solid and fluid).

Calculation time is another critical factor in this study. Simulations should be completed in a timely manner in order to evaluate results and to determine required analyses for a reliable thermal model. In basic flow problems OpenFOAM completes the simulation usually faster than ANSYS Fluent. However, a major drawback, which can cause serious problems as the study proceeds, was noticed for OpenFOAM during these preliminary simulations. While solving transient flows, OpenFOAM is very sensitive in solution stability and due to this oversensitivity it requires very small time steps for a stable solution. In basic transient flow simulations, small time steps in OpenFOAM can be compensated with its fast calculation procedure at each time step ending up with a relatively short solution time. However, in case of more complex flows, as in this study, calculation speed of OpenFOAM at each time step decreases substantially. On the contrary, considerably larger time steps can be used in ANSYS Fluent solution with an acceptable error level even for flows with high complexity. Therefore, in terms of solution time OpenFOAM becomes inferior to ANSYS Fluent regarding its sluggish transient solution procedure for complex flows. During investigations, a trial simulation of a complex flow was run and solution time for



ANSYS Fluent was received as approximately 2-3 days. On the other hand, OpenFOAM could not complete even half of the solution after 10 days of running due to a maximum time step of 0.001 seconds. Consequently, ANSYS Fluent requires considerably less time for the investigated flow case in comparison with OpenFOAM.

Furthermore, another set-back was encountered while working with OpenFOAM regarding the modeling of the density change and the associated free convection flow.

In the operation of the battery, natural flow over the battery surface is slightly compressible due to the density change induced by temperature gradients. Initially, the flow was modeled using the compressible flow solvers of both programs which resulted in erroneous flow directions and unreasonable flow velocities and temperatures. As an example, vectors of the calculated velocities can be seen in Fig 4.1 clearly demonstrating that the directions of the vectors are downwards which in fact should be upwards due to the temperature increase occurred at the proximity of the battery. After careful investigation of the related literature, it was decided that compressible flow solvers of CFD programs are more suitable for high speed flows in which density change is induced by velocity change. Therefore, it was decided to use an incompressible flow solver with Boussinesq approximation to consider the density change due to temperature gradient and related free convection flow. Unfortunately, unlike ANSYS Fluent, OpenFOAM did not have an incompressible multi-region solver at the time of the study.

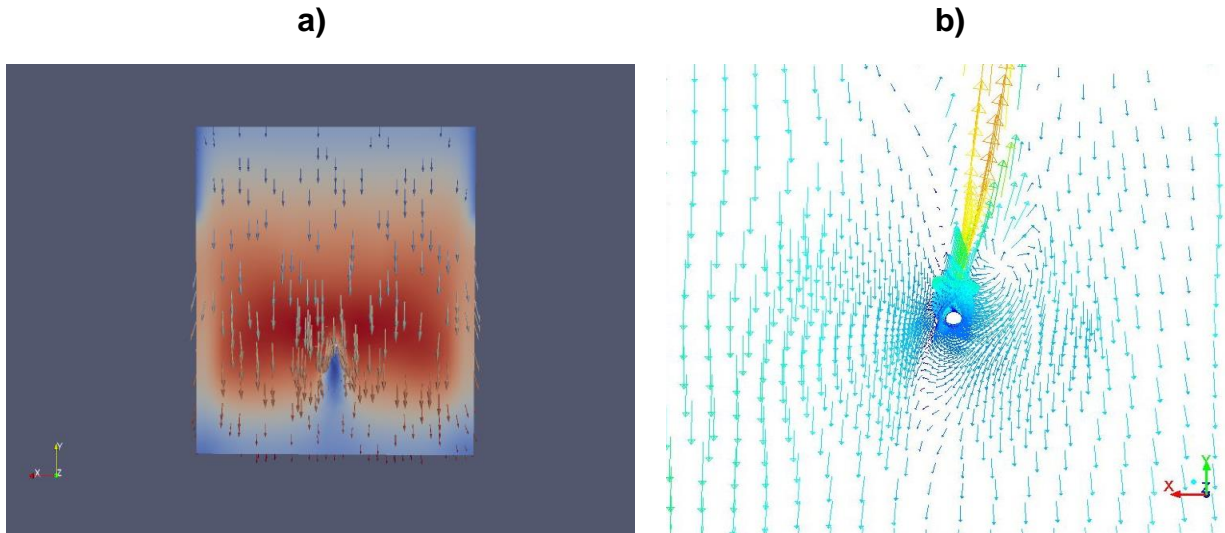


Figure 4.1: Velocity vectors calculated with compressible flow solvers of both programs. a) OpenFOAM b) ANSYS Fluent.

Regarding all of these factors ANSYS Fluent was preferred as the computational tool for this study at the expense of open source structure, the unique advantage of OpenFOAM. It is more user friendly in terms of mesh and geometry design, it solves the flow faster and it has an incompressible flow solver in which Boussinesq approximation can be utilized, as required. Results of comparison made between OpenFOAM and ANSYS Fluent is summarized in Table 4.1.

Table 4.1: Comparison of OpenFOAM and ANSYS Fluent for the investigated flow case in the thesis

	<b>OpenFOAM (version 2.3.0)</b>	<b>ANSYS Fluent (version 14.5)</b>
<b>Open source structure</b>	+	-
<b>Geometry and mesh design</b>	-	+
<b>Solution speed</b>	-	+
<b>Solver options</b>	-	+

## 4.2 Solution Parameters

The model is implemented with CFD approach employing a commercial CFD software, ANSYS Fluent 14.5. A pressure based, laminar, incompressible, transient solver is used in the simulations. The effect of buoyancy forces as a result of density differences due to varying temperature of the air is modeled using Boussinesq approximation in the incompressible solver. Second order upwind scheme is preferred for the momentum and energy equations. The SIMPLE algorithm is selected for pressure and velocity coupling.

Heat generation in the battery -determined as a function of time- is integrated into the solver via a user-defined function (UDF) developed for this study. This UDF takes the battery temperature from the main solver and employs Eq. (6) to calculate the heat generation during the discharge process.

## 4.3 Domain, Mesh, Boundary and Initial Conditions

In order to obtain a reliable mesh structure, mesh dependency analysis was performed with four different meshes. In Fig. 4.2, along with temperature variations, calculated convection coefficients on the top surface of the battery are shown graphically in order to examine their mesh dependency. The convection heat transfer coefficient was determined from the surface energy balance equation given in Eq. (8) using the battery surface temperature obtained from the CFD solution. A first order approximation was used to evaluate the temperature gradient at the battery surface.

$$h = -\frac{k_a \left( \frac{dT_a}{dn} \right)_s}{(T_s - T_\infty)} \quad (8)$$

As seen in Fig. 4.2, all meshes result in similar temperature profiles. However, calculated convection coefficients exhibit substantial variations depending on the mesh structure. Only after mesh 3, the convection coefficient becomes nearly invariant with respect to mesh, so that any further increase in the number of cells does not result in an important difference. On the other hand, despite of giving similar results, solution time of mesh 3 was considerably less than mesh 4. Therefore, Mesh

3 was selected as the mesh structure in this study. Mesh structure of the model was efficiently designed by employing a mesh grading to have a higher mesh density in the proximity of the battery. Other parts of the domain have a coarser mesh so that any unnecessary computational effort was prevented during simulations. As a result of that, a mesh structure having 326708 cells was obtained with the smallest cell height of  $1e-4$  m just above the battery and with the maximum cell volume of  $3.002438e-6$  m<sup>3</sup>. Using this mesh structure the model runs approximately 2 days on a HP Z640 workstation to obtain a converged solution. The mesh structure of the battery surface at the symmetry plane can be seen in Fig. 4.3.

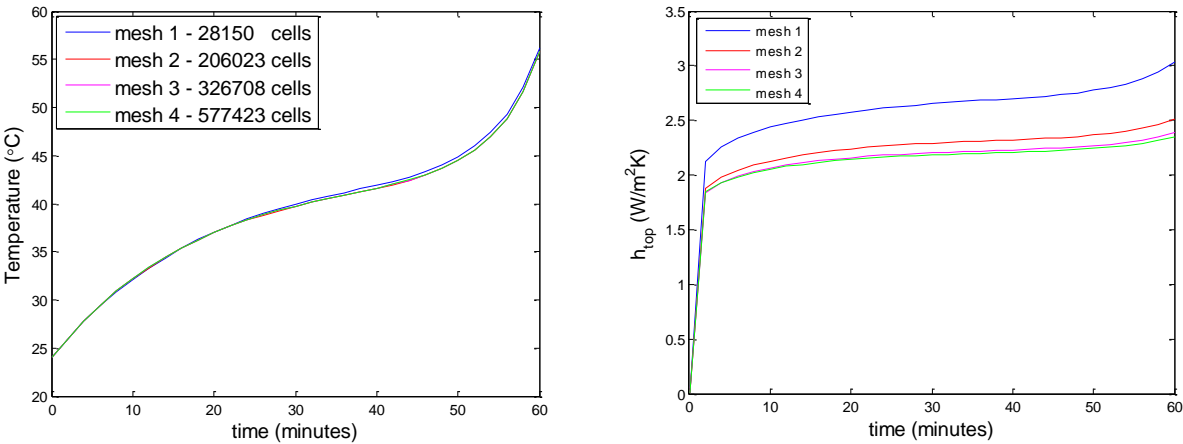


Figure 4.2: Mesh dependency analysis.  $k = 28.05$  W/mK,  $c_p = 1300$  J/kgK, discharge rate = 1.0C.

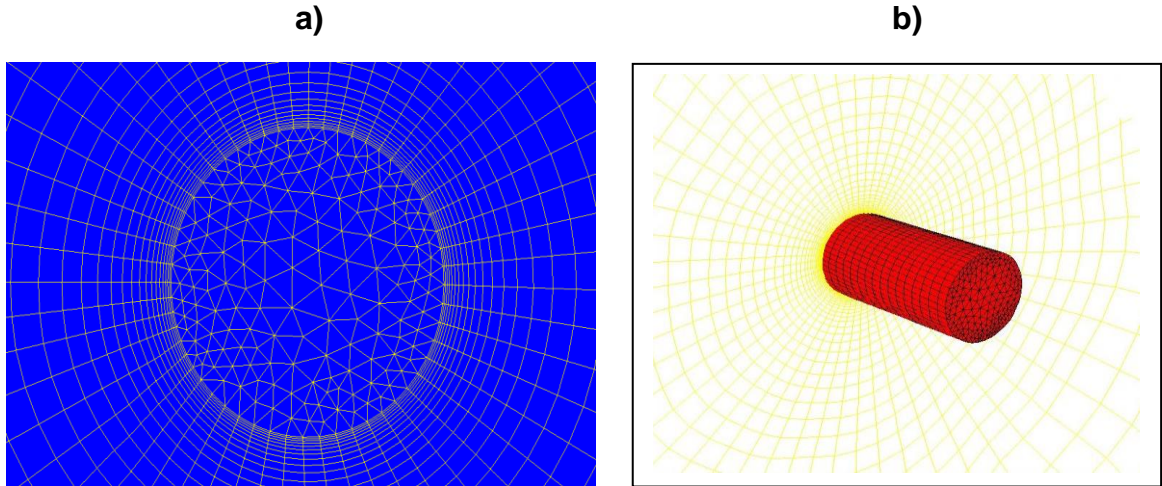


Figure 4.3: Mesh Structure. a) 2D view of the region, in the vicinity of the battery, at the middle plane b) 3D view of the region close to the battery

The specified boundary and initial conditions are shown in Table 4.2. The total pressure and temperature at the domain boundaries are always equal to atmospheric pressure and temperature. No slip condition is valid on the solid surface. As an initial condition, temperature of the whole domain, including the battery, is equal to ambient temperature. At the beginning of the simulation, air pressure also equals to atmospheric pressure and velocity of the air is zero.

Table 4.2: Boundary and initial conditions

<b>Boundary Conditions</b>	
<i>Battery Surface</i>	No slip condition
<i>Flow Domain Boundary</i>	$p_{total,a} = p_{\infty}, T_{total,a} = T_{\infty}$
<b>Initial Conditions</b>	
<i>Battery</i>	$T_b = T_{\infty}$
<i>Flow Domain</i>	$T_a = T_{\infty}, V_a = 0, p_a = p_{\infty},$
$p_{total,a} = p_{static,a} + \frac{1}{2} \rho_a V_a^2$ $T_{total,a} = T_{static,a} \text{ (based on incompressible flow assumption)}$ $p_{\infty} = 90.8 \text{ kPa}, T_{\infty} = 25 \text{ }^{\circ}\text{C}$	

#### 4.4 Evaluation of the Thermophysical Properties

Temperature dependent air properties are incorporated in the simulations using their corresponding values at standard atmospheric pressure. Physical properties of the battery were determined using the values from the literature.

In the literature, thermal conductivity of the Li-ion batteries varies substantially. In some studies it was specified assuming the battery as an isotropic material [21, 28, 58, 59] while in some other studies anisotropy was taken into account [1, 27, 60–62]. In studies with anisotropic battery approximation, thermal conductivity values range from 0.219 W/mK to 3.40 W/mK in radial direction while the range is in between 20 W/mK and 30 W/mK in the axial one [1, 27, 60–62]. For isotropic batteries, thermal conductivity varies between 0.219 W/mK and 3 W/mK in the literature [21, 28, 58, 59]. Specific heat is also a controversial property in the literature. It was presented in the range of 814 J/kgK and 2400 J/kgK [1, 21, 27, 28, 58–62].

The density of the battery was assumed to be uniform and calculated by dividing its mass to its volume. All thermophysical properties of the battery are presumed to be independent of temperature. Properties of the battery are shown in Table 4.3.

The surface of the battery includes an aluminum sheet and a protective plastic coverage. Thermophysical properties of PVC were used as the material properties of the protective plastic. These aluminum sheet and plastic coverage are assumed as a unique composite material having 0.4 mm thickness and its properties were derived by averaging the properties of aluminum and PVC. It is modeled with a shell conduction approach in the simulation without creating any mesh for the shell itself. Properties of the resultant composite material are also shown in Table 4.3.

Table 4.3: Thermophysical properties

<b>Thermophysical Properties</b>	<b>Battery</b>	<b>Shell</b>
$\rho$ (kg/m <sup>3</sup> )	2939	2059
$c_p$ (J/kgK)	814-2400	875
$k$ (W/mK)	0.219-28.05	0.638

## CHAPTER 5

### RESULTS AND DISCUSSIONS

#### 5.1 Effect of thermophysical properties

##### 5.1.1 Specific Heat

Thermophysical properties of a battery are one of the most important parameters for the development of a computational model to predict the thermal behavior. Due to a wide range of materials used in the composition of Li-ion batteries, these properties are found to be highly diversified in the literature so that the determination of properties of a specific battery is a difficult task. Moreover, their effects on a computational solution have not been systematically investigated. In order to elaborate the problem systematically, a range of values from the literature for each thermophysical property is specified, and their effects on the computational solution are examined. Additionally, comparing the results against the experimental data provides a means to quantify their effects.

As has been shown in Table 4.3, specific heat values range from 814 J/kgK to 2400 J/kgK for Li-ion batteries in the literature. Four different values of specific heat were chosen within this interval and used in the model with 3 W/mK thermal conductivity. The model was run at various discharge rates of 0.5C, 1.0C and 1.5C and results are compared with the corresponding experimental data.



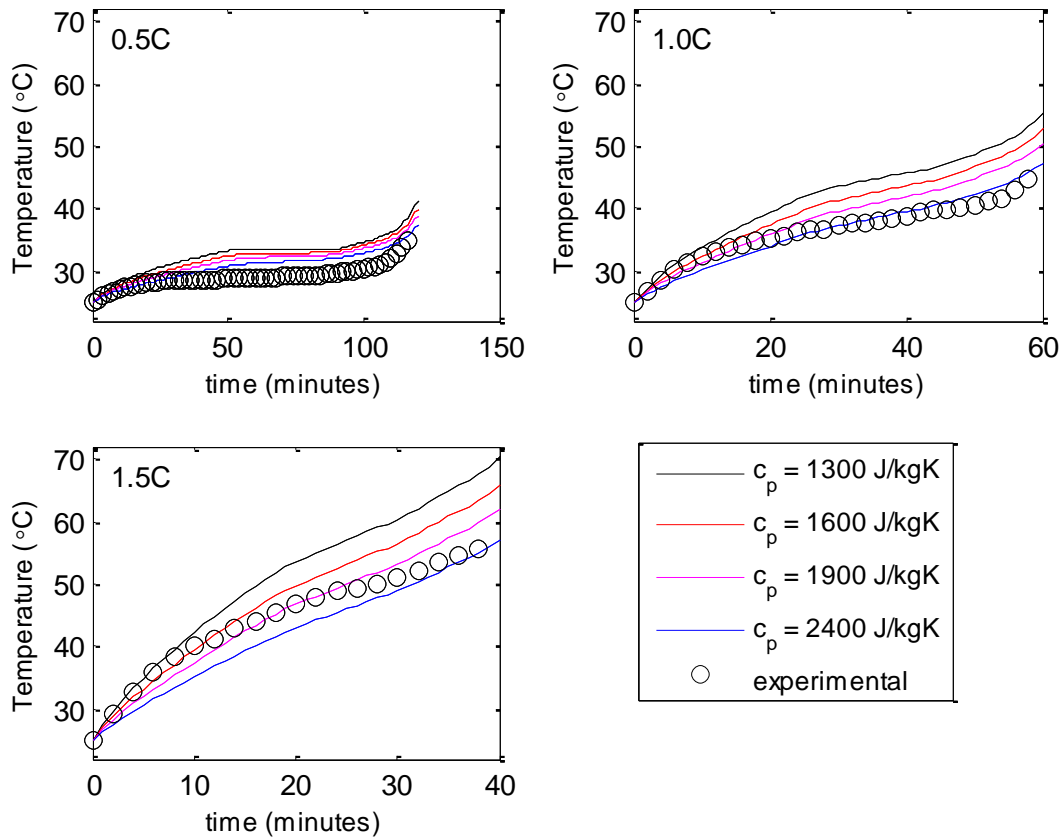


Figure 5.1: Variation of surface temperature with time for different specific heats at various discharge rates.  $k = 3$  W/mK.

All model results are comparable with experimental data in terms of error and trend as shown in Fig. 5.1 and Table 5.1. However as seen in Table 5.1, the lower two specific heat values (1300 J/kgK and 1600 J/kgK) result in higher errors for all discharge rates compared to 1900 J/kgK and 2400 J/kgK. Among the higher two specific heat values, 2400 J/kgK gives the most accurate result for all discharge rates, so it is preferred to be used as the nominal specific heat value of the battery for the rest of the study.

Table 5.1: Root mean square errors ( $^{\circ}\text{C}$ ) for different specific heats at different discharge rates

<b>Specific heats (J/kgK)</b> <b>Discharge rates</b>	<b>1300</b>	<b>1600</b>	<b>1900</b>	<b>2400</b>
<b>0.5C</b>	3.4	2.8	2.3	1.6
<b>1.0C</b>	5.1	3.4	2.2	1.1
<b>1.5C</b>	6.0	3.2	1.8	3.0
<b>Average</b>	4.8	3.1	2.1	1.9

### 5.1.2 Thermal Conductivity

Following the selection of the specific heat value a similar procedure is applied to determine the effects of the thermal conductivity. Six different thermal conductivity values, ranging between the minimum and the maximum values given in Table 4.3, are chosen from the literature to investigate. The computational model is run separately with each of these thermal conductivity values at 1.0C discharge rate. In addition to different thermal conductivities, anisotropic battery assumption is also investigated by defining axial and radial thermal conductivities separately in one of the simulations.

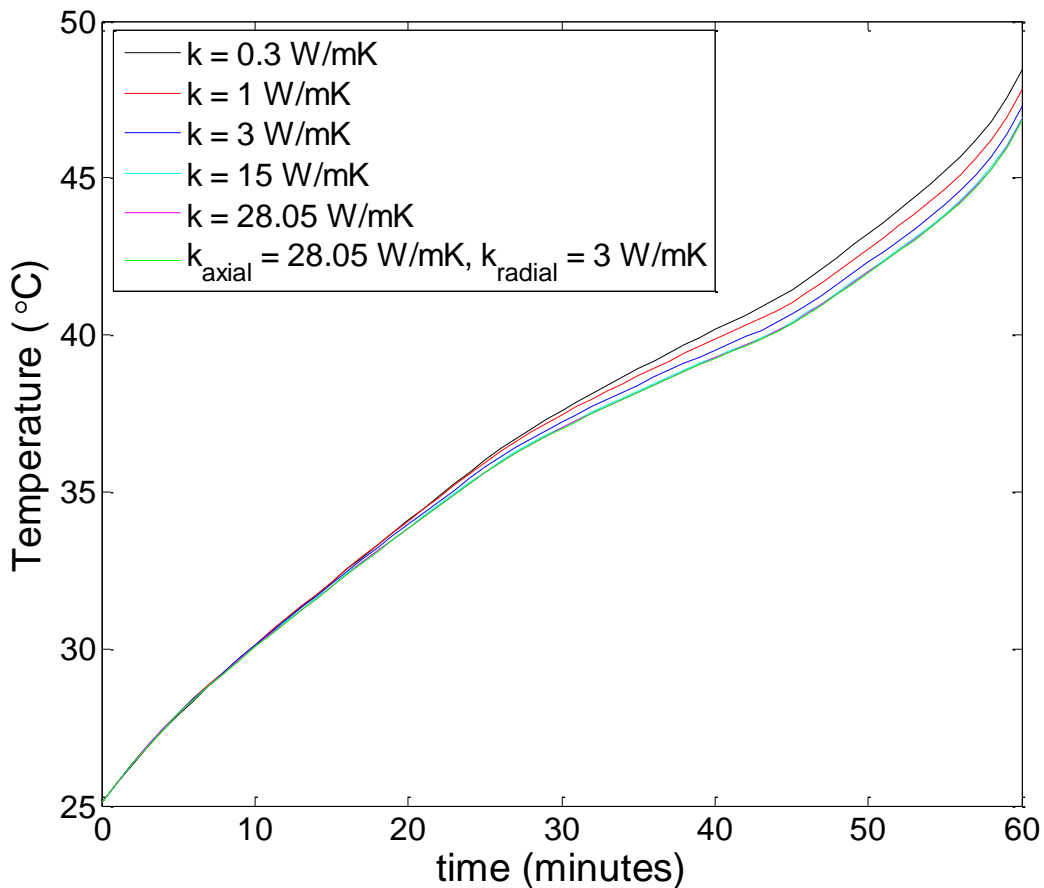


Figure 5.2: Variation of surface temperature with time for different thermal conductivities.  $c_p = 2400 \text{ J/kgK}$ , discharge rate = 1.0C.

Fig. 5.2 shows that the choice of a thermal conductivity value has a minor impact on the predicted temperature values. It is seen that an increase in the thermal conductivity causes a slight decrease, which is less than 2°C, in the calculated temperatures. It is also important to note that a non-isotropic approach by assigning different thermal conductivity values in axial and radial directions has negligible effect on the results. Similar results are obtained for 0.5C and 1.5C discharge rates and consequently, it is found that an isotropic material approach in thermal modelling seems to be accurate enough for the regular discharge rates investigated in this study.

The relatively small effect of thermal conductivity values in the thermal behavior can be further investigated by considering both the convection and conduction heat transfer processes during a discharge. During a typical discharge, the average convection coefficient around the battery is numerically calculated and plotted along with the results of the well-known free convection empirical correlations proposed by Churchill and Morgan, as cited in Incropera et al. [63] in Fig. 5.3. Except the very early times of discharge, a good agreement is obtained especially with the correlation of Morgan. It is important to note that, the main reason of discrepancy at early times is due to different initial conditions, i.e., the battery or cylinder is assumed to be heated from the beginning of the process in the correlations whereas its temperature is the same as the environment temperature at the beginning in the numerical calculation as in the case of experiments.

In order to quantify the relative importance of the conduction heat transfer compared to the convective heat transfer the Biot number is also calculated. According to Fig. 5.4, Biot number is below 0.1 for all of the thermal conductivity values except for 0.3 W/mK. It means that majority of the suggested thermal conductivity values in the literature result in a nearly uniform temperature distribution inside the battery. As a result, while most of the thermal conductivity values give almost identical results, only values close to the lowest limit of the literature create a slightly different temperature

profile, still less than 2°C compared to the others, during a regular discharge. Therefore, the thermal conductivity value of 3 W/mK, a widely used value in the literature, is chosen as the nominal value for the simulations conducted in this study.

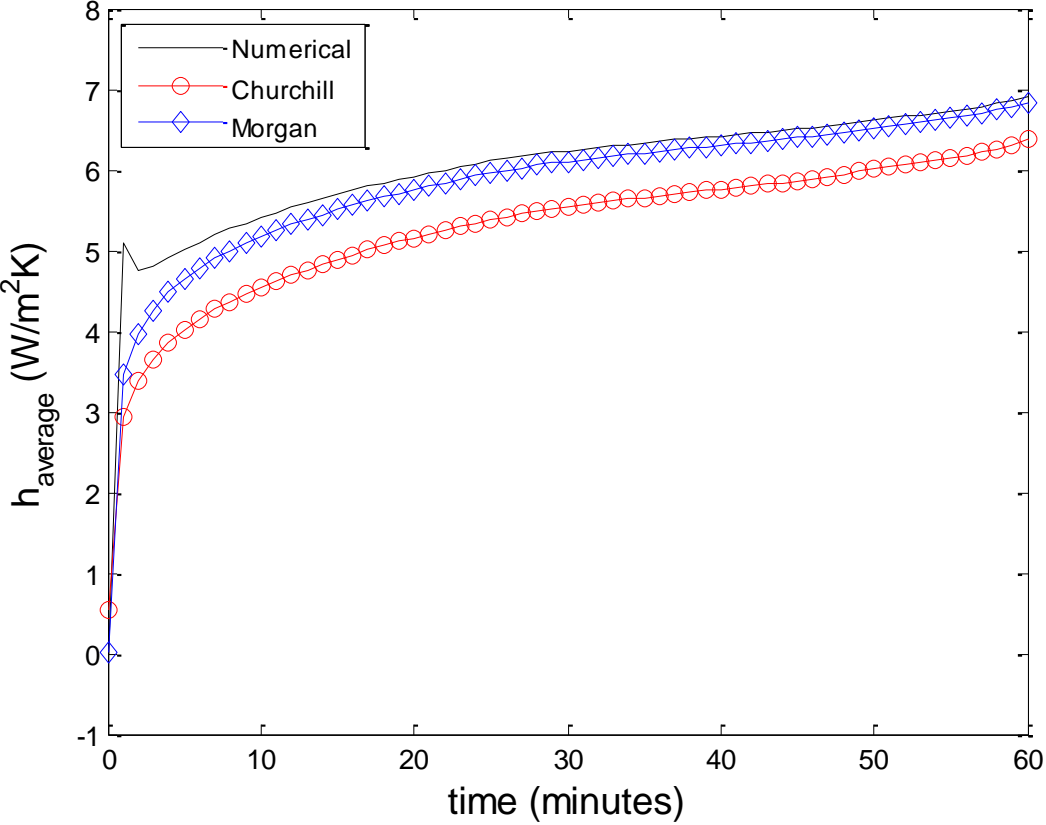


Figure 5.3: Variation of the calculated convection coefficient with time in comparison with correlations in the literature.  $k = 3 \text{ W/mK}$ ,  $c_p = 2400 \text{ J/kgK}$ , discharge rate = 1.0C.

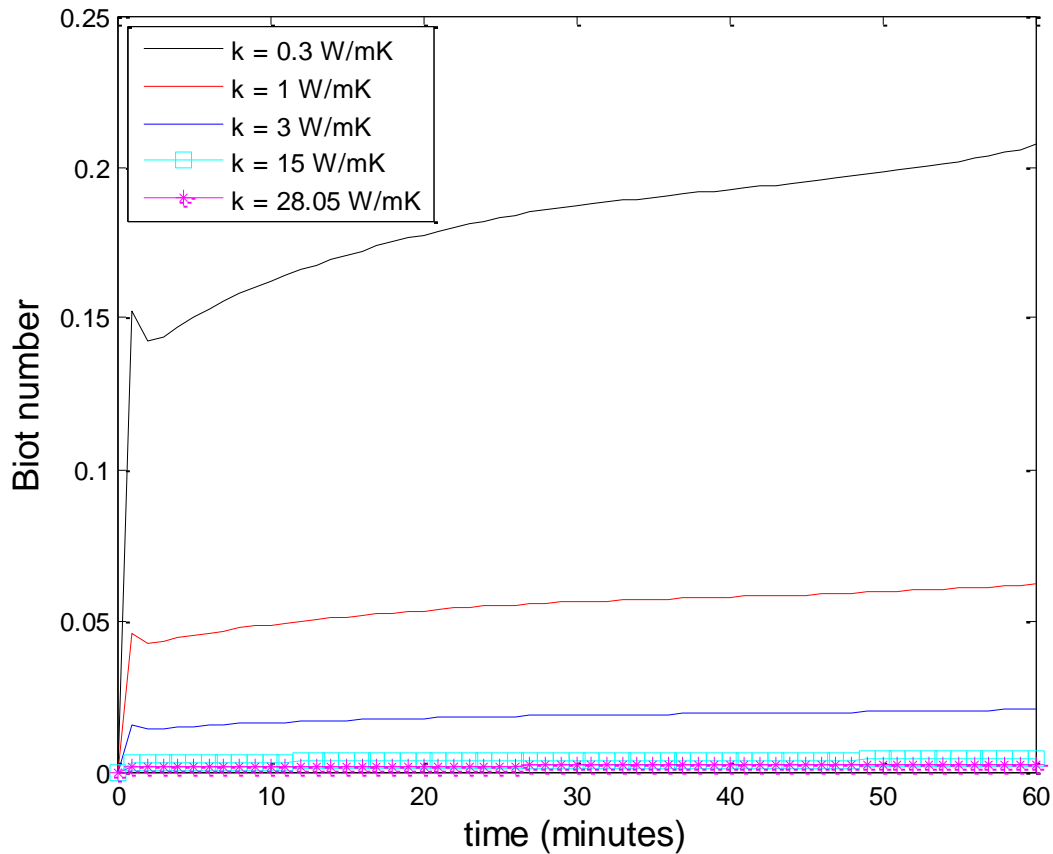


Figure 5.4: Variation of the Biot number with time for different thermal conductivities.  
 $c_p = 2400 \text{ J/kgK}$ , discharge rate = 1.0C.

## 5.2 Effect of Discharge Rate

Electrical response of a battery changes with a discharge rate as shown in Fig. 3.3 before. This variation in electrical response affects thermal behavior of the battery as well. Discharge rate affects both the irreversible and reversible heat generations, while the variation of the irreversible part constitutes a larger portion in magnitude and dominates the overall increase. As it is presented in Fig. 5.5, the irreversible heat generation increases with an increasing discharge rate, whereas the reversible one decreases. Heat generation values shown in Fig. 5.5 are consistent with studies of Al Hallaj et al. and Bandhauer et al. [21, 51]. UDFs developed for the model to calculate heat generation can be seen in Appendix C.

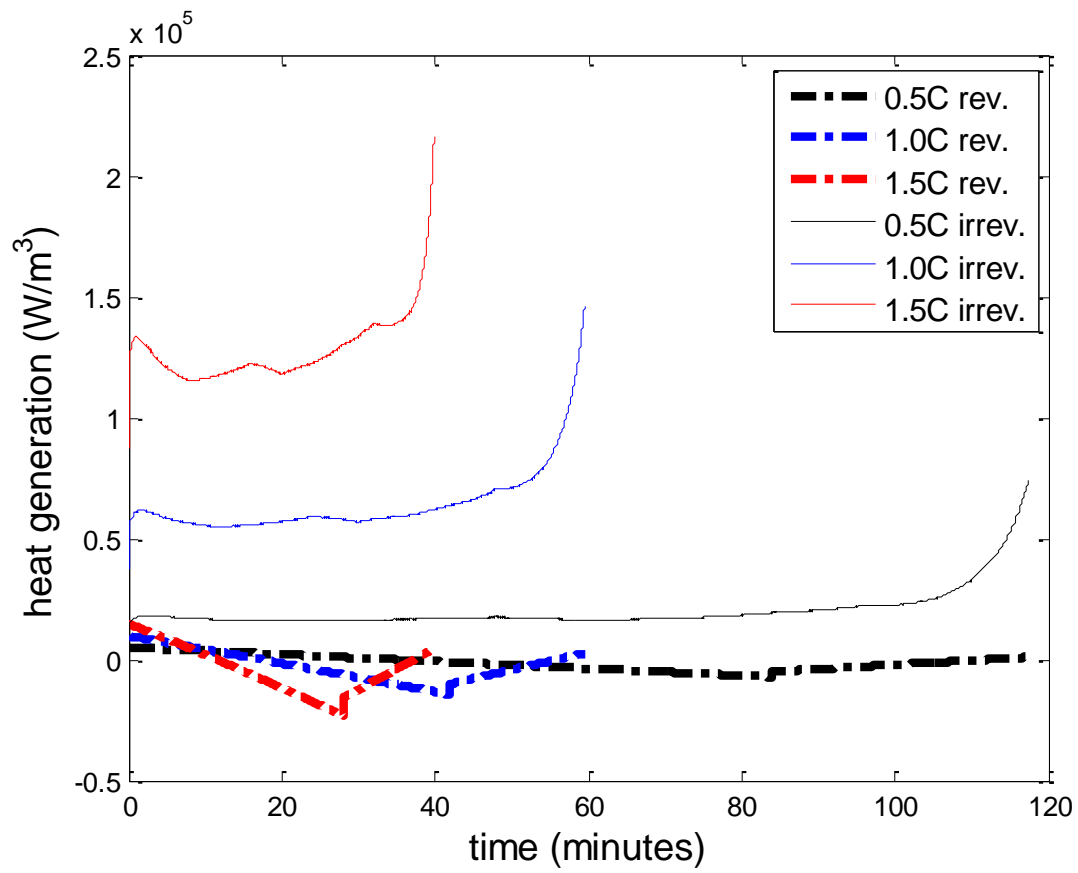


Figure 5.5: Variation of heat generation in the battery with time for different discharge rates.

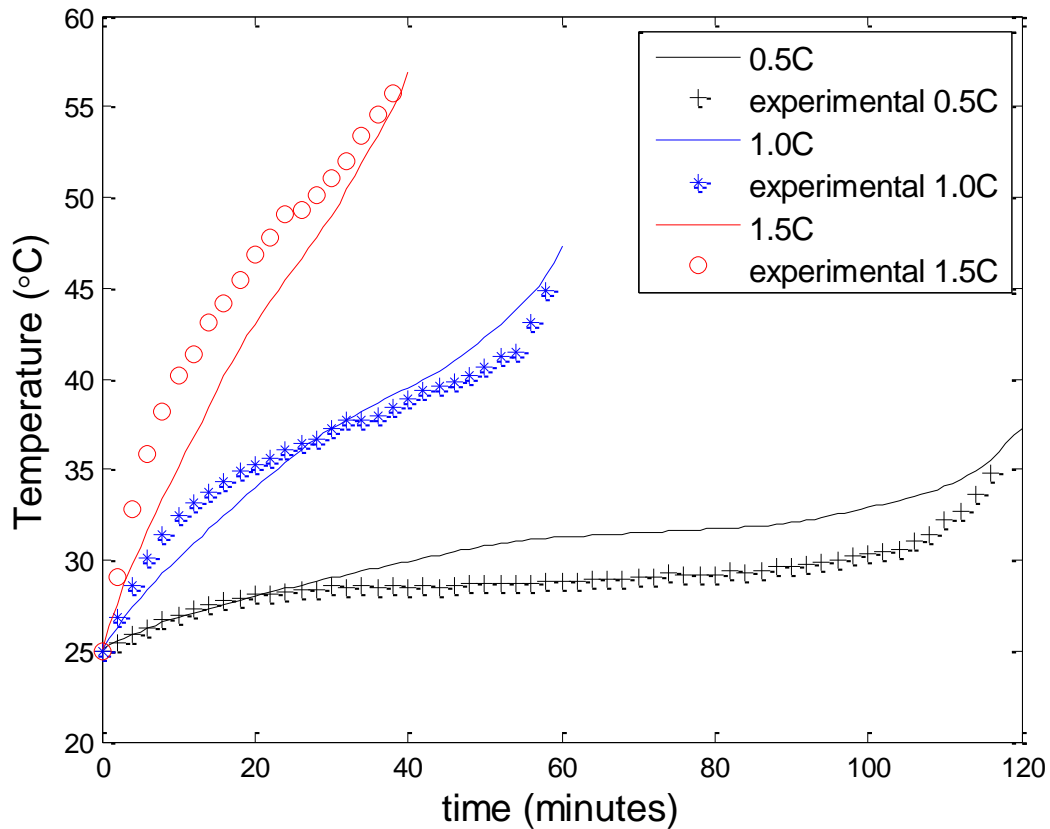


Figure 5.6: Variation of the surface temperature with time for different discharge rates.  
 $k = 3 \text{ W/mK}$ ,  $c_p = 2400 \text{ J/kgK}$ .

In Fig. 5.6, calculated transient surface temperature results for three different discharge rates are compared with the experimental results. Calculated and measured temperature profiles are consistent with the experimental results in the literature [21]. According to the experimental data and model results the surface temperature increases substantially with discharge rate. In addition to temperature increase, the tendency of the temperature profile also changes. At 0.5C discharge rate the temperature profile is nearly constant in most of the discharge process. Then the profile becomes steadily incremental at 1.0C discharge rate with a variable slope. In the case of 1.5C discharge rate, the temperature profile shows an almost linear increase. These experimental tendencies are well predicted and can be seen in



the model results for all of the three discharge rates. The maximum average error of the model results is obtained at 1.5C discharge rate as 3.0°C as presented in Table 5.1.

### **5.3 Effect of the Entropic Term**

As mentioned in earlier sections, the entropic term is used to calculate the reversible heat generation in the battery. On account of being a parameter requiring significant efforts to measure, the entropic term should be investigated to understand its effect on the process and on the reliability of the model. This is accomplished through employing four different approaches to model discharge test at 1.0C rate. The first approach uses piecewise linear equations to obtain an entropic term function with respect to DoD. The second approach mimics the main trend of the entropic term which increases before 0.7 DoD and then shows a decrease. Therefore, it employs two linear equations fitted to the experimental data set. The third approach considers the whole data set as a linear equation and the fourth approach assumes zero entropic term in the whole discharge process neglecting the reversible heat generation in the battery completely. These approximations are presented graphically in Fig. 5.7.

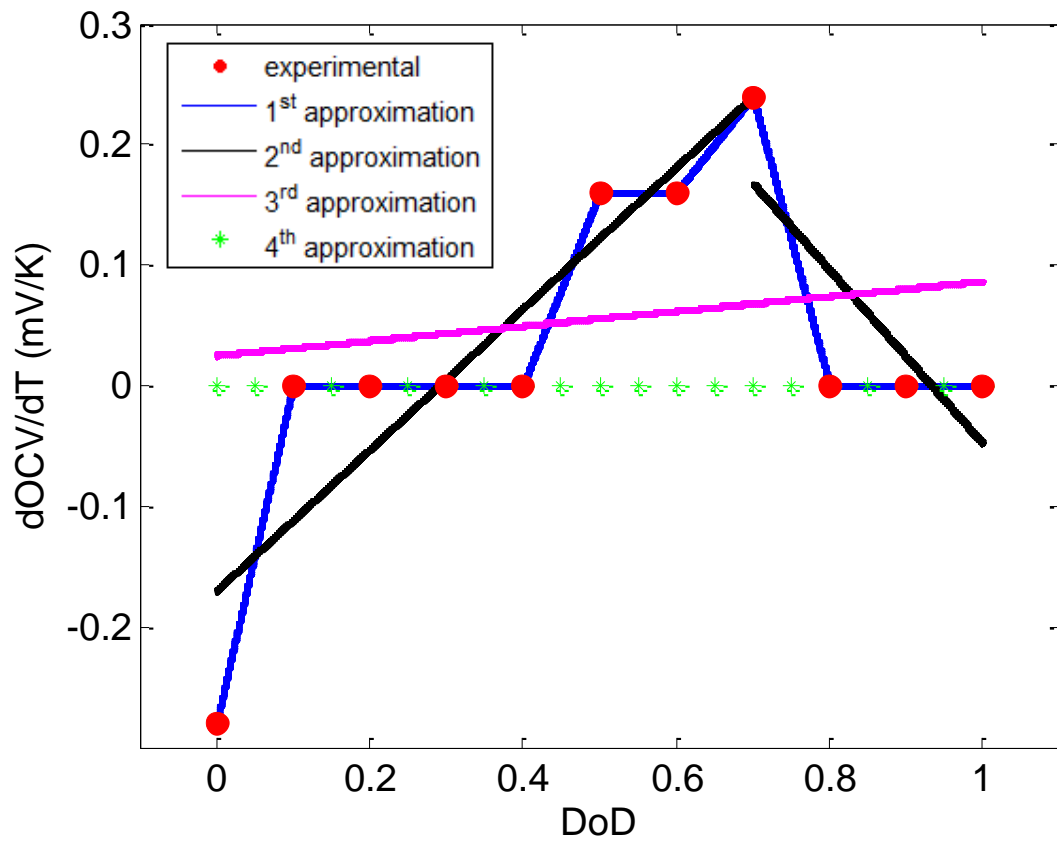


Figure 5.7: Various approximations for the entropic term.

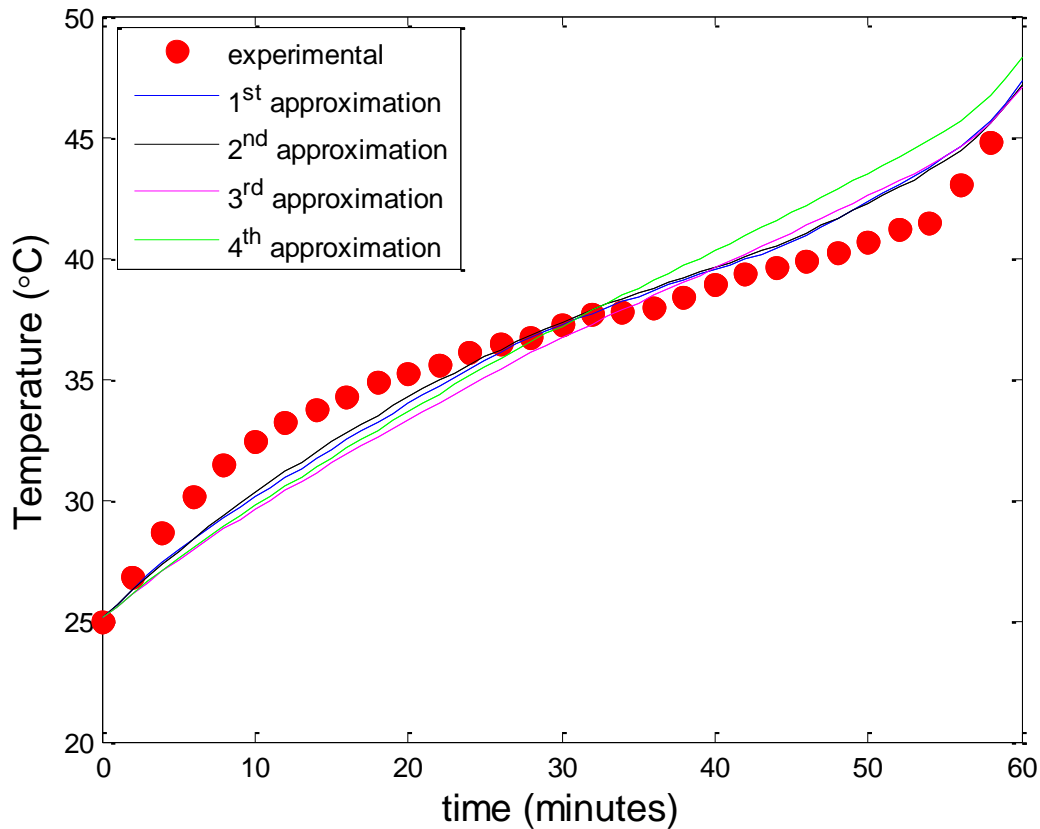


Figure 5.8: Variation of the surface temperature with time for different entropic term approximations.  $k=3 \text{ W/mK}$ ,  $c_p=2400 \text{ J/kgK}$ , discharge rate = 1.0C.

As seen in Fig. 5.8, the surface temperature can be accurately predicted with all of the four entropic term approaches. On the other hand, the difference between the case of zero entropic term, 4<sup>th</sup> approximation, and the others becomes more pronounced after 30 minutes.

The main conclusion drawn from these results is that the irreversible heat generation is the major parameter defining the battery temperature during discharge. Considering the tedious process of the entropic term measurement, using only the irreversible heat which can be calculated easily and precisely, one can have accurate results in terms of battery temperature variation.

#### 5.4 Effect of Usage History

As explained before, usage history or cycling is one of the two ways of battery ageing and during experimental studies it is noticed as an important parameter affecting both electrical performance and thermal behavior of the lithium ion batteries. In order to reveal the effects of usage, five different batteries, having various operational backgrounds depicted in Table 5.2, are used to discharge at 1.0C discharge rate. During these tests both electrical and thermal responses of these batteries are measured and corresponding temperature variations are shown in Fig. 5.9.

Table 5.2: Usage details of five different batteries

	<b>B1</b>	<b>B2</b>	<b>B3</b>	<b>B4</b>	<b>B5</b>
<b>Usage (Charge + Discharge)</b>	>36×2	29×2	10×2	3×2	2×2

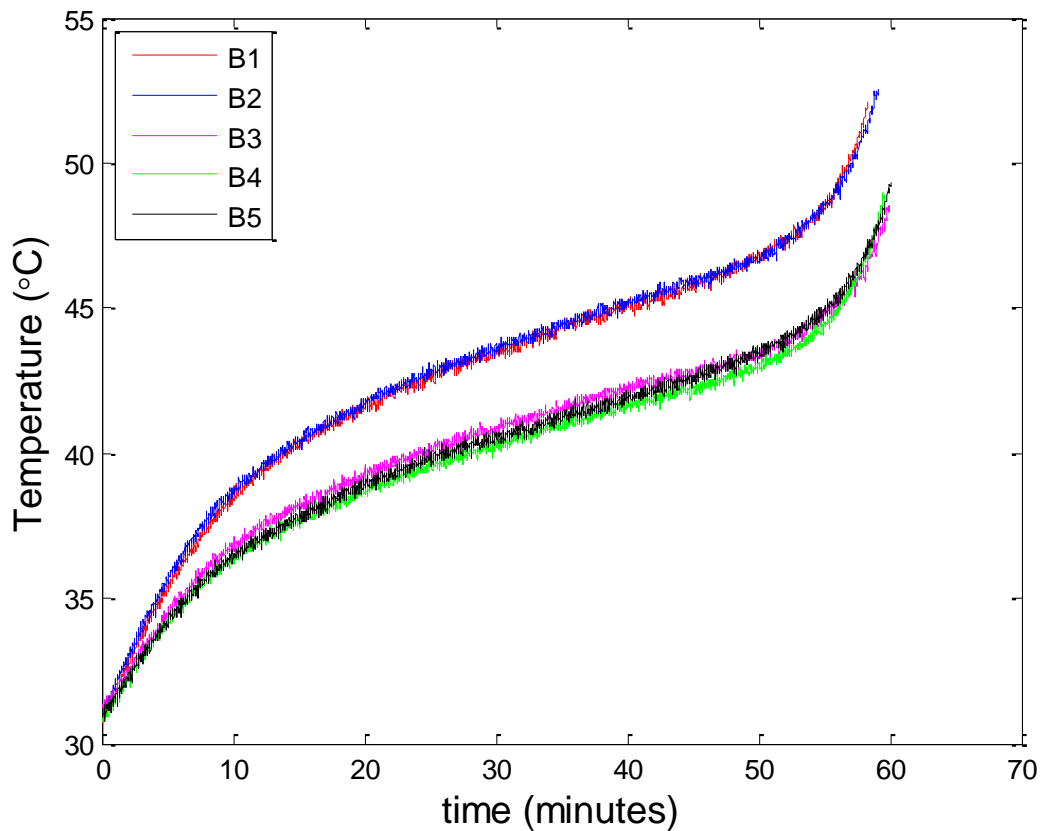


Figure 5.9: Variation of surface temperature with time using batteries of different usage history. Discharge rate = 1.0C.

Fig. 5.9 clearly shows that thermal responses of the batteries separate from each other depending on their operational backgrounds. Generally the more the battery is used, the higher temperature increase it demonstrates. The main difference occurs at the beginning of the discharge. Batteries which are used more face with faster temperature increase approximately during first 10 minutes, which can be deduced from the difference in the slopes. The remaining part of discharge has almost the same slope for all batteries.

The developed model was run to simulate temperature behaviors of a used and a new battery. As seen in Fig. 5.10, the model gives accurate results regardless of the battery usage history as long as the corresponding electrical data for each battery are provided to the model. UDF codes developed for the calculation of heat generation in the old battery can be seen in Appendix C.

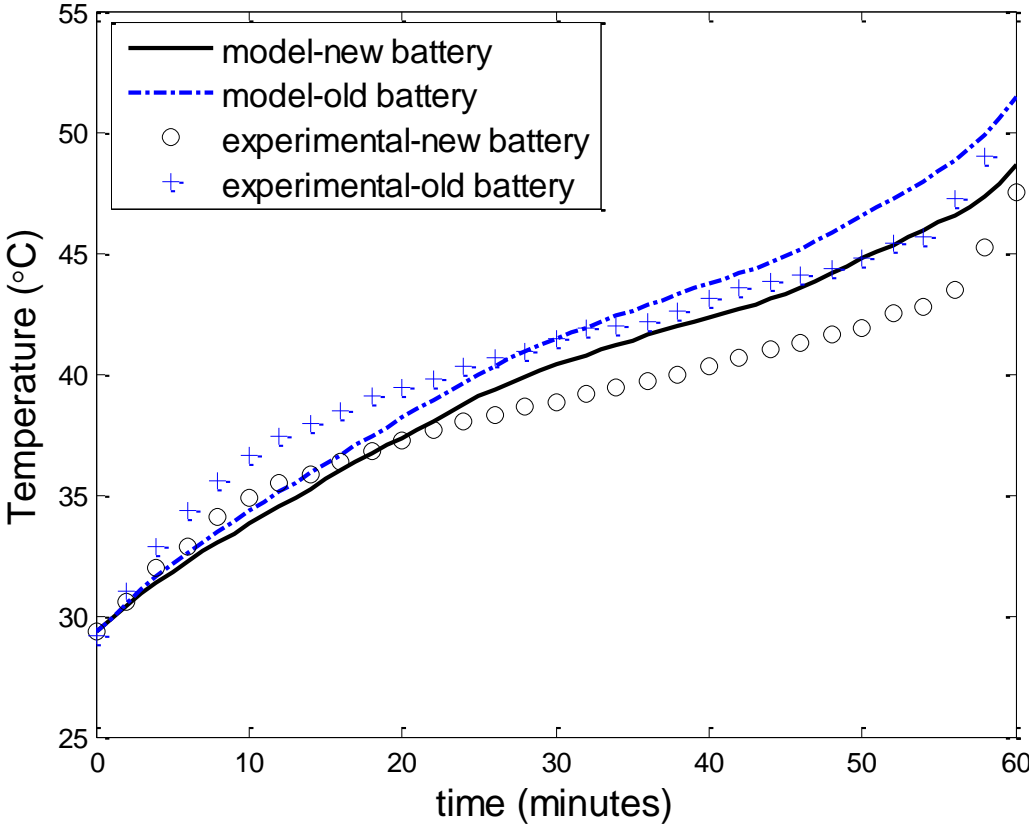
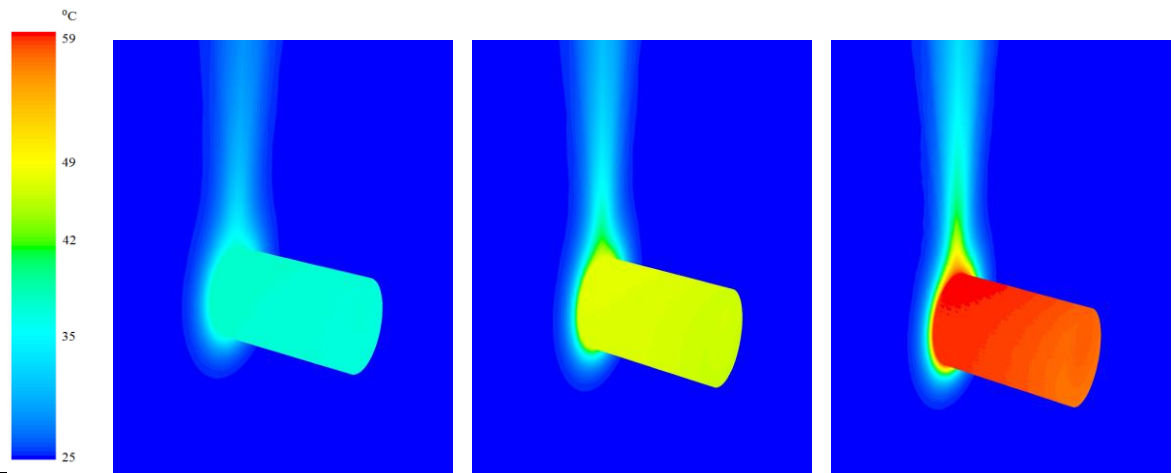


Figure 5.10: Model and experimental results for a new and old battery.  $k = 3 \text{ W/mK}$ ,  $C_p = 2400 \text{ J/kgK}$ , discharge rate = 1.0C.

## 5.5 Temperature Distribution and Velocity Profile at the End of the Discharge

a)



b)

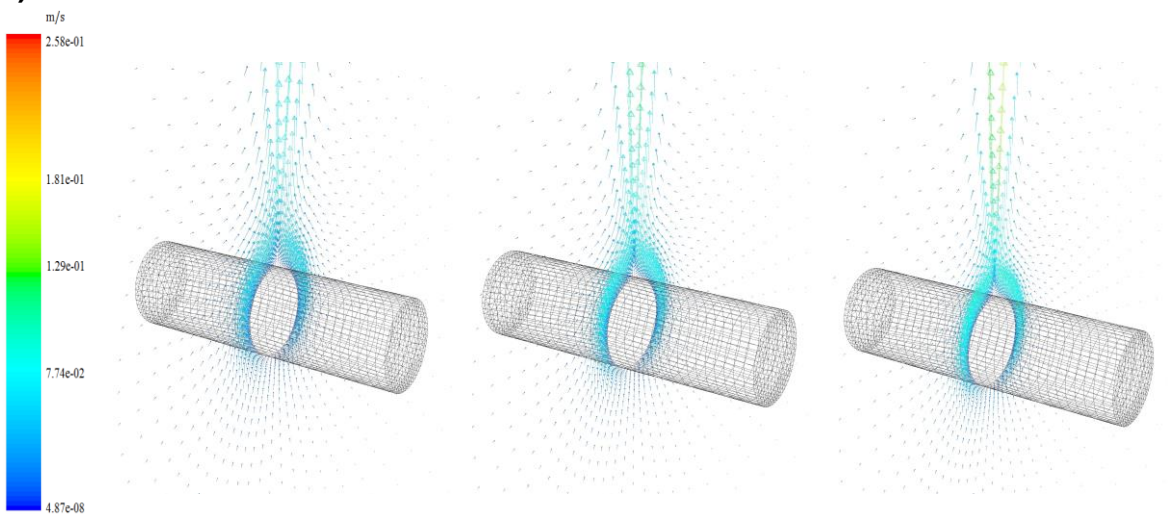


Figure 5.11: Temperature distribution ( $^{\circ}\text{C}$ ) and velocity profile (m/s) at the end of discharge.  $k = 3 \text{ W/mK}$ ,  $c_p = 2400 \text{ J/kgK}$ , 1.0C discharge rate. a) Temperature distribution b) Velocity Profile. For 0.5C, 1.0C and 1.5C discharge rates. (from left to right)

As seen in Fig. 5.11(a), temperature increase of the battery affects air temperature in the proximity of the surface. In addition, above the battery a thermal plume is observed at all discharge rates as a result of natural convection. As expected, the symmetry plane at the upper side of the battery has higher temperature compared to lower side and end points. Temperature distribution throughout the battery is nearly uniform; only small temperature differences occur in the battery, as seen in Table 5.3. At the lowest discharge rate temperature variations are lower due to smaller heat generation and longer discharge duration. Higher discharge rates cause higher temperature differences in the battery especially in axial direction. In radial direction, no variation in temperature difference is observed at 1.0C and 1.5C discharge rates. It can be argued that, temperature variation in radial direction reaches a stable condition at higher discharge rates but the difference in axial direction continues to increase.

In Fig. 5.11(b) velocity vectors are shown graphically. Flow velocities around the battery are low and symmetrical with respect to vertical axis of battery's cross section as expected. At 1.5C discharge rate, the highest velocity is observed due to the highest temperature increase but the difference in velocity values between discharge rates is not significant.

Table 5.3: Maximum temperature variation in the battery at the end of the discharge

$\Delta T_{\max}$ Discharge rates	Radial Direction (°C)	Axial Direction (°C)
0.5C	0.2	0.5
1.0C	0.5	1.1
1.5C	0.5	2.0



## CHAPTER 6

### CONCLUSIONS AND RECOMMENDATIONS FOR FUTURE WORK

#### 6.1 Conclusions

Supply and utilization of clean and safe energy is one of the most important problems of 21<sup>st</sup> century affecting our lives and civilization. New methods of energy generation are being continuously investigated and storage of the energy becomes more critical, especially when one of the most prominent methods of the future energy production strategy, renewable energy is considered [5, 64]. Fluctuations and unpredictable nature of the renewable energy can be tolerated only with an appropriate storage capability [5, 9]. In this respect, batteries are considered to have the potential to address the storage problem of the renewable energy [64].

In addition to energy back up, such a capability gained with efficient battery systems may provide cleaner transportation replacing internal combustion engines [5], because energy storage is also the main obstacle ahead of the full electric transportation [7].

Among all other battery technologies, Li-Ion batteries are one of the most potent battery types [7]. Their high energy and power densities make them ideal to power high performance machines and devices [1]. However, safety is a substantial problem impeding widespread usage of these batteries [3]. Safety issues of these batteries are generally related to their thermal behavior [3, 4]. Therefore, in order to solve the safety problem, thermal behavior of these batteries must be well understood and modeled.

In the thesis, modeling and experimental studies were conducted to investigate thermal behavior of Li-Ion batteries. A 3D CFD model was developed to predict the

temperature variation of a Li-ion battery subjected to natural convection during discharge using electrical performance data of the battery.

Selection of the computational tool was based on a detailed investigation in which a commercial software ANSYS Fluent 14.5 and an open source software OpenFOAM 2.3.0 were analyzed with respect to their suitability for the thesis. During this investigation, ANSYS Fluent was observed as a more advantageous tool regarding its simpler geometry and mesh design elements as well as its faster solution time for the flow problem studied in the thesis. Consequently, although OpenFOAM has an advantage of open source structure, ANSYS Fluent was preferred as the computational tool of the study.

The developed model solves both the conduction heat transfer in the battery and convection heat transfer between the battery surface and the surrounding medium along with the fluid flow around the battery. Comparison of the model results with the in-house experimental data shows that the model can predict the battery temperature with an average error of 2<sup>o</sup>C considering all of the three discharge rates (0.5C, 1.0C, 1.5C) tested in this work.

The model was employed to investigate the effects of the thermophysical properties of the battery on the computational solution. A wide range of specific heat values were tested and results showed that it was a major parameter affecting battery temperature. Therefore, an accurate prediction of battery temperature requires the usage of the correct value of specific heat in the simulations. On the other hand, thermal conductivity was found to have a minor impact on the results. Furthermore, no considerable difference was obtained in the results of isotropic and anisotropic battery models.

The heat generation in the battery was modeled using the equation proposed by Bernardi et al. [15], which is comprised of irreversible (Joule heating) and reversible (entropic) terms. The Entropic term is the most intractable parameter for the calculation of the heat generation. The entropic term was calculated based on experimental OCV measurements and it was shown that battery temperature can be successfully predicted by only taking the irreversible term into account in the calculation of the heat generation. The entropic term slightly affects the time evolution of the temperature only during a limited part of the discharge process.

## **6.2 Recommendations for Future Work**

Based on the results of the thesis, research about Li-Ion batteries can be further expanded. Thermal behavior of Li-Ion batteries in various packaging options can be studied using the same modeling approach developed in this thesis. On the other hand, battery operations can be analyzed under different and adverse environmental conditions, such as cold or hot environments close to the operational limits of the battery. Effect of the battery orientation on its thermal behavior and modeling can also be studied simply by investigating a battery standing vertically.

Another area of study in the future could be modeling of these batteries in high performance demanding applications including variable load patterns, such as electric vehicles etc. Thermal behavior of these batteries under such kinds of conditions can be investigated by further developing the current model and experimental procedures.

Battery chemistry is an ongoing concern substantially affecting thermal behavior of the battery. Regarding that, different battery chemistries can be tested under similar conditions and the comprehension about battery chemistries could be enhanced.

Finally, thermal abuse of these batteries and modeling the abuse conditions will be an important challenge for the future. The thesis can also be a stepping stone for future investigations related to thermal abuse studies.

## References

- [1] Chen, S. C., Wan, C. C., and Wang, Y. Y., Thermal analysis of lithium-ion batteries, *Journal of Power Sources*, 140, 111–124, **2005**.
- [2] Wu, S.-L. *et al.*, High Rate Capability of Li(Ni $\frac{1}{3}$ Mn $\frac{1}{3}$ Co $\frac{1}{3}$ )O $_2$  Electrode for Li-Ion Batteries, *Journal of The Electrochemical Society*, 159, A438, **2012**.
- [3] Bandhauer, T. M., Garimella, S., and Fuller, T. F., A Critical Review of Thermal Issues in Lithium-Ion Batteries, *Journal of The Electrochemical Society*, 158, R1, **2011**.
- [4] Doughty, D. and Roth, E. P., A general discussion of Li Ion battery safety, *Electrochemical Society Interface*, 21, 37–44, **2012**.
- [5] Thackeray, M. M., Wolverton, C., and Isaacs, E. D., Electrical energy storage for transportation—approaching the limits of, and going beyond, lithium-ion batteries, *Energy & Environmental Science*, 5, 7854, **2012**.
- [6] Zhu, C., Li, X., Song, L., and Xiang, L., Development of a theoretically based thermal model for lithium ion battery pack, *Journal of Power Sources*, 223, 155–164, **2013**.
- [7] Wang, Q., Jiang, B., Li, B., and Yan, Y., A critical review of thermal management models and solutions of lithium-ion batteries for the development of pure electric vehicles, *Renewable and Sustainable Energy Reviews*, 64, 106–128, **2016**.
- [8] Miller, P., Automotive Lithium-ion Batteries, *Johnson Matthey Technol. Rev.*, 59, 4–13, **2015**.
- [9] Etacheri, V., Marom, R., Elazari, R., Salitra, G., and Aurbach, D., Challenges in the development of advanced Li-ion batteries: a review, *Energy & Environmental Science*, 3243–3262, **2011**.
- [10] Tarascon, J. M. and Armand, M., Issues and challenges facing rechargeable lithium batteries., *Nature*, 414, 359–67, **2001**.
- [11] Karimi, G. and Li, X., Thermal management of lithium-ion batteries for electric vehicles, *International Journal of Energy Research*, **2013**.
- [12] Mohammadian, S. K. and Zhang, Y., Thermal management optimization of an air-cooled Li-ion battery module using pin-fin heat sinks for hybrid electric vehicles, *Journal of Power Sources*, 273, 431–439, **2015**.
- [13] Panasonic, Lithium Ion Batteries Overview, <https://industrial.panasonic.com/cdbs/www-data/pdf/ACA4000/ACA4000PE3.pdf>. (October, **2015**).
- [14] Drake, S. J. *et al.*, Heat generation rate measurement in a Li-ion cell at large C-rates through temperature and heat flux measurements, *Journal of Power Sources*, 285, 266–273, **2015**.

- [15] Bernardi, D., Pawlikowski, E., and Newman, J., A General Energy Balance for Battery Systems, *Journal of The Electrochemical Society*, 132, 5, **1985**.
- [16] Yayathi, S., Walker, W., Doughty, D., and Ardebili, H., Energy distributions exhibited during thermal runaway of commercial lithium ion batteries used for human spaceflight applications, *Journal of Power Sources*, 329, 197–206, **2016**.
- [17] Finegan, D. P. *et al.*, Power failure, *TCE The Chemical Engineer*, 6, 23, **2015**.
- [18] Barré, A., Deguilhem, B., Grolleau, S., Gérard, M., Suard, F., and Riu, D., A review on lithium-ion battery ageing mechanisms and estimations for automotive applications, *Journal of Power Sources*, 241, 680–689, **2013**.
- [19] Vetter, J. *et al.*, Ageing mechanisms in lithium-ion batteries, *Journal of Power Sources*, 147, 269–281, **2005**.
- [20] Broussely, M. *et al.*, Main aging mechanisms in Li ion batteries, *Journal of Power Sources*, 146, 90–96, **2005**.
- [21] Al Hallaj, S., Maleki, H., Hong, J. S., and Selman, J. R., Thermal modeling and design considerations of lithium-ion batteries, *Journal of Power Sources*, 83, 1–8, **1999**.
- [22] Chen, Y. and Evans, J. W., Heat transfer phenomena in lithium/polymer-electrolyte batteries for electric vehicle application, *Journal of the Electrochemical Society*, 140, 1833–1838, **1993**.
- [23] Chen, Y. and Evans, J. W., Thermal analysis of lithium polymer electrolyte batteries by a two dimensional model—thermal behaviour and design optimization, *Electrochimica Acta*, 39, 517–526, **1994**.
- [24] Chen, Y. and Evans, J. W., Thermal Analysis of Lithium-Ion Batteries, *Journal of The Electrochemical Society*, 143, 2708, **1996**.
- [25] Chen, Y. and Evans, J. W., Three-Dimensional Thermal Modeling of Lithium-Polymer Batteries under Galvanostatic Discharge and Dynamic Power Profile, *Journal of The Electrochemical Society*, 141, 2947, **1994**.
- [26] Evans, T. I. and White, R. E., A Thermal Analysis of a Spirally Wound Battery Using a Simple Mathematical Model, *Journal of The Electrochemical Society*, 136, 2145, **1989**.
- [27] Sabbah, R., Kizilel, R., Selman, J. R., and Al-Hallaj, S., Active (air-cooled) vs. passive (phase change material) thermal management of high power lithium-ion packs: Limitation of temperature rise and uniformity of temperature distribution, *Journal of Power Sources*, 182, 630–638, **2008**.
- [28] Mills, A. and Al-Hallaj, S., Simulation of passive thermal management system for lithium-ion battery packs, *Journal of Power Sources*, 141, 307–315, **2005**.
- [29] Khateeb, S. A., Farid, M. M., Selman, J. R., and Al-Hallaj, S., Design and simulation of a lithium-ion battery with a phase change material thermal management system for an electric scooter, *Journal of Power Sources*, 128, 292–307, **2004**.

- [30] Kizilel, R., Sabbah, R., Selman, J. R., and Al-Hallaj, S., An alternative cooling system to enhance the safety of Li-ion battery packs, *Journal of Power Sources*, 194, 1105–1112, **2009**.
- [31] Newman, J. and Tiedemann, W., Temperature Rise in a Battery Module with Constant Heat Generation, *Journal of The Electrochemical Society*, 142, 1054–1057, **1995**.
- [32] Li, X., He, F., and Ma, L., Thermal management of cylindrical batteries investigated using wind tunnel testing and computational fluid dynamics simulation, *Journal of Power Sources*, 238, 395–402, **2013**.
- [33] Mahamud, R. and Park, C., Reciprocating air flow for Li-ion battery thermal management to improve temperature uniformity, *Journal of Power Sources*, 196, 5685–5696, **2011**.
- [34] Sun, H., Wang, X., Tossan, B., and Dixon, R., Three-dimensional thermal modeling of a lithium-ion battery pack, *Journal of Power Sources*, 206, 349–356, **2012**.
- [35] Chen, D., Jiang, J., Kim, G. H., Yang, C., and Pesaran, A., Comparison of different cooling methods for lithium ion battery cells, *Applied Thermal Engineering*, 94, 846–854, **2016**.
- [36] Moraga, N. O., Xaman, J. P., and Araya, R. H., Cooling Li-ion batteries of racing solar car by using multiple phase change materials, *Applied Thermal Engineering*, 108, 1041–1054, **2016**.
- [37] Wang, T., Tseng, K. J., and Zhao, J., Development of efficient air-cooling strategies for lithium-ion battery module based on empirical heat source model, *Applied Thermal Engineering*, 90, 521–529, **2015**.
- [38] Tran, T. H., Harmand, S., Desmet, B., and Filangi, S., Experimental investigation on the feasibility of heat pipe cooling for HEV/EV lithium-ion battery, *Applied Thermal Engineering*, 63, 551–558, **2014**.
- [39] Martin, L., Gastelurrutia, J., Nieto, N., Ramos, J. C., Rivas, A., and Gil, I., Modeling based on design of thermal management systems for vertical elevation applications powered by lithium-ion batteries, *Applied Thermal Engineering*, 102, 1081–1094, **2016**.
- [40] Javani, N., Dincer, I., Naterer, G. F., and Rohrauer, G. L., Modeling of passive thermal management for electric vehicle battery packs with PCM between cells, *Applied Thermal Engineering*, 73, 305–314, **2014**.
- [41] Lan, C., Xu, J., Qiao, Y., and Ma, Y., Thermal management for high power lithium-ion battery by minichannel aluminum tubes, *Applied Thermal Engineering*, 101, 284–292, **2016**.
- [42] Zhao, J., Rao, Z., Huo, Y., Liu, X., and Li, Y., Thermal management of cylindrical power battery module for extending the life of new energy electric vehicles, *Applied Thermal Engineering*, 85, 33–43, **2015**.
- [43] Botte, G. G., Johnson, B. A., and White, R. E., Influence of Some Design

- Variables on the Thermal Behavior of a Lithium-Ion Cell, *Journal of The Electrochemical Society*, 146, 914, **1999**.
- [44] Basu, S., Hariharan, K. S., Kolake, S. M., Song, T., Sohn, D. K., and Yeo, T., Coupled electrochemical thermal modelling of a novel Li-ion battery pack thermal management system, *Applied Energy*, 181, 1–13, **2016**.
- [45] Pals, C. R. and Newman, J., Thermal Modeling of the Lithium / Polymer Battery - II. Temperature profiles in cell stack, *Journal of The Electrochemical Society*, 142, 3282–3288, **1995**.
- [46] Tong, W., Somasundaram, K., Birgersson, E., Mujumdar, A. S., and Yap, C., Thermo-electrochemical model for forced convection air cooling of a lithium-ion battery module, *Applied Thermal Engineering*, 99, 672–682, **2016**.
- [47] Newman, J. S., *Electrochemical Systems*, 2nd ed. Prentice Hall, Inc: New jersey, **1991**.
- [48] Jeon, D. H. and Baek, S. M., Thermal modeling of cylindrical lithium ion battery during discharge cycle, *Energy Conversion and Management*, 52, 2973–2981, **2011**.
- [49] Shadman Rad, M., Danilov, D. L., Baghalha, M., Kazemeini, M., and Notten, P. H. L., Adaptive thermal modeling of Li-ion batteries, *Electrochimica Acta*, 102, 183–195, **2013**.
- [50] Wang, Y., Peng, C., and Zhang, W., Thermal analysis of multifunctional structural battery for satellite applications, *Applied Thermal Engineering*, 78, 209–216, **2015**.
- [51] Bandhauer, T. M., Garimella, S., and Fuller, T. F., Temperature-dependent electrochemical heat generation in a commercial lithium-ion battery, *Journal of Power Sources*, 247, 618–628, **2014**.
- [52] Hallaj, S. Al, Prakash, J., and Selman, J. R., Characterization of commercial Li-ion batteries using electrochemical – calorimetric measurements, *Journal of Power Sources*, 186–194, **2000**.
- [53] Zhang, S. S., The effect of the charging protocol on the cycle life of a Li-ion battery, *Journal of Power Sources*, 161, 1385–1391, **2006**.
- [54] Lu, L., Han, X., Li, J., Hua, J., and Ouyang, M., A review on the key issues for lithium-ion battery management in electric vehicles, *Journal of Power Sources*, 226, 272–288, **2013**.
- [55] Arora, P., White, R. E., and Doyle, M., Capacity Fade Mechanisms and Side Reactions in Lithium-Ion Batteries, *Journal of The Electrochemical Society*, 145, 3647, **1998**.
- [56] Liu, Y. H., Hsieh, C. H., and Luo, Y. F., Search for an optimal five-step charging pattern for li-ion batteries using consecutive orthogonal arrays, *IEEE Transactions on Energy Conversion*, 26, 654–661, **2011**.
- [57] Panasonic, NCR18650B Type Lithium Ion Battery Data Sheet, 2012, <http://na.industrial.panasonic.com/products/batteries/rechargeable->

batteries/lithium-ion/series/cylindrical-series/CS474/model/NCR18650B.  
(October, **2015**).

- [58] Hong, J.-S., Maleki, H., Hallaj, S. Al, Redey, L., and Selman, J. R., Electrochemical-Calorimetric Studies of Lithium-Ion Cells, *Journal of The Electrochemical Society*, 145, 1489, **1998**.
- [59] Barsoukov, E., Jang, J. H., and Lee, H., Thermal impedance spectroscopy for Li-ion batteries using heat-pulse response analysis, *Journal of Power Sources*, 109, 313–320, **2002**.
- [60] Maleki, H., Al Hallaj, S., Selman, J. R., Dinwiddie, R. B., and Wang, H., Thermal Properties of Lithium-Ion Battery and Components, *Journal of The Electrochemical Society*, 146, 947–954, **1999**.
- [61] Chen, S.-C., Wang, Y.-Y., and Wan, C.-C., Thermal Analysis of Spirally Wound Lithium Batteries, *Journal of The Electrochemical Society*, 153, A637–A648, **2006**.
- [62] Spinner, N. S., Mazurick, R., Brandon, A., Rose-Pehrsson, S. L., and Tuttle, S. G., Analytical, Numerical and Experimental Determination of Thermophysical Properties of Commercial 18650 LiCoO<sub>2</sub> Lithium-Ion Battery, *Journal of The Electrochemical Society*, 162, A2789–A2795, **2015**.
- [63] Incropera, F. P., Dewitt, D. P., Bergman, T. L., and Lavine, A. S., *Principles of Heat and Mass Transfer*, 7th ed. John Wiley and Sons, **2013**.
- [64] Dunn, B., Kamath, H., and Tarascon, J.-M., Electrical Energy Storage for the Grid: A Battery of Choices, *Science*, 334, 928–935, **2011**.



# APPENDIX A

## Panasonic General Overview about Li-Ion Batteries

**Panasonic**

### Overview

\*A Lithium ion battery must include a safety unit(SU). Also for safety reasons cells are not sold individually.

Dedicated to support various types of mobile equipment with its high-energy density

## Lithium Ion Batteries



### ■ Overview

The battery is a rechargeable battery best suited to mobile devices that require small-size, light weight and high performance. Its characteristics of high energy and high voltage (3.6V) powerfully fulfill these three key requirements. Its standard battery-pack, coupled with a charger, facilitates simple equipment design.

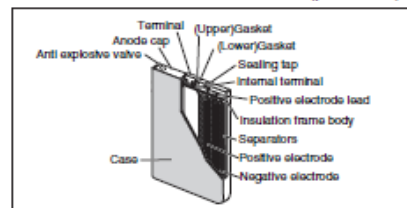
### ■ Characteristics

1. Less self-discharge (approx. 1/10) compared with a Ni-MH or Ni-Cd batteries as well as no memory effect.
2. A newly developed NNP\* series is achieving both high capacity & safety by the use of new positive electrode & high reliable technology by the present charging system (4.2V)  
\* NNP = Nickel oxide based New Platform
3. The PSS\* series adopts nickel and the manganese in new positive electrode.  
The safety of a battery to heat improved further.  
\* PSS = Panasonic Solid Solution

### ■ Structure

A lithium-ion rechargeable battery consists of a spiral structure with 4 layers. A positive electrode activated by cobalt acid lithium, a negative electrode activated by special carbon, and separator are put together in a whirl pattern and stored in the case. It also incorporates a variety of safety protection systems such as a gas discharge valve which helps prevent the battery from exploding by releasing internal gas pressure if it exceeds the design limit.

Structure of Lithium Ion Batteries (prismatic)



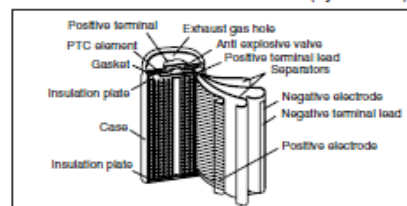
### ■ Safety

Our lithium ion batteries have acquired UL1642. Contact us for further details.

### ■ Applications

Cellular phone, Note PC etc.  
DVC/DSC/DVD/Portable LCD TV etc.  
Portable CD player, MD player, Semiconductor-driven audio etc.

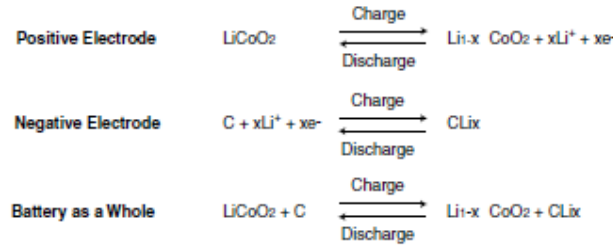
Structure of Lithium Ion Batteries (cylindrical)



• **Battery Reaction**

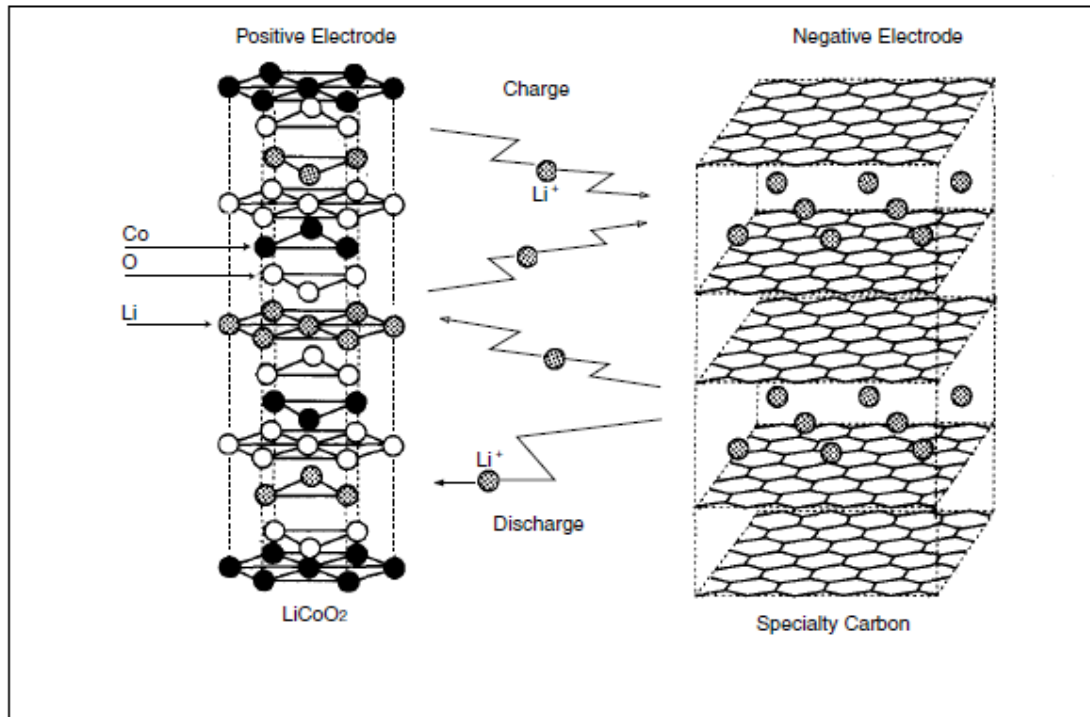
The lithium ion battery makes use of lithium cobalt oxide (which has superior cycling properties at high voltages) as the positive electrode and a highly-crystallized specialty carbon as the negative electrode. It uses an organic solvent, optimized for the specialty carbon, as the electrolytic fluid.

The chemical reactions for charge and discharge are as shown below:



The principle behind the chemical reaction in the lithium ion battery is one where the lithium in the positive electrode lithium cobalt oxide material is ionized during charge, and moves from layer to layer in the negative electrode. During discharge, the ions move to the positive electrode and return to the original compound.

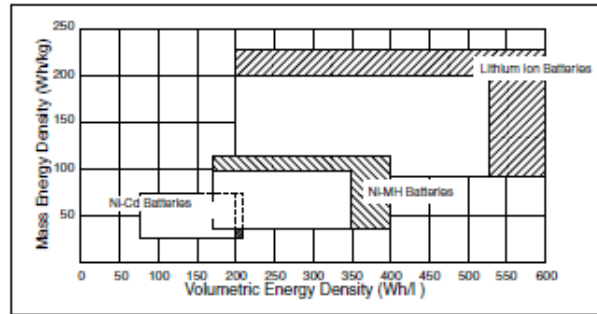
**Schematic Diagram of the Chemical Reaction of the Lithium Ion Battery**



Features

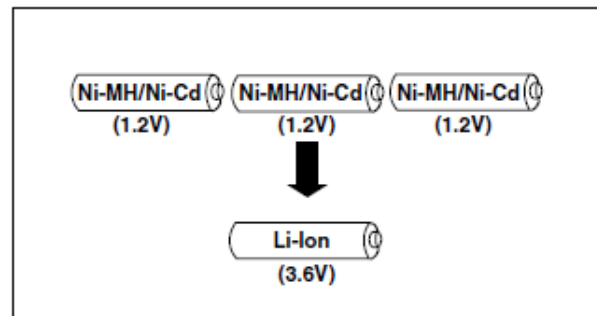
• High Energy Density

Because the lithium ion batteries are high voltage/light weight batteries, they boast a higher energy density than nickel metal hydride (Ni-MH) batteries or nickel cadmium (Ni-Cd) batteries.



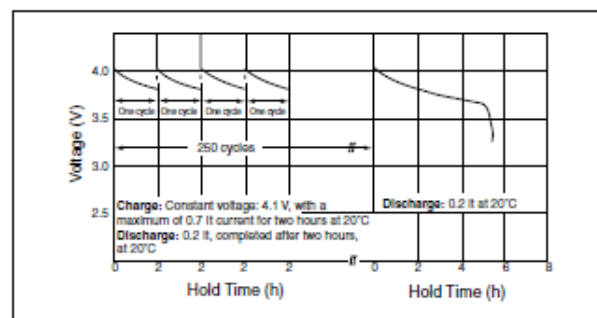
• High Voltage

Lithium ion batteries produce 3.6 volts, approximately three times the voltage of Ni-MH batteries or Ni-Cd batteries. This will make it possible to make smaller, lighter equipment.



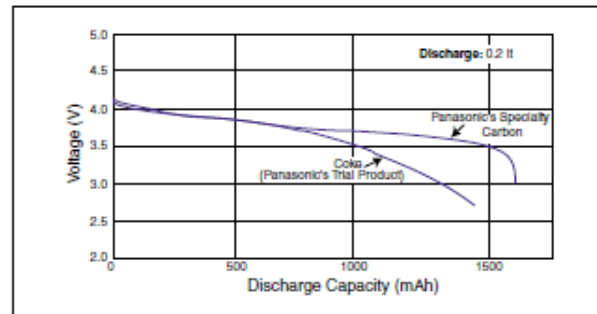
• No Memory Effect

Lithium ion batteries have none of the memory effects seen in Ni-Cd batteries ("memory effect" refers to the phenomenon where the apparent discharge capacity of a battery is reduced when it is repetitively discharged incompletely and then recharged).



• Flat Discharge Voltage

The use of the specialty carbon creates an extremely flat discharge voltage profile, allowing the production of stable power throughout the discharge period of the battery.



\*The data in this document are for descriptive purposes only and are not intended to make or imply any guarantee or warranty.

# APPENDIX B

## Panasonic Specification Sheet for NCR18650B Type Battery

# Panasonic

# Lithium Ion NCR18650B

### Features & Benefits

- High energy density
- Long stable power and long run time
- Ideal for notebook PCs, boosters, portable devices, etc.

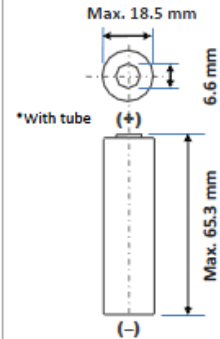
### Specifications

Rated capacity <sup>(1)</sup>	Min. 3200mAh
Capacity <sup>(2)</sup>	Min. 3250mAh Typ. 3350mAh
Nominal voltage	3.6V
Charging	CC-CV, Std. 1625mA, 4.20V, 4.0 hrs
Weight (max.)	48.5 g
Temperature	Charge*: 0 to +45°C Discharge: -20 to +60°C Storage: -20 to +50°C
Energy density <sup>(3)</sup>	Volumetric: 676 Wh/l Gravimetric: 243 Wh/kg

\* At temperatures below 10°C, charge at a 0.25C rate.

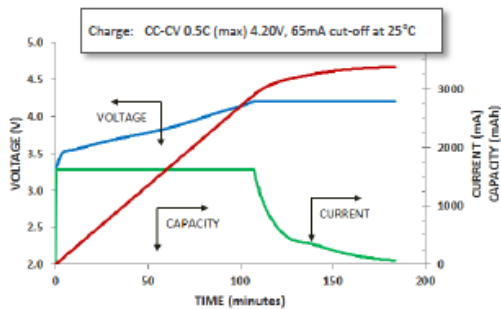
<sup>(1)</sup> At 20°C <sup>(2)</sup> At 25°C <sup>(3)</sup> Energy density based on bare cell dimensions

### Dimensions

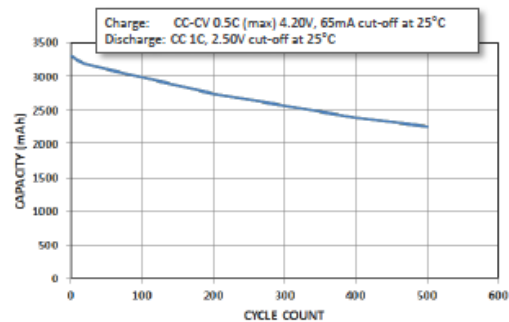


For Reference Only

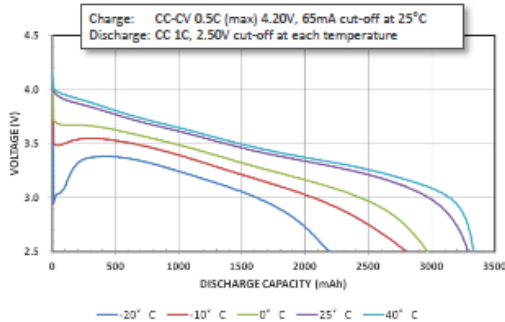
### Charge Characteristics



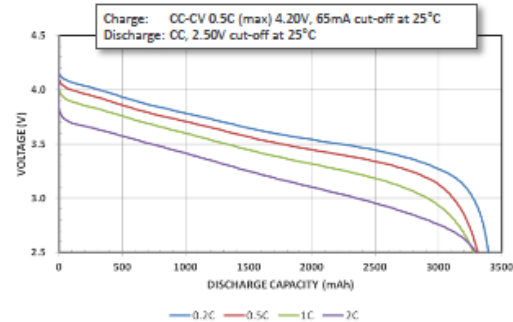
### Cycle Life Characteristics



### Discharge Characteristics (by temperature)



### Discharge Characteristics (by rate of discharge)



The data in this document is for descriptive purposes only and is not intended to make or imply any guarantee or warranty.

For more information on how Panasonic can assist you with your battery power solution needs, visit us at [www.panasonic.com/industrial/batteries-oem](http://www.panasonic.com/industrial/batteries-oem), e-mail [secsales@us.panasonic.com](mailto:secsales@us.panasonic.com), or call (469) 362-5600.

## APPENDIX C

### UDF Codes

#### Heat generation at 0.5C with 1st approximation for entropic term

```
/******  
UDF for time dependent volumetric heat generation of 18650 cell  
*****/  
  
#include "udf.h"  
  
//qirreversible  
  
//.....  
  
//0-1  
  
#define p1_0 4126.2  
  
#define p2_0 9726.1  
  
  
//1-130  
  
#define a1_1 1.458e+004  
  
#define b1_1 160.1  
  
#define c1_1 57.86  
  
#define a2_1 1.554e+004  
  
#define b2_1 72.21  
  
#define c2_1 64.09  
  
#define a3_1 1937  
  
#define b3_1 50.99  
  
#define c3_1 18.92  
  
#define a4_1 209.9
```

```
#define b4_1 49.9
#define c4_1 6.818
#define a5_1 899.2
#define b5_1 39.72
#define c5_1 10
#define a6_1 5355
#define b6_1 23.95
#define c6_1 17.05
#define a7_1 63.11
#define b7_1 108.8
#define c7_1 6.531
#define a8_1 8506
#define b8_1 -0.3125
#define c8_1 19

//130-1270
#define a1_2 1.4e+004
#define b1_2 4.337
#define c1_2 398.2
#define a2_2 1920
#define b2_2 403.1
#define c2_2 266.2
#define a3_2 1.573e+004
#define b3_2 795.8
```

```
#define c3_2 603.3
#define a4_2 4230
#define b4_2 1170
#define c4_2 209.7
#define a5_2 2302
#define b5_2 1277
#define c5_2 105.9
#define a6_2 9056
#define b6_2 1440
#define c6_2 140
#define a7_2 144
#define b7_2 901.8
#define c7_2 109.9
#define a8_2 331
#define b8_2 1170
#define c8_2 81.38
//1270-3200
#define a1_3 1576
#define b1_3 2950
#define c1_3 243.1
#define a2_3 1.686e+004
#define b2_3 2579
#define c2_3 1246
#define a3_3 1200
```

```
#define b3_3 2016
#define c3_3 310.5
#define a4_3 4016
#define b4_3 1620
#define c4_3 384.6
#define a5_3 1.212e+004
#define b5_3 975.8
#define c5_3 530.1
#define a6_3 3980
#define b6_3 3301
#define c6_3 244.2
#define a7_3 -118.9
#define b7_3 1435
#define c7_3 68.26
#define a8_3 43.9
#define b8_3 1799
#define c8_3 109.2
```

```
//3200-5321
```

```
#define a1_4 2.038e+004
#define b1_4 5690
#define c1_4 1189
#define a2_4 444.4
#define b2_4 5027
```



```
#define c2_4 171.8
#define a3_4 311
#define b3_4 4765
#define c3_4 188
#define a4_4 1.169e+004
#define b4_4 4165
#define c4_4 816.5
#define a5_4 1.449e+004
#define b5_4 3066
#define c5_4 640.5
#define a6_4 1296
#define b6_4 3877
#define c6_4 294.6
#define a7_4 187.5
#define b7_4 3712
#define c7_4 86.73
#define a8_4 195.7
#define b8_4 3484
#define c8_4 98.45
```

```
//5321-6664
```

```
#define a1_5 3.343e+004
#define b1_5 7073
#define c1_5 357.4
```

```
#define a2_5 51.99
#define b2_5 6626
#define c2_5 38.45
#define a3_5 3199
#define b3_5 6566
#define c3_5 228.1
#define a4_5 670.4
#define b4_5 6315
#define c4_5 175
#define a5_5 45.13
#define b5_5 6137
#define c5_5 71.25
#define a6_5 495.9
#define b6_5 5752
#define c6_5 125.4
#define a7_5 14.55
#define b7_5 5934
#define c7_5 34.28
#define a8_5 2.464e+004
#define b8_5 7386
#define c8_5 4586
```

```
//6664-7049
```

```
#define a1_6 1.842e+004
```

```
#define b1_6 7076
#define c1_6 48.56
#define a2_6 5583
#define b2_6 7019
#define c2_6 38.57
#define a3_6 8007
#define b3_6 6971
#define c3_6 56.8
#define a4_6 2255
#define b4_6 6903
#define c4_6 38.59
#define a5_6 691.5
#define b5_6 6864
#define c5_6 25.36
#define a6_6 191
#define b6_6 6838
#define c6_6 8.124
#define a7_6 1870
#define b7_6 6835
#define c7_6 72.78
#define a8_6 1.447e+005
#define b8_6 8785
#define c8_6 1796
```

//.....

//reversible

//0-719

#define p11 0.03826

#define p21 -27.51

//719-2881

#define p12 0

#define p22 0

//2881-3599

#define p13 0.02189

#define p23 -63.08

//3599-4321

#define p14 0

#define p24 15.72

//4321-5039

#define p15 0.01095

#define p25 -31.58

//5039-5041

#define p16 0

#define p26 23.58

//5041-5759

#define p17 -0.03284

#define p27 189.1

```

//5759-7049

#define p18 0

#define p28 0

//.....

DEFINE_SOURCE(heat_gen_0_5C2,cell,thread)
{

real entropic_term, rev, irrev, source;

real time;

time = CURRENT_TIME; //taking time value;

//.....

if (time < 719)
entropic_term = p11*time + p21;
else if (time <= 2881)
entropic_term = p12*time + p22;
else if (time < 3599)
entropic_term = p13*time + p23;
else if (time <= 4321)
entropic_term = p14*time + p24;

```

```

else if (time < 5039)
entropic_term = p15*time + p25;
else if (time <= 5041)
entropic_term = p16*time + p26;
else if (time < 5759)
entropic_term = p17*time + p27;
else
entropic_term = p18*time + p28;

rev=-(C_T(cell,thread))*entropic_term;

//.....
//irreversible
//irreversible=I(OCV-V)/volume
if (time <= 1)
    irrev =p1_0*time + p2_0 ;
else if (time <= 130)
    irrev = a1_1*exp(-pow(((time-b1_1)/c1_1),2)) + a2_1*exp(-pow(((time-
b2_1)/c2_1),2)) + a3_1*exp(-pow(((time-b3_1)/c3_1),2)) + a4_1*exp(-
pow(((time-b4_1)/c4_1),2)) + a5_1*exp(-pow(((time-b5_1)/c5_1),2)) +
a6_1*exp(-pow(((time-b6_1)/c6_1),2)) + a7_1*exp(-pow(((time-b7_1)/c7_1),2))
+ a8_1*exp(-pow(((time-b8_1)/c8_1),2));
else if (time <= 1270)
    irrev = a1_2*exp(-pow(((time-b1_2)/c1_2),2)) + a2_2*exp(-pow(((time-
b2_2)/c2_2),2)) + a3_2*exp(-pow(((time-b3_2)/c3_2),2)) + a4_2*exp(-
pow(((time-b4_2)/c4_2),2)) + a5_2*exp(-pow(((time-b5_2)/c5_2),2)) +

```

$a6\_2 \cdot \exp(-\text{pow}(((\text{time}-b6\_2)/c6\_2),2)) + a7\_2 \cdot \exp(-\text{pow}(((\text{time}-b7\_2)/c7\_2),2))$   
 $+ a8\_2 \cdot \exp(-\text{pow}(((\text{time}-b8\_2)/c8\_2),2));$

else if (time <= 3200)

$\text{irrev} = a1\_3 \cdot \exp(-\text{pow}(((\text{time}-b1\_3)/c1\_3),2)) + a2\_3 \cdot \exp(-\text{pow}(((\text{time}-$   
 $b2\_3)/c2\_3),2)) + a3\_3 \cdot \exp(-\text{pow}(((\text{time}-b3\_3)/c3\_3),2)) + a4\_3 \cdot \exp(-$   
 $\text{pow}(((\text{time}-b4\_3)/c4\_3),2)) + a5\_3 \cdot \exp(-\text{pow}(((\text{time}-b5\_3)/c5\_3),2)) +$   
 $a6\_3 \cdot \exp(-\text{pow}(((\text{time}-b6\_3)/c6\_3),2)) + a7\_3 \cdot \exp(-\text{pow}(((\text{time}-b7\_3)/c7\_3),2))$   
 $+ a8\_3 \cdot \exp(-\text{pow}(((\text{time}-b8\_3)/c8\_3),2));$

else if (time <= 5321)

$\text{irrev} = a1\_4 \cdot \exp(-\text{pow}(((\text{time}-b1\_4)/c1\_4),2)) + a2\_4 \cdot \exp(-\text{pow}(((\text{time}-$   
 $b2\_4)/c2\_4),2)) + a3\_4 \cdot \exp(-\text{pow}(((\text{time}-b3\_4)/c3\_4),2)) + a4\_4 \cdot \exp(-$   
 $\text{pow}(((\text{time}-b4\_4)/c4\_4),2)) + a5\_4 \cdot \exp(-\text{pow}(((\text{time}-b5\_4)/c5\_4),2)) +$   
 $a6\_4 \cdot \exp(-\text{pow}(((\text{time}-b6\_4)/c6\_4),2)) + a7\_4 \cdot \exp(-\text{pow}(((\text{time}-b7\_4)/c7\_4),2))$   
 $+ a8\_4 \cdot \exp(-\text{pow}(((\text{time}-b8\_4)/c8\_4),2));$

else if (time <= 6664)

$\text{irrev} = a1\_5 \cdot \exp(-\text{pow}(((\text{time}-b1\_5)/c1\_5),2)) + a2\_5 \cdot \exp(-\text{pow}(((\text{time}-$   
 $b2\_5)/c2\_5),2)) + a3\_5 \cdot \exp(-\text{pow}(((\text{time}-b3\_5)/c3\_5),2)) + a4\_5 \cdot \exp(-$   
 $\text{pow}(((\text{time}-b4\_5)/c4\_5),2)) + a5\_5 \cdot \exp(-\text{pow}(((\text{time}-b5\_5)/c5\_5),2)) +$   
 $a6\_5 \cdot \exp(-\text{pow}(((\text{time}-b6\_5)/c6\_5),2)) + a7\_5 \cdot \exp(-\text{pow}(((\text{time}-b7\_5)/c7\_5),2))$   
 $+ a8\_5 \cdot \exp(-\text{pow}(((\text{time}-b8\_5)/c8\_5),2));$

else

$\text{irrev} = a1\_6 \cdot \exp(-\text{pow}(((\text{time}-b1\_6)/c1\_6),2)) + a2\_6 \cdot \exp(-\text{pow}(((\text{time}-$   
 $b2\_6)/c2\_6),2)) + a3\_6 \cdot \exp(-\text{pow}(((\text{time}-b3\_6)/c3\_6),2)) + a4\_6 \cdot \exp(-$   
 $\text{pow}(((\text{time}-b4\_6)/c4\_6),2)) + a5\_6 \cdot \exp(-\text{pow}(((\text{time}-b5\_6)/c5\_6),2)) +$   
 $a6\_6 \cdot \exp(-\text{pow}(((\text{time}-b6\_6)/c6\_6),2)) + a7\_6 \cdot \exp(-\text{pow}(((\text{time}-b7\_6)/c7\_6),2))$   
 $+ a8\_6 \cdot \exp(-\text{pow}(((\text{time}-b8\_6)/c8\_6),2));$

source=irrev+rev;//W/m<sup>3</sup>

```
return source;  
}
```



## Heat generation at 1.0C with 1st approximation for entropic term

```
/******  
UDF for time dependent volumetric heat generation of 18650 cell  
*****/  
  
#include "udf.h"  
  
//qirreversible  
  
//.....  
  
//0-  
  
#define p1_0 13493  
#define p2_0 37529  
  
//1-130  
  
#define a1_1 4.882e+004  
#define b1_1 45.27  
#define c1_1 98.75  
#define a2_1 5.231e+004  
#define b2_1 190.8  
#define c2_1 108.2  
#define a3_1 2394  
#define b3_1 33.16  
#define c3_1 13.04  
#define a4_1 1853  
#define b4_1 25.33
```

```
#define c4_1 9.029
#define a5_1 1344
#define b5_1 17.95
#define c5_1 7.062
#define a6_1 2053
#define b6_1 45.36
#define c6_1 22.04
#define a7_1 4022
#define b7_1 210
#define c7_1 28.79
#define a8_1 9287
#define b8_1 5.245
#define c8_1 15.45

//130-1500
#define a1_2 6.17e+004
#define b1_2 3205
#define c1_2 1727
#define a2_2 8.454e+004
#define b2_2 -1601
#define c2_2 2889
#define a3_2 5013
#define b3_2 1502
#define c3_2 209.9
#define a4_2 3094
```

```
#define b4_2 1906
#define c4_2 240
#define a5_2 7360
#define b5_2 1180
#define c5_2 390.7
#define a6_2 1292
#define b6_2 1677
#define c6_2 99.46
#define a7_2 848.8
#define b7_2 853.5
#define c7_2 134.6
#define a8_2 1006
#define b8_2 585.4
#define c8_2 155.4

//1500-1800
#define a1_6 5.904e+004
#define b1_6 1468
#define c1_6 1094
#define a2_6 8962
#define b2_6 1976
#define c2_6 168.7
#define a3_6 657.2
#define b3_6 1717
#define c3_6 46.18
```

```
#define a4_6 493.2
#define b4_6 1649
#define c4_6 53.48
#define a5_6 284.1
#define b5_6 1763
#define c5_6 26.8
#define a6_6 58.39
#define b6_6 1582
#define c6_6 25.35

//1800-2500
#define a1_5 6.429e+004
#define b1_5 2637
#define c1_5 704.6
#define a2_5 5090
#define b2_5 2244
#define c2_5 179
#define a3_5 2677
#define b3_5 2144
#define c3_5 112.7
#define a4_5 6226
#define b4_5 1990
#define c4_5 126
#define a5_5 4.929e+004
#define b5_5 1595
```

```
#define    c5_5    457.7
#define    a6_5    1149
#define    b6_5    1859
#define    c6_5    70.83
#define    a7_5    -327.3
#define    b7_5    1816
#define    c7_5    55.14
#define    a8_5    591.3
#define    b8_5    2087
#define    c8_5    64.99

//2500-3500
#define    a1_3    9.549e+004
#define    b1_3    3650
#define    c1_3    129.1
#define    a2_3    1.191e+004
#define    b2_3    3471
#define    c2_3    73.51
#define    a3_3    5554
#define    b3_3    3392
#define    c3_3    72.98
#define    a4_3    6298
#define    b4_3    3335
#define    c4_3    130.1
#define    a5_3    1.705e+006
```

```
#define b5_3 1.253e+004
```

```
#define c5_3 4211
```

```
#define a6_3 1459
```

```
#define b6_3 2880
```

```
#define c6_3 70.2
```

```
#define a7_3 287.6
```

```
#define b7_3 2796
```

```
#define c7_3 25
```

```
#define a8_3 6.782e+004
```

```
#define b8_3 5402
```

```
#define c8_3 7180
```

```
//3500-3570
```

```
#define a1_4 2.517e+004
```

```
#define b1_4 3629
```

```
#define c1_4 69.24
```

```
#define a2_4 1.66e+005
```

```
#define b2_4 3816
```

```
#define c2_4 531
```

```
//.....
```

```
//reversible
```

```
//0-360
```

```
#define p11 0.1528
#define p21 -55.02
//360-1440
#define p12 0
#define p22 0
//1440-1800
#define p13 0.08733
#define p23 -125.8
//1800-2160
#define p14 0
#define p24 31.44
//2160-2520
#define p15 0.04367
#define p25 -62.88
//2520
#define p18 0
#define p28 47.16
//2520-2880
#define p16 -0.131
#define p26 377.3
//2880-3570
#define p17 0
#define p27 0
//.....
```

```

DEFINE_SOURCE(heat_gen_1C2,cell,thread)
{

real entropic_term, rev, irrev, source;

real time;

time = CURRENT_TIME; //taking time value;

//.....

//reversible+entropic_term

//entropic_term is equal to I*entropic_term/volume so only multiplication with T must
be done to calculate qreversible

if (time < 360)

entropic_term = p11*time + p21;

else if (time <= 1440)

entropic_term = p12*time + p22;

else if (time < 1800)

entropic_term = p13*time + p23;

else if (time <= 2160)

entropic_term = p14*time + p24;

else if (time < 2520)

entropic_term = p15*time + p25;

else if (time == 2520)

```



```
entropic_term = p18*time + p28;
```

```
else if (time < 2880)
```

```
entropic_term = p16*time + p26;
```

```
else
```

```
entropic_term = p17*time + p27;
```

```
rev=-(C_T(cell,thread))*entropic_term;
```

```
//.....
```

```
//irreversible
```

```
//irreversible=I(OCV-V)/volume
```

```
if (time <= 1)
```

```
    irrev =p1_0*time + p2_0 ;
```

```
else if (time <= 130)
```

```
    irrev = a1_1*exp(-pow(((time-b1_1)/c1_1),2)) + a2_1*exp(-pow(((time-  
b2_1)/c2_1),2)) + a3_1*exp(-pow(((time-b3_1)/c3_1),2)) + a4_1*exp(-pow(((time-  
b4_1)/c4_1),2)) + a5_1*exp(-pow(((time-b5_1)/c5_1),2)) + a6_1*exp(-pow(((time-  
b6_1)/c6_1),2)) + a7_1*exp(-pow(((time-b7_1)/c7_1),2)) + a8_1*exp(-pow(((time-  
b8_1)/c8_1),2));
```

```
else if (time <= 1500)
```

```
    irrev = a1_2*exp(-pow(((time-b1_2)/c1_2),2)) + a2_2*exp(-pow(((time-  
b2_2)/c2_2),2)) + a3_2*exp(-pow(((time-b3_2)/c3_2),2)) + a4_2*exp(-pow(((time-  
b4_2)/c4_2),2)) + a5_2*exp(-pow(((time-b5_2)/c5_2),2)) + a6_2*exp(-pow(((time-  
b6_2)/c6_2),2)) + a7_2*exp(-pow(((time-b7_2)/c7_2),2)) + a8_2*exp(-pow(((time-  
b8_2)/c8_2),2));
```

```
else if (time <= 1800)
```

```
    irrev = a1_6*exp(-pow(((time-b1_6)/c1_6),2)) + a2_6*exp(-pow(((time-  
b2_6)/c2_6),2)) + a3_6*exp(-pow(((time-b3_6)/c3_6),2)) + a4_6*exp(-pow(((time-  
b4_6)/c4_6),2)) + a5_6*exp(-pow(((time-b5_6)/c5_6),2)) + a6_6*exp(-pow(((time-  
b6_6)/c6_6),2)) ;
```

```
else if (time <= 2500)
```

```
    irrev = a1_5*exp(-pow(((time-b1_5)/c1_5),2)) + a2_5*exp(-pow(((time-  
b2_5)/c2_5),2)) + a3_5*exp(-pow(((time-b3_5)/c3_5),2)) + a4_5*exp(-pow(((time-  
b4_5)/c4_5),2)) + a5_5*exp(-pow(((time-b5_5)/c5_5),2)) + a6_5*exp(-pow(((time-  
b6_5)/c6_5),2)) + a7_5*exp(-pow(((time-b7_5)/c7_5),2)) + a8_5*exp(-pow(((time-  
b8_5)/c8_5),2));
```

```
else if (time <= 3500)
```

```
    irrev = a1_3*exp(-pow(((time-b1_3)/c1_3),2)) + a2_3*exp(-pow(((time-  
b2_3)/c2_3),2)) + a3_3*exp(-pow(((time-b3_3)/c3_3),2)) + a4_3*exp(-pow(((time-  
b4_3)/c4_3),2)) + a5_3*exp(-pow(((time-b5_3)/c5_3),2)) + a6_3*exp(-pow(((time-  
b6_3)/c6_3),2)) + a7_3*exp(-pow(((time-b7_3)/c7_3),2)) + a8_3*exp(-pow(((time-  
b8_3)/c8_3),2));
```

```
else
```

```
    irrev = a1_4*exp(-pow(((time-b1_4)/c1_4),2)) + a2_4*exp(-pow(((time-  
b2_4)/c2_4),2));
```

```
source=irrev+rev;/W/m^3
```

```
    return source;
```

```
}
```

## Heat generation at 1.5C with 1st approximation for entropic term

```
/******  
UDF for time dependent volumetric heat generation of 18650 cell  
*****/  
  
#include "udf.h"  
  
//qirreversible  
  
//.....  
  
//0-1  
  
#define p1_0 28197  
#define p2_0 87240  
  
//1-60  
  
#define a1_1 1.311e+005  
#define b1_1 87.43  
#define c1_1 149.3  
#define a2_1 546.6  
#define b2_1 34.41  
#define c2_1 4.599  
#define a3_1 2379  
#define b3_1 18.77  
#define c3_1 6.095  
#define a4_1 3501  
#define b4_1 11.06
```

```
#define c4_1 5.161
#define a5_1 1.992e+004
#define b5_1 11.71
#define c5_1 45.48
#define a6_1 2921
#define b6_1 2.149
#define c6_1 2.754
#define a7_1 2986
#define b7_1 6.019
#define c7_1 3.295
#define a8_1 1036
#define b8_1 26.98
#define c8_1 4.901
```

```
//60-1700
```

```
#define a1_2 1.39e+005
#define b1_2 2208
#define c1_2 1992
#define a2_2 6.957e+004
#define b2_2 -5.428
#define c2_2 217.4
#define a3_2 7580
#define b3_2 1006
#define c3_2 191.9
```

```
#define a4_2 2078
#define b4_2 1328
#define c4_2 103.1
#define a5_2 4.405e+004
#define b5_2 507.2
#define c5_2 525.1
#define a6_2 973.7
#define b6_2 411.2
#define c6_2 71.37
#define a7_2 613.2
#define b7_2 545.3
#define c7_2 60.94
#define a8_2 1.847e+004
#define b8_2 269.8
#define c8_2 181.8
```

```
//1700-2170
```

```
#define a1_3 5.371e+005
#define b1_3 2735
#define c1_3 232.8
#define a2_3 1.436e+005
#define b2_3 2491
#define c2_3 1267
#define a3_3 636.7
```

```
#define b3_3 1919
#define c3_3 22.01
#define a4_3 3605
#define b4_3 1915
#define c4_3 127.4
#define a5_3 251.3
#define b5_3 1725
#define c5_3 45.33
#define a6_3 303.9
#define b6_3 1680
#define c6_3 24.53
#define a7_3 4.682e+004
#define b7_3 1381
#define c7_3 534.3
#define a8_3 665.7
#define b8_3 1926
#define c8_3 50.39
```

```
//2170-2392
```

```
#define a1_4 2.877e+005
#define b1_4 2527
#define c1_4 85.48
#define a2_4 9.816e+004
#define b2_4 2482
```

```
#define c2_4 132.1
#define a3_4 4.494e+004
#define b3_4 2375
#define c3_4 197.1
#define a4_4 1.354e+005
#define b4_4 2017
#define c4_4 565.1
```

```
//.....
```

```
//reversible
```

```
//0-240
```

```
#define p11 0.3438
```

```
#define p21 -82.52
```

```
//240-960
```

```
#define p12 0
```

```
#define p22 0
```

```
//960-1200
```

```
#define p13 0.1965
```

```
#define p23 -188.6
```

```
//1200-1440
#define p14 0
#define p24 47.16

//1440-1680
#define p15 0.09825
#define p25 -94.32

//1680-1920
#define p16 -0.2948
#define p26 565.9

//1920-2392
#define p17 0
#define p27 0

//.....

DEFINE_SOURCE(heat_gen_1_5C2,cell,thread)
{

real entropic_term, rev, irrev, source;

real time;
```



```
time = CURRENT_TIME; //taking time value;
```

```
//.....
```

```
//reversible+entropic_term
```

```
//entropic_term is equal to I*entropic_term/volume so only multiplication with T must  
be done to calculate qreversible
```

```
if (time < 240)
```

```
entropic_term = p11*time + p21;
```

```
else if (time <= 960)
```

```
entropic_term = p12*time + p22;
```

```
else if (time < 1200)
```

```
entropic_term = p13*time + p23;
```

```
else if (time <= 1440)
```

```
entropic_term = p14*time + p24;
```

```
else if (time <= 1680)
```

```
entropic_term = p15*time + p25;
```

```
else if (time < 1920)
```

```
entropic_term = p16*time + p26;
```

```
else
```

```
entropic_term = p17*time + p27;
```

```
rev=-(C_T(cell,thread))*entropic_term;
```

```

//.....

//irreversible

//irreversible=I(OCV-V)/volume

if (time <= 1)

    irrev =p1_0*time + p2_0 ;

else if (time <= 60)

    irrev  =  a1_1*exp(-pow(((time-b1_1)/c1_1),2))  +      a2_1*exp(-pow(((time-
b2_1)/c2_1),2))  +  a3_1*exp(-pow(((time-b3_1)/c3_1),2))  +  a4_1*exp(-pow(((time-
b4_1)/c4_1),2))  +  a5_1*exp(-pow(((time-b5_1)/c5_1),2))  +  a6_1*exp(-pow(((time-
b6_1)/c6_1),2))  +  a7_1*exp(-pow(((time-b7_1)/c7_1),2))  +  a8_1*exp(-pow(((time-
b8_1)/c8_1),2));

else if (time <= 1700)

    irrev  =  a1_2*exp(-pow(((time-b1_2)/c1_2),2))  +      a2_2*exp(-pow(((time-
b2_2)/c2_2),2))  +  a3_2*exp(-pow(((time-b3_2)/c3_2),2))  +  a4_2*exp(-pow(((time-
b4_2)/c4_2),2))  +  a5_2*exp(-pow(((time-b5_2)/c5_2),2))  +  a6_2*exp(-pow(((time-
b6_2)/c6_2),2))  +  a7_2*exp(-pow(((time-b7_2)/c7_2),2))  +  a8_2*exp(-pow(((time-
b8_2)/c8_2),2));

else if (time <= 2170)

    irrev  =  a1_3*exp(-pow(((time-b1_3)/c1_3),2))  +      a2_3*exp(-pow(((time-
b2_3)/c2_3),2))  +  a3_3*exp(-pow(((time-b3_3)/c3_3),2))  +  a4_3*exp(-pow(((time-
b4_3)/c4_3),2))  +  a5_3*exp(-pow(((time-b5_3)/c5_3),2))  +  a6_3*exp(-pow(((time-
b6_3)/c6_3),2))  +  a7_3*exp(-pow(((time-b7_3)/c7_3),2))  +  a8_3*exp(-pow(((time-
b8_3)/c8_3),2));

else

    irrev  =  a1_4*exp(-pow(((time-b1_4)/c1_4),2))  +      a2_4*exp(-pow(((time-
b2_4)/c2_4),2))  +  a3_4*exp(-pow(((time-b3_4)/c3_4),2))  +  a4_4*exp(-pow(((time-
b4_4)/c4_4),2));

```

```
source=irrev+rev; //W/m^3
```

```
return source;
```

```
}
```

## Heat generation at 1.0C with 2nd approximation for entropic term

```
/******  
UDF for time dependent volumetric heat generation of 18650 cell  
*****/  
  
#include "udf.h"  
  
//qirreversible  
  
//.....  
  
//0-  
  
#define p1_0 13493  
#define p2_0 37529  
  
//1-130  
  
#define a1_1 4.882e+004  
#define b1_1 45.27  
#define c1_1 98.75  
#define a2_1 5.231e+004  
#define b2_1 190.8  
#define c2_1 108.2  
#define a3_1 2394  
#define b3_1 33.16  
#define c3_1 13.04  
#define a4_1 1853  
#define b4_1 25.33
```

```
#define c4_1 9.029
#define a5_1 1344
#define b5_1 17.95
#define c5_1 7.062
#define a6_1 2053
#define b6_1 45.36
#define c6_1 22.04
#define a7_1 4022
#define b7_1 210
#define c7_1 28.79
#define a8_1 9287
#define b8_1 5.245
#define c8_1 15.45

//130-1500
#define a1_2 6.17e+004
#define b1_2 3205
#define c1_2 1727
#define a2_2 8.454e+004
#define b2_2 -1601
#define c2_2 2889
#define a3_2 5013
#define b3_2 1502
#define c3_2 209.9
#define a4_2 3094
```

```
#define b4_2 1906
#define c4_2 240
#define a5_2 7360
#define b5_2 1180
#define c5_2 390.7
#define a6_2 1292
#define b6_2 1677
#define c6_2 99.46
#define a7_2 848.8
#define b7_2 853.5
#define c7_2 134.6
#define a8_2 1006
#define b8_2 585.4
#define c8_2 155.4

//1500-1800
#define a1_6 5.904e+004
#define b1_6 1468
#define c1_6 1094
#define a2_6 8962
#define b2_6 1976
#define c2_6 168.7
#define a3_6 657.2
#define b3_6 1717
#define c3_6 46.18
```

```
#define a4_6 493.2
#define b4_6 1649
#define c4_6 53.48
#define a5_6 284.1
#define b5_6 1763
#define c5_6 26.8
#define a6_6 58.39
#define b6_6 1582
#define c6_6 25.35

//1800-2500
#define a1_5 6.429e+004
#define b1_5 2637
#define c1_5 704.6
#define a2_5 5090
#define b2_5 2244
#define c2_5 179
#define a3_5 2677
#define b3_5 2144
#define c3_5 112.7
#define a4_5 6226
#define b4_5 1990
#define c4_5 126
#define a5_5 4.929e+004
#define b5_5 1595
```

```
#define c5_5 457.7
#define a6_5 1149
#define b6_5 1859
#define c6_5 70.83
#define a7_5 -327.3
#define b7_5 1816
#define c7_5 55.14
#define a8_5 591.3
#define b8_5 2087
#define c8_5 64.99

//2500-3500
#define a1_3 9.549e+004
#define b1_3 3650
#define c1_3 129.1
#define a2_3 1.191e+004
#define b2_3 3471
#define c2_3 73.51
#define a3_3 5554
#define b3_3 3392
#define c3_3 72.98
#define a4_3 6298
#define b4_3 3335
#define c4_3 130.1
#define a5_3 1.705e+006
```



```
#define b5_3 1.253e+004
```

```
#define c5_3 4211
```

```
#define a6_3 1459
```

```
#define b6_3 2880
```

```
#define c6_3 70.2
```

```
#define a7_3 287.6
```

```
#define b7_3 2796
```

```
#define c7_3 25
```

```
#define a8_3 6.782e+004
```

```
#define b8_3 5402
```

```
#define c8_3 7180
```

```
//3500-3570
```

```
#define a1_4 2.517e+004
```

```
#define b1_4 3629
```

```
#define c1_4 69.24
```

```
#define a2_4 1.66e+005
```

```
#define b2_4 3816
```

```
#define c2_4 531
```

```
//.....
```

```
//reversible
```

```
//0-2520
```

```

#define p11 0.03197
#define p21 -33.4
//2520-3570
#define p12 -0.03926
#define p22 131.9

//.....

DEFINE_SOURCE(heat_gen_1C3,cell,thread)
{

real entropic_term, rev, irrev, source;

real time;

time = CURRENT_TIME; //taking time value;

//.....

//reversible+entropic_term
//entropic_term is equal to I*entropic_term/volume so only multiplication with T must
be done to calculate qreversible
if (time <= 2520)
entropic_term = p11*time + p21;
else
entropic_term = p12*time + p22;

```

```

rev=-(C_T(cell,thread))*entropic_term;

//.....

//irreversible

//irreversible=I(OCV-V)/volume

if (time <= 1)

    irrev =p1_0*time + p2_0 ;

else if (time <= 130)

    irrev = a1_1*exp(-pow(((time-b1_1)/c1_1),2)) + a2_1*exp(-pow(((time-
b2_1)/c2_1),2)) + a3_1*exp(-pow(((time-b3_1)/c3_1),2)) + a4_1*exp(-pow(((time-
b4_1)/c4_1),2)) + a5_1*exp(-pow(((time-b5_1)/c5_1),2)) + a6_1*exp(-pow(((time-
b6_1)/c6_1),2)) + a7_1*exp(-pow(((time-b7_1)/c7_1),2)) + a8_1*exp(-pow(((time-
b8_1)/c8_1),2));

else if (time <= 1500)

    irrev = a1_2*exp(-pow(((time-b1_2)/c1_2),2)) + a2_2*exp(-pow(((time-
b2_2)/c2_2),2)) + a3_2*exp(-pow(((time-b3_2)/c3_2),2)) + a4_2*exp(-pow(((time-
b4_2)/c4_2),2)) + a5_2*exp(-pow(((time-b5_2)/c5_2),2)) + a6_2*exp(-pow(((time-
b6_2)/c6_2),2)) + a7_2*exp(-pow(((time-b7_2)/c7_2),2)) + a8_2*exp(-pow(((time-
b8_2)/c8_2),2));

else if (time <= 1800)

    irrev = a1_6*exp(-pow(((time-b1_6)/c1_6),2)) + a2_6*exp(-pow(((time-
b2_6)/c2_6),2)) + a3_6*exp(-pow(((time-b3_6)/c3_6),2)) + a4_6*exp(-pow(((time-
b4_6)/c4_6),2)) + a5_6*exp(-pow(((time-b5_6)/c5_6),2)) + a6_6*exp(-pow(((time-
b6_6)/c6_6),2)) ;

else if (time <= 2500)

    irrev = a1_5*exp(-pow(((time-b1_5)/c1_5),2)) + a2_5*exp(-pow(((time-
b2_5)/c2_5),2)) + a3_5*exp(-pow(((time-b3_5)/c3_5),2)) + a4_5*exp(-pow(((time-

```

```
b4_5)/c4_5),2)) + a5_5*exp(-pow(((time-b5_5)/c5_5),2)) + a6_5*exp(-pow(((time-  
b6_5)/c6_5),2)) + a7_5*exp(-pow(((time-b7_5)/c7_5),2)) + a8_5*exp(-pow(((time-  
b8_5)/c8_5),2));
```

```
else if (time <= 3500)
```

```
    irrev = a1_3*exp(-pow(((time-b1_3)/c1_3),2)) + a2_3*exp(-pow(((time-  
b2_3)/c2_3),2)) + a3_3*exp(-pow(((time-b3_3)/c3_3),2)) + a4_3*exp(-pow(((time-  
b4_3)/c4_3),2)) + a5_3*exp(-pow(((time-b5_3)/c5_3),2)) + a6_3*exp(-pow(((time-  
b6_3)/c6_3),2)) + a7_3*exp(-pow(((time-b7_3)/c7_3),2)) + a8_3*exp(-pow(((time-  
b8_3)/c8_3),2));
```

```
else
```

```
    irrev = a1_4*exp(-pow(((time-b1_4)/c1_4),2)) + a2_4*exp(-pow(((time-  
b2_4)/c2_4),2));
```

```
source=irrev+rev;//W/m^3
```

```
    return source;
```

```
}
```

## Heat generation at 1.0C with 3rd approximation for entropic term

```
/******  
  
UDF for time dependent volumetric heat generation of 18650 cell  
*****/  
  
#include "udf.h"  
  
//qirreversible  
  
//.....  
  
//0-  
  
#define p1_0 13493  
#define p2_0 37529  
  
//1-130  
  
#define a1_1 4.882e+004  
#define b1_1 45.27  
#define c1_1 98.75  
#define a2_1 5.231e+004  
#define b2_1 190.8  
#define c2_1 108.2  
#define a3_1 2394  
#define b3_1 33.16  
#define c3_1 13.04  
#define a4_1 1853  
#define b4_1 25.33
```

```
#define c4_1 9.029
#define a5_1 1344
#define b5_1 17.95
#define c5_1 7.062
#define a6_1 2053
#define b6_1 45.36
#define c6_1 22.04
#define a7_1 4022
#define b7_1 210
#define c7_1 28.79
#define a8_1 9287
#define b8_1 5.245
#define c8_1 15.45

//130-1500
#define a1_2 6.17e+004
#define b1_2 3205
#define c1_2 1727
#define a2_2 8.454e+004
#define b2_2 -1601
#define c2_2 2889
#define a3_2 5013
#define b3_2 1502
#define c3_2 209.9
#define a4_2 3094
```

```
#define b4_2 1906
#define c4_2 240
#define a5_2 7360
#define b5_2 1180
#define c5_2 390.7
#define a6_2 1292
#define b6_2 1677
#define c6_2 99.46
#define a7_2 848.8
#define b7_2 853.5
#define c7_2 134.6
#define a8_2 1006
#define b8_2 585.4
#define c8_2 155.4

//1500-1800
#define a1_6 5.904e+004
#define b1_6 1468
#define c1_6 1094
#define a2_6 8962
#define b2_6 1976
#define c2_6 168.7
#define a3_6 657.2
#define b3_6 1717
#define c3_6 46.18
```

```
#define a4_6 493.2
#define b4_6 1649
#define c4_6 53.48
#define a5_6 284.1
#define b5_6 1763
#define c5_6 26.8
#define a6_6 58.39
#define b6_6 1582
#define c6_6 25.35

//1800-2500
#define a1_5 6.429e+004
#define b1_5 2637
#define c1_5 704.6
#define a2_5 5090
#define b2_5 2244
#define c2_5 179
#define a3_5 2677
#define b3_5 2144
#define c3_5 112.7
#define a4_5 6226
#define b4_5 1990
#define c4_5 126
#define a5_5 4.929e+004
#define b5_5 1595
```



```
#define    c5_5    457.7
#define    a6_5    1149
#define    b6_5    1859
#define    c6_5    70.83
#define    a7_5    -327.3
#define    b7_5    1816
#define    c7_5    55.14
#define    a8_5    591.3
#define    b8_5    2087
#define    c8_5    64.99

//2500-3500
#define    a1_3    9.549e+004
#define    b1_3    3650
#define    c1_3    129.1
#define    a2_3    1.191e+004
#define    b2_3    3471
#define    c2_3    73.51
#define    a3_3    5554
#define    b3_3    3392
#define    c3_3    72.98
#define    a4_3    6298
#define    b4_3    3335
#define    c4_3    130.1
#define    a5_3    1.705e+006
```

```
#define b5_3 1.253e+004
```

```
#define c5_3 4211
```

```
#define a6_3 1459
```

```
#define b6_3 2880
```

```
#define c6_3 70.2
```

```
#define a7_3 287.6
```

```
#define b7_3 2796
```

```
#define c7_3 25
```

```
#define a8_3 6.782e+004
```

```
#define b8_3 5402
```

```
#define c8_3 7180
```

```
//3500-3570
```

```
#define a1_4 2.517e+004
```

```
#define b1_4 3629
```

```
#define c1_4 69.24
```

```
#define a2_4 1.66e+005
```

```
#define b2_4 3816
```

```
#define c2_4 531
```

```
//.....
```

```
//reversible
```

```
//0-3570
```

```

#define p11 0.0033572
#define p21 5.0006

//.....

DEFINE_SOURCE(heat_gen_1C3_1,cell,thread)
{

real entropic_term, rev, irrev, source;
real time;
time = CURRENT_TIME; //taking time value;

//.....

//reversible+entropic_term
//entropic_term is equal to l*entropic_term/volume so only multiplication with T must
    be done to calculate qreversible

entropic_term = p11*time + p21;

rev=-(C_T(cell,thread))*entropic_term;

//.....

//irreversible

```

//irreversible=l(OCV-V)/volume

if (time <= 1)

irrev =p1\_0\*time + p2\_0 ;

else if (time <= 130)

irrev = a1\_1\*exp(-pow(((time-b1\_1)/c1\_1),2)) + a2\_1\*exp(-pow(((time-b2\_1)/c2\_1),2)) + a3\_1\*exp(-pow(((time-b3\_1)/c3\_1),2)) + a4\_1\*exp(-pow(((time-b4\_1)/c4\_1),2)) + a5\_1\*exp(-pow(((time-b5\_1)/c5\_1),2)) + a6\_1\*exp(-pow(((time-b6\_1)/c6\_1),2)) + a7\_1\*exp(-pow(((time-b7\_1)/c7\_1),2)) + a8\_1\*exp(-pow(((time-b8\_1)/c8\_1),2));

else if (time <= 1500)

irrev = a1\_2\*exp(-pow(((time-b1\_2)/c1\_2),2)) + a2\_2\*exp(-pow(((time-b2\_2)/c2\_2),2)) + a3\_2\*exp(-pow(((time-b3\_2)/c3\_2),2)) + a4\_2\*exp(-pow(((time-b4\_2)/c4\_2),2)) + a5\_2\*exp(-pow(((time-b5\_2)/c5\_2),2)) + a6\_2\*exp(-pow(((time-b6\_2)/c6\_2),2)) + a7\_2\*exp(-pow(((time-b7\_2)/c7\_2),2)) + a8\_2\*exp(-pow(((time-b8\_2)/c8\_2),2));

else if (time <= 1800)

irrev = a1\_6\*exp(-pow(((time-b1\_6)/c1\_6),2)) + a2\_6\*exp(-pow(((time-b2\_6)/c2\_6),2)) + a3\_6\*exp(-pow(((time-b3\_6)/c3\_6),2)) + a4\_6\*exp(-pow(((time-b4\_6)/c4\_6),2)) + a5\_6\*exp(-pow(((time-b5\_6)/c5\_6),2)) + a6\_6\*exp(-pow(((time-b6\_6)/c6\_6),2)) ;

else if (time <= 2500)

irrev = a1\_5\*exp(-pow(((time-b1\_5)/c1\_5),2)) + a2\_5\*exp(-pow(((time-b2\_5)/c2\_5),2)) + a3\_5\*exp(-pow(((time-b3\_5)/c3\_5),2)) + a4\_5\*exp(-pow(((time-b4\_5)/c4\_5),2)) + a5\_5\*exp(-pow(((time-b5\_5)/c5\_5),2)) + a6\_5\*exp(-pow(((time-b6\_5)/c6\_5),2)) + a7\_5\*exp(-pow(((time-b7\_5)/c7\_5),2)) + a8\_5\*exp(-pow(((time-b8\_5)/c8\_5),2));

else if (time <= 3500)

irrev = a1\_3\*exp(-pow(((time-b1\_3)/c1\_3),2)) + a2\_3\*exp(-pow(((time-

```
b2_3)/c2_3),2)) + a3_3*exp(-pow(((time-b3_3)/c3_3),2)) + a4_3*exp(-  
pow(((time-b4_3)/c4_3),2)) + a5_3*exp(-pow(((time-b5_3)/c5_3),2)) +  
a6_3*exp(-pow(((time-b6_3)/c6_3),2)) + a7_3*exp(-pow(((time-b7_3)/c7_3),2))  
+ a8_3*exp(-pow(((time-b8_3)/c8_3),2));
```

```
else
```

```
irrev = a1_4*exp(-pow(((time-b1_4)/c1_4),2)) + a2_4*exp(-pow(((time-  
b2_4)/c2_4),2));
```

```
source=irrev+rev;//W/m^3
```

```
return source;
```

```
}
```

## Heat generation at 1.0C with 4th approximation for entropic term

```
/******  
UDF for time dependent volumetric heat generation of 18650 cell  
*****/  
  
#include "udf.h"  
  
//qirreversible  
  
//.....  
  
//0-  
  
#define p1_0 13493  
#define p2_0 37529  
  
//1-130  
  
#define a1_1 4.882e+004  
#define b1_1 45.27  
#define c1_1 98.75  
#define a2_1 5.231e+004  
#define b2_1 190.8  
#define c2_1 108.2  
#define a3_1 2394  
#define b3_1 33.16  
#define c3_1 13.04  
#define a4_1 1853  
#define b4_1 25.33
```

```
#define c4_1 9.029
#define a5_1 1344
#define b5_1 17.95
#define c5_1 7.062
#define a6_1 2053
#define b6_1 45.36
#define c6_1 22.04
#define a7_1 4022
#define b7_1 210
#define c7_1 28.79
#define a8_1 9287
#define b8_1 5.245
#define c8_1 15.45

//130-1500
#define a1_2 6.17e+004
#define b1_2 3205
#define c1_2 1727
#define a2_2 8.454e+004
#define b2_2 -1601
#define c2_2 2889
#define a3_2 5013
#define b3_2 1502
#define c3_2 209.9
#define a4_2 3094
```

```
#define b4_2 1906
#define c4_2 240
#define a5_2 7360
#define b5_2 1180
#define c5_2 390.7
#define a6_2 1292
#define b6_2 1677
#define c6_2 99.46
#define a7_2 848.8
#define b7_2 853.5
#define c7_2 134.6
#define a8_2 1006
#define b8_2 585.4
#define c8_2 155.4

//1500-1800
#define a1_6 5.904e+004
#define b1_6 1468
#define c1_6 1094
#define a2_6 8962
#define b2_6 1976
#define c2_6 168.7
#define a3_6 657.2
#define b3_6 1717
#define c3_6 46.18
```



```
#define a4_6 493.2
#define b4_6 1649
#define c4_6 53.48
#define a5_6 284.1
#define b5_6 1763
#define c5_6 26.8
#define a6_6 58.39
#define b6_6 1582
#define c6_6 25.35

//1800-2500
#define a1_5 6.429e+004
#define b1_5 2637
#define c1_5 704.6
#define a2_5 5090
#define b2_5 2244
#define c2_5 179
#define a3_5 2677
#define b3_5 2144
#define c3_5 112.7
#define a4_5 6226
#define b4_5 1990
#define c4_5 126
#define a5_5 4.929e+004
#define b5_5 1595
```

```
#define    c5_5    457.7
#define    a6_5    1149
#define    b6_5    1859
#define    c6_5    70.83
#define    a7_5    -327.3
#define    b7_5    1816
#define    c7_5    55.14
#define    a8_5    591.3
#define    b8_5    2087
#define    c8_5    64.99

//2500-3500
#define    a1_3    9.549e+004
#define    b1_3    3650
#define    c1_3    129.1
#define    a2_3    1.191e+004
#define    b2_3    3471
#define    c2_3    73.51
#define    a3_3    5554
#define    b3_3    3392
#define    c3_3    72.98
#define    a4_3    6298
#define    b4_3    3335
#define    c4_3    130.1
#define    a5_3    1.705e+006
```

```
#define b5_3 1.253e+004
```

```
#define c5_3 4211
```

```
#define a6_3 1459
```

```
#define b6_3 2880
```

```
#define c6_3 70.2
```

```
#define a7_3 287.6
```

```
#define b7_3 2796
```

```
#define c7_3 25
```

```
#define a8_3 6.782e+004
```

```
#define b8_3 5402
```

```
#define c8_3 7180
```

```
//3500-3570
```

```
#define a1_4 2.517e+004
```

```
#define b1_4 3629
```

```
#define c1_4 69.24
```

```
#define a2_4 1.66e+005
```

```
#define b2_4 3816
```

```
#define c2_4 531
```

```
//.....
```

```
DEFINE_SOURCE(heat_gen_1C4,cell,thread)
```

```
{
```

```

real entropic_term, rev, irrev, source;

real time;

time = CURRENT_TIME; //taking time value;

//.....

//irreversible

//irreversible=I(OCV-V)/volume

if (time <= 1)

    irrev =p1_0*time + p2_0 ;

else if (time <= 130)

    irrev = a1_1*exp(-pow(((time-b1_1)/c1_1),2)) + a2_1*exp(-pow(((time-
        b2_1)/c2_1),2)) + a3_1*exp(-pow(((time-b3_1)/c3_1),2)) + a4_1*exp(-
        pow(((time-b4_1)/c4_1),2)) + a5_1*exp(-pow(((time-b5_1)/c5_1),2)) +
        a6_1*exp(-pow(((time-b6_1)/c6_1),2)) + a7_1*exp(-pow(((time-b7_1)/c7_1),2))
        + a8_1*exp(-pow(((time-b8_1)/c8_1),2));

else if (time <= 1500)

    irrev = a1_2*exp(-pow(((time-b1_2)/c1_2),2)) + a2_2*exp(-pow(((time-
        b2_2)/c2_2),2)) + a3_2*exp(-pow(((time-b3_2)/c3_2),2)) + a4_2*exp(-
        pow(((time-b4_2)/c4_2),2)) + a5_2*exp(-pow(((time-b5_2)/c5_2),2)) +
        a6_2*exp(-pow(((time-b6_2)/c6_2),2)) + a7_2*exp(-pow(((time-b7_2)/c7_2),2))
        + a8_2*exp(-pow(((time-b8_2)/c8_2),2));

else if (time <= 1800)

    irrev = a1_6*exp(-pow(((time-b1_6)/c1_6),2)) + a2_6*exp(-pow(((time-
        b2_6)/c2_6),2)) + a3_6*exp(-pow(((time-b3_6)/c3_6),2)) + a4_6*exp(-
        pow(((time-b4_6)/c4_6),2)) + a5_6*exp(-pow(((time-b5_6)/c5_6),2)) +
        a6_6*exp(-pow(((time-b6_6)/c6_6),2)) ;

```

```

else if (time <= 2500)

    irrev = a1_5*exp(-pow(((time-b1_5)/c1_5),2)) + a2_5*exp(-pow(((time-
        b2_5)/c2_5),2)) + a3_5*exp(-pow(((time-b3_5)/c3_5),2)) + a4_5*exp(-
        pow(((time-b4_5)/c4_5),2)) + a5_5*exp(-pow(((time-b5_5)/c5_5),2)) +
        a6_5*exp(-pow(((time-b6_5)/c6_5),2)) + a7_5*exp(-pow(((time-b7_5)/c7_5),2))
        + a8_5*exp(-pow(((time-b8_5)/c8_5),2));

else if (time <= 3500)

    irrev = a1_3*exp(-pow(((time-b1_3)/c1_3),2)) + a2_3*exp(-pow(((time-
        b2_3)/c2_3),2)) + a3_3*exp(-pow(((time-b3_3)/c3_3),2)) + a4_3*exp(-
        pow(((time-b4_3)/c4_3),2)) + a5_3*exp(-pow(((time-b5_3)/c5_3),2)) +
        a6_3*exp(-pow(((time-b6_3)/c6_3),2)) + a7_3*exp(-pow(((time-b7_3)/c7_3),2))
        + a8_3*exp(-pow(((time-b8_3)/c8_3),2));

else

    irrev = a1_4*exp(-pow(((time-b1_4)/c1_4),2)) + a2_4*exp(-pow(((time-
        b2_4)/c2_4),2));

source=irrev;//W/m^3

    return source;
}

```

## Heat generation at 1.0C for the new battery

```
/******  
UDF for time dependent volumetric heat generation of 18650 cell  
*****/  
  
#include "udf.h"  
  
//qirreversible  
  
//.....  
  
//0-1  
  
#define p1_0 5829.9  
#define p2_0 35957  
  
//1-130  
  
#define a1_1 3.991e+004  
#define b1_1 67.55  
#define c1_1 94.58  
  
#define a2_1 4.782e+004  
#define b2_1 215.1  
#define c2_1 116.3  
  
#define a3_1 237.7  
#define b3_1 66.02  
#define c3_1 6.578  
  
#define a4_1 1155  
#define b4_1 55.04  
#define c4_1 12.87
```

```
#define a5_1 1.223e+004
#define b5_1 23.59
#define c5_1 31.16
#define a6_1 1422
#define b6_1 74.57
#define c6_1 18.35
#define a7_1 162.1
#define b7_1 20.41
#define c7_1 1.361
#define a8_1 8816
#define b8_1 -0.376
#define c8_1 18.55

//130-1500
#define a1_2 3.876e+004
#define b1_2 1607
#define c1_2 393.9
#define a2_2 5.062e+004
#define b2_2 63.57
#define c2_2 471.7
#define a3_2 4.723e+004
#define b3_2 967.5
#define c3_2 535.3
#define a4_2 6916
#define b4_2 551
```

```
#define c4_2 158.4
#define a5_2 2653
#define b5_2 770
#define c5_2 137.6
#define a6_2 630.3
#define b6_2 646.6
#define c6_2 64.85
#define a7_2 1.341e+004
#define b7_2 1818
#define c7_2 175.9
#define a8_2 2587
#define b8_2 372.2
#define c8_2 130.2

//1500-1800

#define a1_6 5.167e+004
#define b1_6 1424
#define c1_6 304.4
#define a2_6 5905
#define b2_6 1654
#define c2_6 115.3
#define a3_6 4.876e+004
#define b3_6 1939
#define c3_6 282.1
#define a4_6 1559
```



```
#define b4_6 1746
#define c4_6 74.76
#define a5_6 1.464e+004
#define b5_6 1219
#define c5_6 118.2
#define a6_6 367.4
#define b6_6 1554
#define c6_6 57.19

//1800-2500
#define a1_5 5.477e+004
#define b1_5 2649
#define c1_5 383.3
#define a2_5 2.339e+004
#define b2_5 2253
#define c2_5 235.5
#define a3_5 1.499e+004
#define b3_5 2054
#define c3_5 175.3
#define a4_5 6587
#define b4_5 1923
#define c4_5 133.2
#define a5_5 4.604e+004
#define b5_5 1511
#define c5_5 560.7
```

```
#define a6_5 409.9
#define b6_5 1864
#define c6_5 48.58
#define a7_5 1.114e+004
#define b7_5 1749
#define c7_5 211.4
#define a8_5 86.98
#define b8_5 2056
#define c8_5 34.21

//2500-3500
#define a1_3 7.167e+004
#define b1_3 3609
#define c1_3 99.48
#define a2_3 1.897e+004
#define b2_3 3487
#define c2_3 106.9
#define a3_3 6.175e+004
#define b3_3 3377
#define c3_3 279.8
#define a4_3 2.736e+004
#define b4_3 2806
#define c4_3 141.8
#define a5_3 4.697e+004
#define b5_3 2992
```

```
#define c5_3 237.2
#define a6_3 5742
#define b6_3 2735
#define c6_3 80.41
#define a7_3 2.784e+004
#define b7_3 2642
#define c7_3 113.1
#define a8_3 5.223e+004
#define b8_3 2469
#define c8_3 160.1

//3500-3601
#define a1_4 6.376e+007
#define b1_4 4281
#define c1_4 248.4
#define a2_4 2.517e+005
#define b2_4 4489
#define c2_4 967.9

//.....

//reversible

//0-360
#define p11 0.1528
```

```
#define p21 -55.02
//360-1440
#define p12 0
#define p22 0
//1440-1800
#define p13 0.08733
#define p23 -125.8
//1800-2160
#define p14 0
#define p24 31.44
//2160-2520
#define p15 0.04367
#define p25 -62.88
//2520
#define p18 0
#define p28 47.16
//2520-2880
#define p16 -0.131
#define p26 377.3
//2880-3601
#define p17 0
#define p27 0
//.....
```

```

DEFINE_SOURCE(heat_gen_1C5,cell,thread)
{

real entropic_term, rev, irrev, source;

real time;

time = CURRENT_TIME; //taking time value;

//.....

//reversible+entropic_term
//entropic_term is equal to I*entropic_term/volume so only multiplication with T must
    be done to calculate qreversible
if (time < 360)
entropic_term = p11*time + p21;
else if (time <= 1440)
entropic_term = p12*time + p22;
else if (time < 1800)
entropic_term = p13*time + p23;
else if (time <= 2160)
entropic_term = p14*time + p24;
else if (time < 2520)
entropic_term = p15*time + p25;
else if (time == 2520)
entropic_term = p18*time + p28;

```

```

else if (time < 2880)
entropic_term = p16*time + p26;
else
entropic_term = p17*time + p27;

rev=-(C_T(cell,thread))*entropic_term;

//.....

//irreversible
//irreversible=l(OCV-V)/volume
if (time <= 1)
    irrev =p1_0*time + p2_0 ;
else if (time <= 130)
    irrev = a1_1*exp(-pow(((time-b1_1)/c1_1),2)) + a2_1*exp(-pow(((time-
        b2_1)/c2_1),2)) + a3_1*exp(-pow(((time-b3_1)/c3_1),2)) + a4_1*exp(-
        pow(((time-b4_1)/c4_1),2)) + a5_1*exp(-pow(((time-b5_1)/c5_1),2)) +
        a6_1*exp(-pow(((time-b6_1)/c6_1),2)) + a7_1*exp(-pow(((time-b7_1)/c7_1),2))
        + a8_1*exp(-pow(((time-b8_1)/c8_1),2));
else if (time <= 1500)
    irrev = a1_2*exp(-pow(((time-b1_2)/c1_2),2)) + a2_2*exp(-pow(((time-
        b2_2)/c2_2),2)) + a3_2*exp(-pow(((time-b3_2)/c3_2),2)) + a4_2*exp(-
        pow(((time-b4_2)/c4_2),2)) + a5_2*exp(-pow(((time-b5_2)/c5_2),2)) +
        a6_2*exp(-pow(((time-b6_2)/c6_2),2)) + a7_2*exp(-pow(((time-b7_2)/c7_2),2))
        + a8_2*exp(-pow(((time-b8_2)/c8_2),2));
else if (time <= 1800)
    irrev = a1_6*exp(-pow(((time-b1_6)/c1_6),2)) + a2_6*exp(-pow(((time-

```

```
b2_6)/c2_6),2)) + a3_6*exp(-pow(((time-b3_6)/c3_6),2)) + a4_6*exp(-  
pow(((time-b4_6)/c4_6),2)) + a5_6*exp(-pow(((time-b5_6)/c5_6),2)) +  
a6_6*exp(-pow(((time-b6_6)/c6_6),2)) ;
```

```
else if (time <= 2500)
```

```
irrev = a1_5*exp(-pow(((time-b1_5)/c1_5),2)) + a2_5*exp(-pow(((time-  
b2_5)/c2_5),2)) + a3_5*exp(-pow(((time-b3_5)/c3_5),2)) + a4_5*exp(-  
pow(((time-b4_5)/c4_5),2)) + a5_5*exp(-pow(((time-b5_5)/c5_5),2)) +  
a6_5*exp(-pow(((time-b6_5)/c6_5),2)) + a7_5*exp(-pow(((time-b7_5)/c7_5),2))  
+ a8_5*exp(-pow(((time-b8_5)/c8_5),2));
```

```
else if (time <= 3500)
```

```
irrev = a1_3*exp(-pow(((time-b1_3)/c1_3),2)) + a2_3*exp(-pow(((time-  
b2_3)/c2_3),2)) + a3_3*exp(-pow(((time-b3_3)/c3_3),2)) + a4_3*exp(-  
pow(((time-b4_3)/c4_3),2)) + a5_3*exp(-pow(((time-b5_3)/c5_3),2)) +  
a6_3*exp(-pow(((time-b6_3)/c6_3),2)) + a7_3*exp(-pow(((time-b7_3)/c7_3),2))  
+ a8_3*exp(-pow(((time-b8_3)/c8_3),2));
```

```
else
```

```
irrev = a1_4*exp(-pow(((time-b1_4)/c1_4),2)) + a2_4*exp(-pow(((time-  
b2_4)/c2_4),2));
```

```
source=irrev+rev;//W/m^3
```

```
return source;
```

```
}
```

## CURRICULUM VITAE

### Credentials

Name, Surname : Emre, GÜMÜŞSU  
Place of Birth : Ankara, Turkey  
Marital Status : Single  
E-mail : [gmssu\\_emre@hotmail.com](mailto:gmssu_emre@hotmail.com)  
Adress : Altay Sokak No:2/12 Güven Apt. Kolej,  
Çankaya/ANKARA

### Education

B.Sc. : Hacettepe University, Department of Mechanical Engineering (2015)  
M.Sc. : Hacettepe University, Department of Mechanical Engineering (2017)

### Projects and Budgets

#### •Master's Thesis

Thermal modeling of lithium ion batteries, funded by Hacettepe University Scientific Research Projects Coordination Unit, Budget: 139000 TL (47000 USD)

#### •Modeling of Turbulent Flow in an Industrial Chimney

Theoretical analysis of complex flow in an industrial chimney, funded by Enpro Inc., Budget: 6000 TL (2300 USD)

#### •Graduation Project for B.Sc

Design and production of a "Viscous Flow in Pipes Experimental Set Up", funded by Hacettepe University Scientific Research Projects Coordination Unit, Budget: 7400 TL (3300 USD)

### Foreign Languages

English

German



**Areas of Experience**

Thermofluids Sciences, Computational Fluid Dynamics, Clean Energy Technologies, Electrochemical Energy Generation and Storage, Li-ion Batteries

**Publications**

Emre Gümüŝsu, Özgür Ekici, Murat Köksal, 3-D CFD Modeling and Experimental Testing of Thermal Behavior of a Li-Ion Battery, Applied Thermal Engineering 120 (2017) 484–495.

<http://doi.org/10.1016/j.applthermaleng.2017.04.017>



HACETTEPE UNIVERSITY  
GRADUATE SCHOOL OF SCIENCE AND ENGINEERING  
THESIS/DISSERTATION ORIGINALITY REPORT

HACETTEPE UNIVERSITY  
GRADUATE SCHOOL OF SCIENCE AND ENGINEERING  
TO THE DEPARTMENT OF *Mechanical Engineering*

Date: *17/05/2017*

Thesis Title / Topic: *Thermal Modeling of Lithium Ion Batteries*

According to the originality report obtained by myself/my thesis advisor by using the *Turnitin* plagiarism detection software and by applying the filtering options stated below on *17/05/2017* for the total of *58* pages including the a) Title Page, b) Introduction, c) Main Chapters, d) Conclusion sections of my thesis entitled as above, the similarity index of my thesis is *5* %.

Filtering options applied:

1. Bibliography/Works Cited excluded
2. Quotes excluded / included
3. Match size up to 5 words excluded

I declare that I have carefully read Hacettepe University Graduate School of Science and Engineering Guidelines for Obtaining and Using Thesis Originality Reports; that according to the maximum similarity index values specified in the Guidelines, my thesis does not include any form of plagiarism; that in any future detection of possible infringement of the regulations I accept all legal responsibility; and that all the information I have provided is correct to the best of my knowledge.

I respectfully submit this for approval.

Date and Signature

Name Surname: *Emre GÜMÜŞLU*  
Student No: *114225933*  
Department: *Mechanical Engineering*  
Program: *Mechanical Engineering*  
Status:  Masters  Ph.D.  Integrated Ph.D.

*17.05.2017*

*G. Gümüşlü*

**ADVISOR APPROVAL**

*Öğretmen*  
APPROVED.

*Assist. Prof. Dr. Özgür Ekici*  
(Title, Name Surname, Signature)